Role of protein phosphorylation in preprotein targeting to plant organelles

Dissertation

der Fakultät für Biologie

der Ludwig-Maximilians-Universität

München

vorgelegt von

Anna-Elisa Catharina Nickel

München

Juli 2016

Diese Dissertation wurde angefertigt unter der Leitung von PD Dr. Serena Schwenkert an der Fakultät für Biologie der Ludwig-Maximilians-Universität München.

Erstgutachterin: PD Dr. Serena Schwenkert

Zweitgutachter: Prof. Dr. Wolfgang Frank

Tag der Abgabe: 06.07.2016

Tag der mündlichen Prüfung: 23.09.2016

Table of contents

Summary

A majority of the proteins utilized by mitochondria and chloroplasts are nucleus encoded, synthesized at cytosolic ribosomes and need to be posttranslationally imported into the organelles via translocon complexes at the membranes. To ensure correct and successful targeting and import, proteins are translated as preproteins equipped with targeting peptides and are associated with cytosolic chaperones. To regulate protein import phosphorylation is involved at different stages. On the one hand, chloroplast preproteins can be phosphorylated to enhance their import rates. Yet, they have to be dephosphorylated by a still unknown phosphatase before translocation can occur. On the other hand, phosphorylation of translocon subunits can influence their binding affinity to incoming preproteins. During this thesis different examples for the involvement of phosphorylation in protein targeting were investigated.

The function of preprotein phosphorylation in vivo was analyzed by using the phosphorylated preprotein pHCF136, a photosystem II assembly factor, to complement the seedling lethal *hcf136* mutant. A phospho-deficient construct could fully rescue the *hcf136* phenotype while phospho-mimicry within the targeting peptide reduced the import rate of the preprotein and led to hampered photosystem II complex assembly. This in vivo study underlines the relevance of preprotein phosphorylation during early developmental stages and confirms the model of mandatory dephosphorylation prior to translocation.
Since the phosphatase is still unknown and a recent report showed that purple acid phosphatase 2 (PAP2) might be involved in preprotein import *pap2* mutant plants were analyzed concerning their import behavior, however finding no indication that PAP2 is a chloroplast preprotein phosphatase.

Apart from organelle specific protein import there exist dual targeted preproteins with ambiguous targeting signals going to mitochondria and chloroplasts. Since chloroplast targeting signals can be phosphorylated these dual signals were likewise tested for phosphorylation. Indeed, 8 out of 17 dual targeted proteins were shown to be phosphorylated.

The mitochondrial docking protein OM64 was found to be phosphorylated as well. The phosphorylation site was identified and localized within the tetratricopeptide repeat (TPR) domain which is responsible for chaperone binding. OM64 could be shown to be part of the translocase of the outer mitochondrial membrane (TOM complex). In vitro and in vivo analysis using phospho-deficient and phospho-mimicking constructs revealed that phosphorylation of OM64 inhibits protein import by reducing binding affinity to preprotein associated chaperones.

Zusammenfassung

Der Großteil aller in Mitochondrien und Chloroplasten genutzten Proteine ist vom Nukleus kodiert, wird an zytosolischen Ribosomen translatiert und muss posttranslationell über membranständige Translokonkomplexe in die Organellen importiert werden. Um die korrekte und erfolgreiche Zielsteuerung und den folgenden Import zu gewährleisten, werden die Proteine als mit Signalpeptiden versehene Präproteine translatiert und sind mit zytosolischen Chaperonen assoziiert. Bei der Regulation des Proteinimports ist Proteinphosphorylierung auf mehreren Ebenen involviert. Einerseits werden chloroplastidäre Präproteine phosphoryliert um deren Importrate zu erhöhen. Jedoch müssen diese von einer noch unbekannten Phosphatase dephosphoryliert werden, bevor die eigentliche Translokation stattfinden kann. Andererseits kann die Phosphorylierung von Translokonuntereinheiten deren Bindeaffinität zu ankommenden Präproteinen beeinflussen. In dieser Arbeit wurden verschiedene Beispiele für die Involvierung von Phosphorylierung in den Proteinimport untersucht.

Die Funktion der Präproteinphosphorylierung in vivo wurde unter Verwendung des phosphorylierten Präproteins pHCF136, einem Photosystem II Assemblierungsfaktor, analysiert. Verschiedene Formen des Präproteins wurde zur Komplementation der lethalen *hcf136* Mutante genutzt. Ein phospho-defizientes Konstrukt konnte den *hcf136* Phänotyp vollständig retten, während Phospho-Mimikry im Signalpeptid die Importrate des Präproteins reduzierte und zu einer gehinderten Assemblierung des Photosystem II Komplexes führte. Diese in vivo Studie unterstreicht die Beteiligung der Proteinphosphorylierung in frühen Entwicklungsstadien und bestätigt das Modell der obligatorischen Dephosphorylierung vor der Translokation.

Da die Phosphatase noch unbekannt ist und ein aktueller Bericht gezeigt hat, dass die purple acid phosphatase 2 (PAP2) in den Proteinimport involviert seien könnte, wurden *pap2* Pflanzen bezüglich ihres Importverhaltens untersucht. Es konnte allerdings kein Hinweis gefunden werden, dass PAP2 eine Phosphatase für chloroplastidäre Präproteine ist.

Neben dem organellspezifischen Import gibt es dual zielgerichtete Präproteine mit zweideutigen Signalpeptiden, die in Mitochondrien und Chloroplasten importiert werden. Da chloroplastidäre Signalpeptide phosphoryliert werden können, wurden diese dualen Signalpeptide ebenfalls auf eine Phosphorylierung untersucht. Tatsächlich konnte gezeigt werden, dass 8 von 17 dual zielgerichteten Proteinen phosphoryliert werden.

Das mitochondrielle Kopplungsprotein OM64 wird ebenfalls phosphoryliert. Die Phosphorylierungsstelle wurde identifiziert und in der TPR (tetratricopeptide repeat) Domäne lokalisiert, welche für die Chaperonbindung verantwortlich ist. Es wurde gezeigt, dass OM64 Teil der Translokase an der äußeren mitochondriellen Membran (TOM Komplex) ist. In vitro

und in vivo Analysen mit phospho-defizienten und phospho-imitierenden Konstrukten zeigten, dass die Phosphorylierung von OM64 durch eine reduzierte Bindeaffinität zu den mit Präproteinen assoziierten Chaperonen den Proteinimport inhibiert.

Abbreviations

aa	amino acid
ATP	adenosine triphosphate
BN-PAGE	blue native polyacrylamide gel electrophoresis
Co-IP	Co-immunopredipitation
Col-0	*Arabidopsis thaliana* ecotype Columbia
Cyt	cytochrome
DTT	dithiothreitol
GFP	green fluorescent protein
GST	glutathione S-transferase
GTP	guanosine triphosphate
HCF	high chlorophyll fluorescence
His tag	hexahistidine tag
HOP	Hsp70/Hsp90 organizing protein
Hsp	heat shock protein
ITC	isothermal titration calorimetry
kDa	kilodalton
LHC	light harvesting complex
m	mature protein
OEP	outer envelope protein
OM	outer membrane
p	preprotein
PAP	purple acid phosphatase
PMSF	phenylmethylsulfonyl fluoride
ppi	plastid protein import
PS	photosystem
RL	reticulocyte lsyate
RuBisCO	ribulose-1,5-bisphosphate carboxylase/oxygenase
SDS-PAGE	sodium dodecyl sulfate polyacrylamide gel electrophoresis
SSU	small subunit of RuBisCO
STY kinase	serine/threonine/tyrosine kinase
TM	transmembrane domain
TOC	translocase of the outer membrane of chloroplasts
TOM	translocase of the outer membrane of mitochondria
TP	targeting peptide
TPR	tetratricopeptide repeat
WG	wheat germ lysate
WT	wildtype
β-DM	β-dodecyl maltoside

1 Introduction

1.1 Preprotein import into organelles

Plants contain two organelles performing vital functions and provide the cells with energy: mitochondria and chloroplasts. Both organelles originated from endosymbiotic events which occurred early in evolution (Margulis, 1970). Around two billion years ago an anaerobic host cell engulfed an ancestral aerobic α-proteobacterium which over time developed to today's mitochondrion. In a second endosymbiotic event around 1.5 billion years ago this heterotrophic mitochondria containing host cell took up an ancestral photosynthetic cyanobacterium which evolved into chloroplast. During the following evolution the two former autonomous prokaryotes lost their independence by lateral gene transfer of large parts of their genome to the host nucleus. Consequently, nowadays 99 % of all mitochondrial (Rehling et al., 2004) and more than 95 % of all chloroplast (Soll, 2002) proteins are nucleus encoded, synthesized at cytosolic ribosomes and need to be imported into their target organelle. For mitochondria and chloroplasts this occurs predominantly posttranslational. To assure the correct and successful targeting there exist several cytosolic mechanisms. Firstly, proteins are synthesized as preproteins containing a targeting signal which encodes their localization. Moreover, cytosolic chaperones bind to the preprotein and target it to its destination organelle. At the organellar surface receptor proteins interact with the preprotein directly or with the associated chaperone. Finally, posttranslational modifications like phosphorylation can be involved in preprotein import.

1.2 Targeting signals

To ensure specificity of targeting and the subsequent import, proteins are equipped with different types of signals which encode their destination. Most precursor proteins destined for the matrix of mitochondria or the stroma of chloroplasts are translated with a cleavable N-terminal targeting peptide. The mitochondrial targeting peptide is called presequence while the chloroplast targeting signal is called transit peptide. Targeting signals are necessary and sufficient for successful posttranslational import (Keegstra et al., 1989). In addition to cleavable targeting signals there exist different forms of non-cleavable ones which can either be present alone or in combination with cleavable signals. They can direct proteins to inner or outer membrane, the intermembrane space or inside chloroplasts further to the thylakoids (Schleiff and Becker, 2011).

Chloroplast targeting signals are on average longer than mitochondrial ones (58 residues vs. 42 residues in *A. thaliana*) (Zhang, 2002). Concerning their amino acid composition both types are very similar, as they show a high abundance of hydrophobic, hydroxylated and

positively charged amino acids while they have a low content of negatively charged residues (Zhang, 2002). Compared to other species like yeast and mammals it is a unique feature of plants that mitochondrial like chloroplast targeting signals are enriched in serine residues (regarding the total sequence) (Schneider et al., 1998). Apart from the overall similarity clear differences can be found when specifically analyzing the first 16 amino acids where arginine is greatly overrepresented in mitochondrial presequences whereas serine and proline are enriched in chloroplast transit peptides (Bhushan et al., 2006). Besides, mitochondrial targeting signals form amphipathic α-helices (von Heijne, 1986; Moberg et al., 2004) whereas chloroplast ones are generally unstructured (Krimm et al., 1999). After successful import into the organelle the N-terminal targeting peptide is cleaved off by specific peptidases, namely the stroma processing peptidase (SPP) in the stroma of chloroplasts and the matrix processing peptidase (MPP) in the matrix of mitochondria and the mature protein is folded.

1.3 Cytosolic chaperones

Preproteins are prone to aggregation or premature folding. To prevent this, chaperones bind to the freshly synthesized proteins. This keeps the preproteins in a conformational import competent state that is not fully folded (Attardi and Schatz, 1988; Waegemann et al., 1990). Besides, chaperones help targeting the preproteins to the correct organelle and can mediate the initial contact with the organellar translocons (Schleiff and Becker, 2011).

Heat shock protein 70 (Hsp70) belongs to a family of proteins found in eukaryotes and prokaryotes and is highly conserved between organisms (Karlin and Brocchieri, 1998). The monomeric chaperone plays a crucial role in protein folding and proteostasis control (Hartl et al., 2011). It promiscuously recognizes short hydrophobic peptide sequences of non-native proteins and binds early after translation. 97 % of plant mitochondrial presequences and 83 % of chloroplast transit peptides have a Hsp70 binding site (Zhang, 2002). Besides, Hsp70 binding was observed in the mature part of chloroplast targeted proteins (May and Soll, 2000). Hsp70 has an ATPase domain and binding and release of the client protein is regulated by the ATPase cycle (Young, 2010). Hsp70 can act alone or in concert with other chaperones.

A second class of the heat shock proteins which is also involved in preprotein import is Hsp90. Hsp90 is an abundant protein found in prokaryotes and eukaryotes, representing even 1-2 % of the total cellular proteins in the majority of unstressed eukaryotic cells (Lindquist and Craig, 1988). Hsp90 forms a proteostasis hub that controls numerous signaling pathways (Taipale et al., 2010). In plants Hsp90 binds NLR (nucleotide binding and leucine-rich) proteins which function in plant immunity (Shirasu, 2009). Besides, Hsp90 was shown to bind preproteins in mammals and plants (Young et al., 2003b; Fellerer et al., 2011). In contrast to Hsp70, Hsp90 does not promiscuously bind to nascent or unfolded polypeptide

chains but interacts with a limited set of partially folded substrates (Röhl et al., 2013). In many cases, Hsp90 takes over clients from Hsp70 (Dittmar and Pratt, 1997). Therefore, it might also act at a later time point during preprotein targeting. Since only a subset of preproteins is bound by Hsp90, this pathway is possibly restricted to preproteins that tend to adapt a higher-order secondary structure in comparison to preproteins binding only Hsp70 (Fellerer et al., 2011). Hsp90 acts as a flexible dimer and like Hsp70 it has an ATPase domain which regulates binding and release of clients (Young, 2001). Besides, Hsp90 needs assisting cochaperones like Hsp70/Hsp90 organizing protein (HOP) and immunophilins for its function. The mechanism is well studied in yeast and mammals (Bracher and Hartl, 2006; Pearl and Prodromou, 2006). Similarly, in *Arabidopsis* Hsp90 interacts with cochaperones, so far HOP and the immunophilin FKBP73 have been identified (Fellerer et al., 2011). In plants Hsp90 was only found in association with chloroplast preproteins (Fellerer et al., 2011) while up to now no mitochondrial preprotein was shown to be bound by Hsp90. Likewise, during mitochondrial import in yeast only Hsp70 is involved and not Hsp90 (Young et al., 2003b). In contrast to that mitochondrial preproteins in mammals are bound by both Hsp70 and Hsp90 (Fan et al., 2006). Besides their function in preprotein targeting both types of heat shock proteins are involved in the regulation of preprotein abundance in the cytosol (Lee et al., 2009; Tillmann et al., 2015). With the help of E3 ligases they can mark excess or aggregated preproteins for degradation by the ubiquitin proteasome system.

Another class of chaperones is the 14-3-3 family which is ubiquitously found in eukaryotic organisms and tissues and assists a wide range of target proteins with diverse functions like regulation of metabolism, cell cycle, cell growth, cell differentiation, programmed cell death, calcium signaling and flower induction (Mhawech, 2005; de Boer et al., 2013). The protein acts as a dimer and binds to client proteins phosphorylated within a 14-3-3 binding motif (de Boer et al., 2013). Many chloroplast transit peptides contain a 14-3-3 binding motif (May and Soll, 2000; Martin et al., 2006). Together with Hsp70 14-3-3 in plants forms a guidance complex for phosphorylated chloroplast preproteins, enhancing their import rate (May and Soll, 2000; Fellerer et al., 2011). In yeast a cytosolic 14-3-3 protein complex called mitochondrial import stimulating factor (MSF) is promoting mitochondrial protein import (Hachiya et al., 1995). Since for a long time no plant mitochondrial preprotein was found to be associated with 14-3-3 it was hypothesized that the guidance complex plays a role in mediating specificity of targeting to chloroplasts versus mitochondria (May and Soll, 2000). Recently however, plant mitochondrial preproteins were reported to bind 14-3-3 as well (Fellerer, 2012; Law et al., 2015).

1.4 Translocons at the outer membrane

Once the protein reaches the organelle, it has to be recognized, bound and transported through two membranes, the outer and the inner membrane. To facilitate this, each membrane has its own translocon consisting of at least one channel protein and several receptor proteins. The different subunits are named according to their calculated molecular masses in the organism they were first discovered in. Though plastids arose later during evolution in a cell where mitochondria were already present, the import systems in the two organelles have been derived independently and do not share homology (Peeters and Small, 2001).

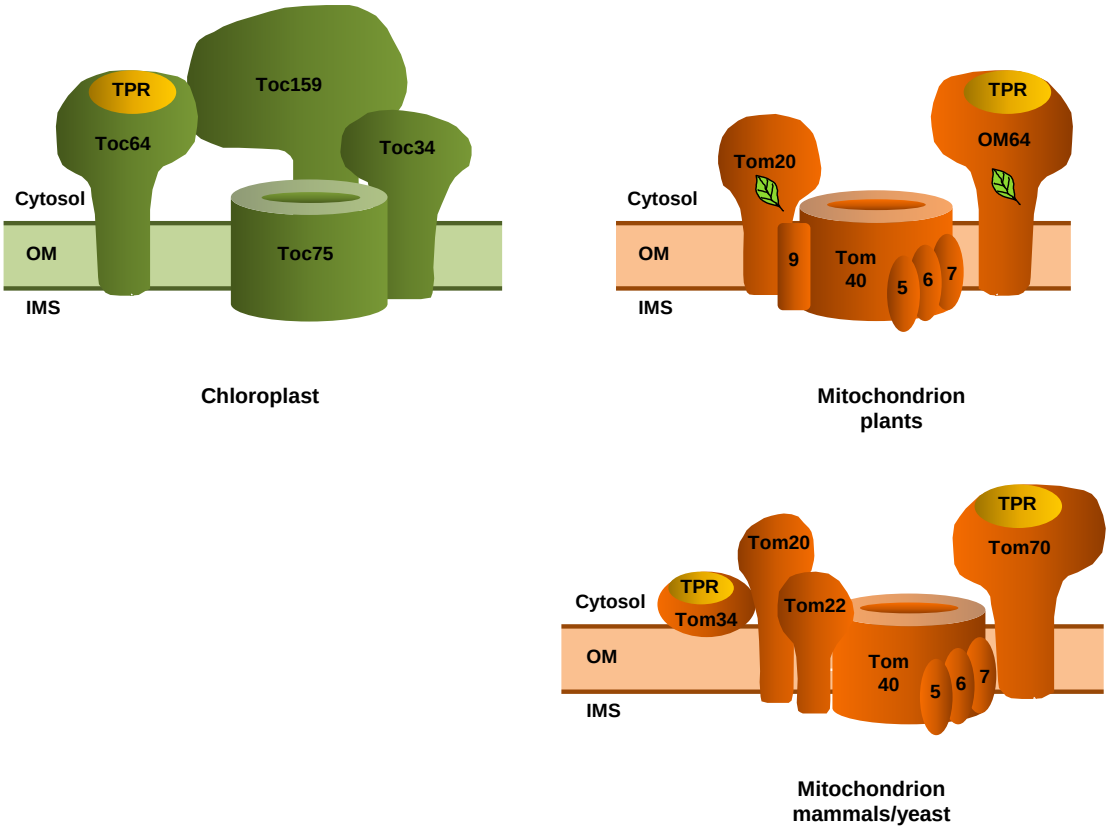

Figure 1: Translocase of the outer membrane (OM) of chloroplasts (TOC) and mitochondria (TOM). Both organelles possess a translocation channel and several receptor proteins including one docking protein exposing a TPR (tetratricopeptide repeat) domain into the cytosol. Plant Tom20 and OM64 are not orthologous to TOM proteins found in mammals and yeast. IMS, intermembran space.

1.4.1 Translocase of the outer membrane of chloroplasts

The TOC complex (translocase of the outer membrane of chloroplasts) directly mediates precursor translocation and is with few exceptions (Nada and Soll, 2004; Miras et al., 2007) the major import pathway into the chloroplast (Figure 1). Toc75 is a β-barrel protein, embedded into the membrane and acts as a translocation channel across the outer

membrane (Hinnah et al., 2002). Toc75 is stably associated with two preprotein binding receptor proteins, Toc34 and Toc159 (Kessler et al., 1994; Seedorf et al., 1995). In *Arabidopsis* deletion of Toc34 (*ppi1* mutant) leads to a pale green phenotype (Jarvis et al., 1998) and deletion of Toc159 (*ppi2* mutant) to albinotic plants (Bauer et al., 2000). This clearly depicts the essential roles of the receptor proteins in chloroplast biogenesis. Both receptors expose GTP binding domains into the cytosol and hydrolysis of GTP is required for protein translocation across the outer membrane. There exist opposing models whether Toc34 (Becker et al., 2004) or Toc159 (Kouranov and Schnell, 1997) is the initial receptor for preprotein binding but both are able to directly interact with the transit peptide.

Another type of docking protein is Toc64 which exposes a tetratricopeptide repeat (TPR) domain into the cytosol (Sohrt and Soll, 2000). Via this TPR domain Toc64 can bind Hsp70 and Hsp90 which can be associated to the preproteins (Qbadou et al., 2006; Schweiger et al., 2013). In contrast to Toc34 and Toc159, Toc64 interacts only transiently with the TOC complex (Qbadou et al., 2006). A knock-out of Toc64 does not show a growth phenotype (Aronsson et al., 2007) but a partly reduced chloroplast protein import (Qbadou et al., 2006).

1.4.2 Translocase of the outer membrane of mitochondria

The TOM complex (translocase of the outer membrane of mitochondria) is the principal outer membrane import complex in mitochondria (Figure 1) and with few exceptions (Ahting et al., 2005) all mitochondrial proteins are thought to pass through the pore forming β-barrel protein Tom40 (Vestweber et al., 1989; Dekker et al., 1998). Tom40 is essential and conserved between yeast, mammals and plants (Duncan et al., 2013).

In yeast (where mitochondrial import has mainly been studied in) and in mammals two receptor proteins can be found as subunits of the TOM complex, Tom20 and Tom70. While Tom20 interacts with the preproteins directly at their N-terminal targeting signals (Abe et al., 2000; Saitoh et al., 2007), Tom70 possesses a cytosolic facing TPR domain which binds to cytosolic chaperones Hsp70 and Hsp90 (Young et al., 2003b). Yeast strains lacking one of the two receptor proteins are viable but grow slower than wild type, a double-deletion mutant however is not viable (Ramage et al., 1993).

Next to Tom20 and Tom70 an additional secondary receptor protein can be found in yeast and mammals, Tom22. Tom22 transfers the incoming mitochondrial preprotein from the primary receptor to the import pore (van Wilpe et al., 1999). Besides, it functions as an organizer of the TOM complex and as an extra step of the presequence binding chain (Moczko et al., 1997; Komiya et al., 1998).

The plant orthologue of Tom22 is Tom9 (Jänsch et al., 1998). Yet, plant Tom9 is a truncated form of yeast Tom22 lacking the large cytosolic region (Jänsch et al., 1998). Instead of binding mitochondrial presequences, Tom9 interacts with plant Tom20 (Rimmer et

al., 2011). Plant Tom20 is not orthologous to yeast or mammalian Tom20 (Perry et al., 2006), yet it has been shown to perform similar functions, namely interacting with the presequence of mitochondrial preproteins (Ramage et al., 1993; Lister et al., 2007). However, plant Tom20 achieves this binding through a different, more complex mechanism (Rimmer et al., 2011). Instead of the single binding domain which is found in yeast and mammalian Tom20 (Abe et al., 2000; Saitoh et al., 2007), plant Tom20 possesses two binding regions separated by a flexible linker segment. This is thought to be an adaption allowing the specific recognition of mitochondrial presequences among similar plastid targeting signal in the cytoplasm (Rimmer et al., 2011). In the *Arabidopsis* genome Tom20 is encoded by four paralogous genes, Tom20-1 to Tom20-4 (Werhahn et al., 2001). Tom20-2 to Tom20-4 are highly expressed in diverse plant organs whereas Tom20-1 transcript is rarely detectable and the protein could not be identified in isolated plant mitochondria (Werhahn et al., 2001; Lister et al., 2004). A single knock-out of one Tom20 isoform shows no phenotype while the triple knock-out of all three relevant isoforms (Tom20-2 to 4) leads to a reduced protein import rate and slower plant growth (Lister et al., 2007).

Furthermore, compared to yeast and mammals there is no orthologue of Tom70 in plants. Yet, in plants the TPR containing docking protein OM64 exists which displays 67 % sequence identity within the TPR domain to the chloroplast docking protein Toc64 (Chew et al., 2004; Lister et al., 2007). In *Arabidopsis* OM64 is a member of a family consisting of three paralogous genes: OM64 (former Toc64-V), Toc64 and Amidase 1. OM64 and Toc64 have a N-terminal transmembrane domain which anchors them in mitochondrial and chloroplast outer membrane, respectively. The TPR domains are located at the C-terminus facing into the cytosol. In the middle part the two proteins have an amidase-like domain. However, the catalytic function has been lost due to two point mutations. In contrast to OM64 and Toc64, Amidase 1 possesses enzymatic activity while it lacks the transmembrane and the TPR domain. It is located in the cytosol and has been reported to be involved in auxin biogenesis (Pollmann et al., 2006). OM64 has been shown to be involved in mitochondrial protein import and to interact with different mitochondrial precursor proteins (Lister et al., 2007) as well as with chaperones Hsp70 and Hsp90 (Schweiger et al., 2013). As it can be observed for Toc64 (Qbadou et al., 2006) and also Tom70 (Dekker et al., 1998) OM64 is suggested to interact dynamically with the TOM complex since it could not be identified in the TOM complex by immunodetection (Lister et al., 2007). Like Toc64 a knock-out of OM64 in *Arabidopsis* does not show a growth phenotype (Aronsson et al., 2007) but a partly reduced mitochondrial protein import (Lister et al., 2007). Interestingly, similar to the lethal double knock-out of Tom20 and Tom70 in yeast (Ramage et al., 1993) also the quadruple knock-out of all three expressed Tom20 isoforms and OM64 in plants leads to embryolethality (Duncan

et al., 2013). If one or several Tom20 isoforms are knocked out expression of OM64 is increased, proposing overlapping roles of these proteins (Lister et al., 2007).

In mammals Tom34 is another TPR domain containing receptor protein which interacts with mitochondrial preproteins in an Hsp70/Hsp90 dependent manner in the cytosol (Faou and Hoogenraad, 2012).

Besides, there exist three associated small Toms, Tom5, 6 and 7, which are partially conserved between yeast, mammals and plants and regulate the formation and function of the TOM complex (Duncan et al., 2013).

1.5 TPR domain

The tetratricopeptide repeat (TPR) domain is generally involved in protein-protein interaction. One TPR domain is made up of at least three TPR motifs each one consisting of 34 degenerated amino acids sharing a loosely conserved pattern of small and large hydrophobic amino acids. No residue is fully invariant but there are positions with certain preferences (Zeytuni and Zarivach, 2012). Structurally a TPR domain consists of three helix-turn-helix motifs capped with an additional seventh solvation helix at the C-terminal end and forms a concave surface via which ligands are usually bound (Zeytuni and Zarivach, 2012). TPR-containing proteins are widespread across all kingdoms of life, where they take part in diverse cellular processes, including peroxisomal targeting and import (Brocard and Hartig, 2006; Fransen et al., 2008), synaptic vesicle fusion (Young et al., 2003a) and import into mitochondria, chloroplast and the endoplasmatic reticulum (Kriechbaumer et al., 2012; Schweiger et al., 2012). TPR domains can bind chemically distinct peptides in a variety of conformations (Zeytuni and Zarivach, 2012). One specific form of the TPR domain is the dicarboxylate clamp type which was first found in Hsp70/Hsp90 organizing protein HOP (Scheufler et al., 2000) and uses basic residues to bind to two carboxylate groups at the conserved C-terminal EEVD motif of its substrates Hsp70 and Hsp90 (Figure 2). The EEVD sequence was found to bind via electrostatic interactions in an extended coil conformation which allows the display of a maximal surface towards the TPR domain and like this promotes specific recognition (Scheufler et al., 2000). HOP consists of three distinct TPR domains which specifically either bind Hsp70 or Hsp90. Besides, there exist TPR domains which can bind both chaperones Hsp70 and Hsp90 like the one of CHIP (C-terminal of Hsp70 interacting protein) (Zhang et al., 2005).

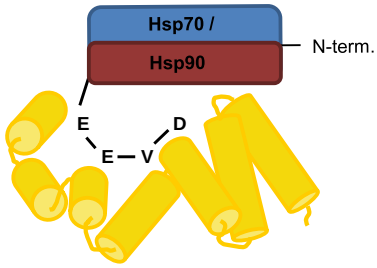

Figure 2: Model of a TPR (tetratricopeptide repeat) domain. One domain consists of at least three TPR motifs of 34 degenerated amino acids. A helix-turn-helix structure creates a concave binding groove for protein-protein-interaction (in yellow). Hsp70 and Hsp90 interact with their conserved EEVD motif at the C-terminus with a clamp type TPR domain.

1.6 Dual import and its regulation

Protein targeting and import is generally very specific. However, an increasing number of proteins with identical sequences, translated from the same gene have been found in both organelles, mitochondria and chloroplasts. This phenomenon is called dual import. Up to now approximately 100 proteins were proposed to be dual targeted (Morgante et al., 2009; Carrie and Small, 2013). These proteins are involved in central processes like nucleotide metabolism, DNA replication, recombination and repair, tRNA biogenesis and translation (Carrie and Small, 2013). There are two basic ways in which a single gene can provide a product to both organelles (Peeters and Small, 2001). Firstly, the protein can have a twin targeting sequence, consisting of a mitochondrial and chloroplast targeting sequence in tandem. By using alternative transcription starts, alternative translation starts, alternative exon splicing or a combination of the above two proteins are made from the same gene which then go to different organelles. The second way of obtaining dual targeting is to use a common ambiguous targeting peptide which allows import into both organelles. These signals share features of both mitochondrial and plastid targeting peptides and often appear intermediate between the two (Pujol et al., 2007; Berglund et al., 2009). How is dual import regulated if the ambiguous targeting signal does not allow a distinction between the two organelles? A general way to direct targeting preferentially to mitochondria could be by expressing more mitochondrial than plastid import components (Howell et al., 2006), whereas with the opposite ratio targeting would be diverted to plastids. Besides, there might be more specific mechanisms at work, like targeting of mRNA to the vicinity of specific organelles prior to translocation (Michaud et al., 2010), redox regulation of the import machineries (Stengel et al., 2010), physicochemical properties of the mature part of the preprotein (von Braun et al., 2007; Leibovitch et al., 2013) or, as it can be seen for chloroplast preproteins, phosphorylation of targeting peptides (Lamberti et al., 2011a).

1.7 Phosphorylation in preprotein targeting

Protein phosphorylation is a widely conserved mechanism of cellular regulation found in prokaryotes and eukaryotes (Kyriakis, 2014). It is a fast and reversible posttranslational modification that can result in conformational changes and modify the function of a protein in almost every conceivable way. Examples are the increase or decrease of its biological activity, its stabilization or its mark for destruction, the facilitation or inhibition of its movement between subcellular compartments or the enhancement or prevention of protein-protein interactions (Cohen, 2002). There are different ways reported how phosphorylation influences preprotein targeting. Chloroplast preproteins can be phosphorylated within their transit peptide (Waegemann and Soll, 1996). The subsequent binding by the guidance complex leads to three- to fourfold higher import rates presumably by enhancing the affinity to the TOC complex (May and Soll, 2000). In *Arabidopsis* three highly homologous cytosolic protein kinases are responsible for the phosphorylation of the transit peptides: STY8, STY17 and STY46 which belong to the plant specific STY (for Ser/Thr/Tyr) kinase family (Martin et al., 2006). A *sty8 sty17 sty46* triple mutant displays a delayed greening process and a reduced accumulation of nuclear encoded phosphorylated proteins in the chloroplast (Lamberti et al., 2011a). The fact that these kinases are important for the differentiation of plastids confirms the involvement of phosphorylation in protein import: during chloroplast development numerous proteins are required, thus at this point the import enhancing effect of phosphorylation is most noticeable. In mammals as well, phosphorylation of precursor proteins stimulates their import into mitochondria (Robin et al., 2002; Robin et al., 2003). In plants there was for long time no evidence that mitochondrial preproteins are also phosphorylated. Recently however, few plant mitochodrial preprotein were reported to be phosphorylated (Fellerer, 2012; Law et al., 2015).

Interestingly, the dephosphorylation of the chloroplast transit peptide is essential for the protein import, as it was shown by in vitro import into chloroplasts (Waegemann and Soll, 1996) and GFP-labeled in vivo import into protoplasts (Lamberti et al., 2011a) both using the small subunit of the ribulose-1,5-bisphosphate carboxylase/oxygenase (SSU). The phosphatase is yet unidentified but thought to be located at the outer membrane.

Apart from the preproteins, another way phosphorylation is involved in import is at the level of the translocon proteins. Toc34 for example is inhibited by phosphorylation since it decreases its affinity to GTP and like this inhibit protein import (Sveshnikova et al., 2000). In yeast, phosphorylation is involved in the biogenesis of the TOM complex (Rao et al., 2012). Phosphorylation of Tom22 not only stimulates the targeting of Tom22 to mitochondria but also the association of Tom20 with the TOM complex (Schmidt et al., 2011). Besides, phosphorylation of the receptor protein Tom70 inhibits protein import by reducing the affinity of Tom70 to Hsp70 (Schmidt et al., 2011). Tom70 is phosphorylated in close proximity to its

TPR domain (Schmidt et al., 2011). Furthermore, phosphorylation within a TPR domain was shown to change affinities to chaperones as well (Röhl et al., 2015). The human HOP and the yeast homolog Sti1 are both phosphorylated within a Hsp70 binding TPR domain. Phospho-mimicry reduces the binding of Hsp70 in both cases (Röhl et al., 2015).

1.8 Aim of this work

During this thesis the role of phosphorylation in preprotein targeting was investigated on several levels. Previously, phosphorylation of chloroplast transit peptides was shown to enhance the import rate. However, dephosphorylation of the preprotein by a yet unidentified phosphatase was stated to be an obligatory prerequisite prior to translocation. In this work a plant complementation study of the phosphorylated preprotein HCF136 was performed to analyze the importance of (de-) phosphorylation in vivo. Furthermore, one potential phosphatase was analyzed for its involvement in chloroplast import. In a third part an in vitro screen was used to investigate whether dual targeted preproteins are phosphorylated as well. Besides preprotein phosphorylation, also phosphorylation of a translocon docking protein was investigated. Mitochondrial outer membrane protein OM64 was shown to be phosphorylated within the TPR domain. The phosphorylation site was determined and the influence of the phosphorylation on chaperone binding and import ability was analyzed.

2 Material and Methods

2.1 Material

2.1.1 Chemicals

If not noted otherwise, all used chemicals were received from Sigma Aldrich (Taufkirchen, Germany), Roth (Karlsruhe, Germany), Merck (Darmstadt, Germany), Thermo Fisher Scientific (Braunschweig, Germany) or Serva (Heidelberg, Germany).

2.1.2 Molecular weight and size markers

For SDS-PAGE peqGOLD protein marker I (VWR, Ismaning, Germany) was used. EcoRI and HindIII digested lambda phage DNA (Thermo Fisher Scientific) was used as a marker for agarose gel electrophoresis. Amersham HMW Calibration Kit For Native Electrophoresis (GE Healthcare, Munich, Germany) was used for BN-PAGE.

2.1.3 Oligonucleotids

DNA oligonucleotids were ordered from Metabion (Martinsried, Germany) and are listed in Table 1.

Table 1: Oligonucleotides used for this work. Capitals indicate exon sequences, small letters introns.

primer	5'-3' oligonucleotid sequence	purpose
At1g12520 TP for	GTCGGATCCGCATCAATTCTCAGG	pGEX6p1
At1g12520 TP rev	GACGAATTCTCACATCGGAGAGCTAACG	pGEX6p1
At1g21400 TP for	GTCGGATCCGCGATCTGGTTTGC	pGEX6p1
At1g21400 TP rev	GACGAATTCTCAATGACGGAGGCTACC	pGEX6p1
At2g04842 TP for	GTCGGATCCGCCTCTTCTC	pGEX6p1
At2g04842 TP rev	GACGAATTCTCACCTTGGCCAAA	pGEX6p1
At2g30320 TP for	GTCGGATCCGCAGTCTCGTTTCTAC	pGEX6p1
At2g30320 TP rev	GACGAATTCTCAGAATCGTAATAACGC	pGEX6p1
At2g39290 TP for	GTCGGATCCCTCAGATCCGGTCTG	pGEX6p1
At2g39290 TP rev	GACGAATTCTCAACGGGAAGTGATAATG	pGEX6p1
At3g02660 TP for	GTCGGATCCGCATATGCAACAGGA	pGEX6p1
At3g02660 TP rev	GACGAATTCTCACTTAACAGAAGAGAA	pGEX6p1
At3g10690 TP for	GTCGGATCCACTCCAGTATTATG	pGEX6p1
At3g10690 TP rev	GACGAATTCTCAGACAACGAATTTG	pGEX6p1
At3g25740 TP for	GTCGGATCCTTGCAGAAGATTTCTC	pGEX6p1
At3g25740 TP rev	GACGAATTCTCATACTAGTGGTGG	pGEX6p1
At3g58140 TP for	GTCGGATCCACCGTTTTCTCAGTTC	pGEX6p1

At3g58140 TP rev	GACGAATTCTCAAGAGACGATTGGGTAG	pGEX6p1
At4g26500 TP for	GTCGGATCCGCAGCAGCGATG	pGEX6p1
At4g26500 TP rev	GACGAATTCTCACGATGGTGGAGG	pGEX6p1
At4g31210 TP for	GTCGGATCCCAGAGAACCATCTC	pGEX6p1
At4g31210 TP rev	GACGAATTCTCATGGGAAATTTTGAATC	pGEX6p1
At4g33760 TP for	GTCGGATCCTCTCTCCTCCTACGAAC	pGEX6p1
At4g33760 TP rev	GACGAATTCTCACACTACTACATCGCCG	pGEX6p1
At5g15700 TP for	GTCGGATCCTCCAGTGCTCAAACC	pGEX6p1
At5g15700 TP rev	GACGAATTCTCACCTCGAAATTGCTTG	pGEX6p1
At5g16200 TP for	GTCGGATCCTCACTCTCCCGTC	pGEX6p1
At5g16200 TP rev	GACGAATTCTCAACGGAGATTCCG	pGEX6p1
At5g26860 TP for	GTCGGATCCAAGGGCTTTGATAC	pGEX6p1
At5g26860 TP rev	GACGAATTCTCAGACGACCCTAC	pGEX6p1
At5g38710 TP for	GTCGGATCCGCAAACCGTTTCC	pGEX6p1
At5g38710 TP rev	GACGAATTCTCAGCGCCTTGCTGCGGC	pGEX6p1
At5g55200 TP for	GTCGGATCCTTGGTGTCTAGGG	pGEX6p1
At5g55200 TP rev	GACGAATTCTCAGTTTCGGAGCGAC	pGEX6p1
OM64 NheI no TM His for	CGATGCTAGCCACCACCACCACCACCACTTAGATCGT	pET21a
OM64 Rev NotI	GATCGCGGCCGCTCATATGTGTTTTCGGAG	pET21a
OM64TPR Dom for	GTCGGATCCGAAGTTATGAAAGAAAAGGGC	pGEX6p1
OM64TPR Dom rev	GACGAATTCTCACTGTGGTTCAAGGACCAATGCG	pGEX6p1
OM64 gateway for	GGGGACAAGTTTGTACAAAAAAGCAGGCTTCATGTCGAATACGCTTTCTTTGATTC	pDONR207
OM64-TPR gateway rev	GGGGACCACTTTGTACAAGAAAGCTGGGTCCTATTCAGAAGCCTCCATGTTAC	pDONR207
OM64 VL gateway rev	GGGGACCACTTTGTACAAGAAAGCTGGGTCTCATATGTGTTTTCGGAGTCTC	pDONR207
OM64 gDNA Gateway for	GGGGACAAGTTTGTACAAAAAAGCAGGCTTCccgcttaatttattacttgg	pDONR207
OM64 gDNA Gateway rev	GGGGACCACTTTGTACAAGAAAGCTGGGTCgaaacagaggagaagatacgg	pDONR207
OM64 S568A for	GAGGGACTGCTAGAGAAGCACTTGTACGGTACAAGGAA	mutagenesis
OM64 S568A rev	TTCTCTAGCAGTCCCTCGTCTCAA	mutagenesis
OM64 S568D for	GGGACTGCTAGAGAAGACCTTGTACGGTACAAG	mutagenesis
OM64 S568E for	GGGA CTGCTAGAGA AGAGCTTGTA CGGTACAAG	mutagenesis
OM64 stop w/oTPR for	GTAACATGGAGGCTTCTTGAGTTATGAAAGAAAAG	mutagenesis
OM64 stop w/oTPR rev	AGAAGCCTCCATGTTACCATTGGTGTCAG	mutagenesis
OM64 bp1860 rev	GGGATTCGAGGCATTGCT	sequencing
OM64 bp2521 for	AGCACTATGGAACTCCTA	sequencing
OM64 bp4265 for	GCATCCAACTTAGC	sequencing
TOM20-2 Mitte UTR for	CGCCTCAAATTCATCTTTGCTC	genotyping
TOM20-2 UTR rev	CTATGGCTTTAGGCTTTATC	genotyping
LBb1.3	ATTTTGCCGATTTCGGAAC	genotyping
TOM20-2 Stop NotI rev	AGTCGCGGCCGCTTATCTGGCAGGAGGTGGAG	genotyping
Hcf136 qPCR for	CTGCAACTCTGCGACGGTTA	qRT-PCR

Hcf136 qPCR rev	TGTTCATCAGCTCTCGCTGG	qRT-PCR
OEP24.1 fw	GGGACTTTGCGATTTCT	qRT-PCR
OEP24.1 rev	CTTTTACTACTAATTGGACTCACTAATA	qRT-PCR
hcf136 f	CGAGTTTCTGGGTTCTTTTGC	genotyping
hcf 136 r	GACTGCGTATAGGTTAGCTGC	genotyping
LB	CGTGACTCCCTTAATTCTCCG	genotyping

2.1.4 Vectors

To overproduce proteins fused to an N-terminal GST-tag pGEX6p1vector was used, for proteins fused to a C-terminal His tag pET21a vector was used. pF3A vector (Promega, Mannheim, Germany) was used for in vitro transcription and translation. For plant transformation the following binary vectors were used: pB7FWG2 for expression under 35 S promoter and pBGW for expression under endogenous promoter (both Plant Systems Biology, Zwijnaarde, Belgium). Cloning into binary vectors was performed using the Gateway system (Thermo Fisher Scientific) via pDONR207 vector. All plasmids used for this thesis are listed in Table 2.

2.1.5 Enzymes

Restriction endonucleases were purchased either from Thermo Fisher Scientific or from New England BioLabs (Frankfurt am Main, Germany). T4 DNA ligase was received from Thermo Fisher Scientific, Phusion DNA polymerase from New England BioLabs, Taq DNA polymerase from Bioron (Ludwigshafen, Germany).

2.1.6 Bacterial strains

E. coli TOP10 cells were used for propagation of plasmid DNA. Overproduction of heterologous proteins was performed using either *E. coli* BL21(DE3)pLysS cells or RIPL (BL21-CodonPlus(DE3)-RIPL strain) cells. For stable transformation of *A. thaliana* plants *A. tumefaciens* GV3101 (pMP90RK) cells were used.

2.1.7 Membranes

PVDF transfer membrane for western blotting was received from Macherey-Nagel (Düren, Germany), blotting paper was obtained from Millipore (Darmstadt, Germany).

Table 2: List of plasmids used for this work

Construct	Organism	Vector	source
At1g12520 TP	*A. thaliana*	pGEX6p1	this work
At1g21400 TP	*A. thaliana*	pGEX6p1	this work
At2g04842 TP	*A. thaliana*	pGEX6p1	this work
At2g30320 TP	*A. thaliana*	pGEX6p1	this work
At2g39290 TP	*A. thaliana*	pGEX6p1	this work
At3g02660 TP	*A. thaliana*	pGEX6p1	this work
At3g10690 TP	*A. thaliana*	pGEX6p1	this work
At3g25740 TP	*A. thaliana*	pGEX6p1	this work
At3g58140 TP	*A. thaliana*	pGEX6p1	this work
At4g26500 TP	*A. thaliana*	pGEX6p1	this work
At4g31210 TP	*A. thaliana*	pGEX6p1	this work
At4g33760 TP	*A. thaliana*	pGEX6p1	this work
At5g15700 TP	*A. thaliana*	pGEX6p1	this work
At5g16200 TP	*A. thaliana*	pGEX6p1	this work
At5g26860 TP	*A. thaliana*	pGEX6p1	this work
At5g38710 TP	*A. thaliana*	pGEX6p1	this work
At5g55200 TP	*A. thaliana*	pGEX6p1	this work
pSSU	*N. tabacum*	pF3A	workgroup Prof. Soll
pSSU S31,34A	*N. tabacum*	pF3A	workgroup Prof. Soll
Hcf136 TP -mSSU	*A. thaliana/ N. tabacum*	pF3A	workgroup Prof. Soll
Hcf136 TP 33-38A -mSSU	*A. thaliana/ N. tabacum*	pF3A	workgroup Prof. Soll
Hcf136 TP S35-37D-mSSU	*A. thaliana/ N. tabacum*	pF3A	workgroup Prof. Soll
STY8	*A. thaliana*	pET21a	workgroup Prof. Soll
Fad	*G. max*	pGEM3zf+	workgroup Prof. Whelan
OM64 w/o TPR	*A. thaliana*	pET21a	this work
OM64 TPR domain	*A. thaliana*	pGEX6p1	this work
OM64 TPR domain S568A	*A. thaliana*	pGEX6p1	this work
OM64 w/o TM	*A. thaliana*	pET21a	this work
OM64 w/o TM S568A	*A. thaliana*	pET21a	this work
OM64 w/o TM S568E	*A. thaliana*	pET21a	this work
OM64	*A. thaliana*	pDONR207	this work
OM64	*A. thaliana*	pB7FWG2	this work
OM64 S568A	*A. thaliana*	pDONR207	this work
OM64 S568A	*A. thaliana*	pB7FWG2	this work
OM64 S568D	*A. thaliana*	pDONR207	this work
OM64 S568D	*A. thaliana*	pB7FWG2	this work
OM64 w/o TPR	*A. thaliana*	pDONR207	this work
OM64 w/o TPR	*A. thaliana*	pB7FWG2	this work
OM64 genomic	*A. thaliana*	pDONR207	this work
OM64 genomic	*A. thaliana*	pBGW	this work
OM64 S568A genomic	*A. thaliana*	pDONR207	this work
OM64 S568A genomic	*A. thaliana*	pBGW	this work

OM64 S568D genomic	*A. thaliana*	pDONR207	this work
OM64 S568D genomic	*A. thaliana*	pBGW	this work
OM64 w/o TPR genomic	*A. thaliana*	pDONR207	this work
OM64 w/o TPR genomic	*A. thaliana*	pBGW	this work

2.1.8 Antisera

D1, CP74, Cytochrome (Cyt) f and PsaF antisera were purchased from Agrisera (Vännäs, Sweden). Antisera against HCF136 were a kind gift from Peter Westhoff (Heinrich-Heine Universität Düsseldorf, Germany). 14-3-3, Tom20, Tom40, Hsp70 and Hsp90 antisera were produced by Biogenes (Berlin, Germany), OM64 antisera by Pineda (Berlin, Germany).

2.1.9 Column material

Ni Sepharose 6 Fast Flow and Protein A Sepharose CL-4B were received from GE Healthcare.

2.1.10 Accession numbers

The gene accession numbers of the proteins involved in this work can be seen in Table 3.

Table 3: Gene accession numbers of proteins involved in this work

gene name	accession number
HCF136	At5g23120
OM64	At5g09420
PAP2	At1g13900
PAP9	At2g02450
STY8	At2g17700
Tom20-2	At1g27390

2.1.11 Software

BioEdit (Ibis Bioscience, Carlbad, USA) was used to align DNA sequences. CLC Genomics Workbench 7 (CLC Bio, Qiagen, Hilden, Germany) was used for protein alignments. NCBI Blast server (http://blast.ncbi.nlm.nih.gov) was used to match DNA or protein sequences. TargetP server (http://www.cbs.dtu.dk) was used to predict targeting peptides and Eukaryotic Linear Motif server (http://elm.eu.org) to analyze 14-3-3 binding sites.

2.2 Molecular biological methods

General methods not listed below were performed according to (Sambrook et al., 1989). Competent cells for DNA transformation were prepared according to (Hanahan, 1985).

2.2.1 Cloning strategies

For overproduction of proteins fused to an N-terminal GST tag pGEX6p1 vector and PCR product created with primes containing the appropriate restriction site were digested with BamHI and EcoRI. For overproduction of proteins fused to an C-terminal His tag pET21a vector and PCR product created with primes containing the appropriate restriction site were digested with NotI and NdeI. Ligation was carried out for 1 h at room temperature using T4 ligase. For stable plant transformation gateway system (Thermo Fisher Scientific) was used to clone constructs via homologous recombination from pDONR207 into binary vectors pB7FWG2 or pBGW. Cloning was performed according to the manufacturer's instructions.

2.2.2 Polymerase chain reaction (PCR)

PCR was performed with gDNA, cDNA or plasmid DNA as templates. For cloning and mutagenesis PCR proof-reading Phusion polymerase was used. For genotyping and colony PCR Taq polymerase was chosen. Annealing temperature and elongation time were adapted concerning oligonucleotids and length of constructs. PCR products for cloning were excised from 1 % agarose gel run in TAE buffer (40 mM Tris, 2.5 mM EDTA, 1 % acetic acid) and purified using NucleoSpin Gel and PCR Clean-up kit (Macherey-Nagel).

2.2.3 Isolation of plasmid DNA from *E. coli*

Plasmid DNA was isolated from 2 ml overnight *E. coli* culture using the NucleoSpin Plasmid EasyPure kit (Macherey-Nagel) according to the manufacturer's instructions.

2.2.4 Sequencing

Each plasmid was confirmed by sequencing which was performed by the sequencing service of the Faculty of Biology (Ludwig-Maximilians-Universität München, Germany) using 100 - 200 ng of vector with appropriate primer.

2.2.5 Isolation of genomic DNA from *A. thaliana* for genotyping PCR

One leaf was homogenized in 300 µl extraction buffer (200 mM Tris pH 7.5, 250 mM NaCl, 25 mM EDTA, 0.5 % SDS) using an electronic pistil. The sample was incubated 5 min at 37 °C then centrifuged for 10 min at 10000 g and 4 °C. Supernatant was incubated for 5 min

at room temperature with equal volume isopropanol then centrifuged as above. Pellet was washed once with 70 % ethanol then dried at 37 °C. DNA was resolved in 50 µl H_2O by freezing the sample at - 20 °C followed by 5 min at 50 °C.

2.2.6 Isolation of genomic DNA from *A. thaliana* for cloning

gDNA from *A. thaliana* leaves was isolated using the DNeasy Plant Mini kit (Qiagen) according to the manufacturer's instructions.

2.2.7 Isolation of RNA from *A. thaliana*

RNA from *A. thaliana* leaves was isolated using the RNeasy Plant Mini kit (Qiagen) according to the manufacturer's instructions. Digestion with DNase was either performed during RNA isolation (DNaseI, Roche, Mannheim, Germany) or in case of preparation of RNA for qRT-PCR done afterwards using TURBO DNA-free kit (Thermo Fisher Scientific).

2.2.8 cDNA synthesis

cDNA was synthesized in 10 µl reaction volume out of 1 µg RNA using M-MLV reverse transcriptase (Promega) according to the manufacturer's instructions.

2.2.9 Quantitative Real Time PCR (qRT-PCR)

cDNA was diluted 20-fold in water supplemented with 0.1 µg/µl tRNA from *E. coli* (Roche). PCR was performed in a LightCycler 96 (Roche) with LightCycler FastStart Essential DNA Green Master kit (Roche). For 20 µl reaction volume 10 µl master mix, 2 µl diluted cDNA and 1 mM oligonucleotids were used. For quantification gene expression was normalized to OEP24 cDNA fragment. Oligonucleotids are listed in Table 1. Quantities of expression were calculated using LightCycler 96 SW 1.1 (Roche).

2.3 Biochemical methods

2.3.1 In vitro transcription

Vectors including either a T7 or SP6 promoter sequence were used for in vitro transcription. Reaction was performed in a total volume of 50 µl containing 1 µg plasmid, 0.05 % BSA (BioLabs), 2 mM DTT (Promega), 0.25 mM m7G(5')ppp(5')G Cap analog (Ambion), 0.4 mM ACU (Roche), 50 U RiboLock RI (Thermo Fisher Scientific), 30 U RNA polymerase (Thermo Fisher Scientific) in transcription buffer (Thermo Fisher Scientific). After 15 min at 37 °C to

yield RNA with CAP structure 1.2 mM GTP is added and transcription is performed for 120 min at 37 °C. pF3A vector (Promega) requires no capping.

2.3.2 In vitro translation

For 50 µl in vitro translation reaction 10 µg of in vitro transcription product was used. 30 µCi ^{35}S methionine and cystein (Perkin Elmer, Walluf, Germany) were used to radiolabel the proteins in the presence of 80 µM amino acid mixture without methionine. The reaction was performed for 1 h using either 50 % wheat germ extract (Promega) with 50 mM KAc at 25 °C or 66 % reticulocyte lysate (Promega) with 70 mM KCl at 30 °C.

2.3.3 Overproduction of recombinant proteins

Transformed *E. coli* bacteria were grown in LB medium (1 % peptone from casein, 0.5 % yeast extract, 171 mM NaCl) at 37 °C to an OD_{600} of 0.6 - 0.8. Overproduction was induced by the addition of 1 mM isopropyl β-D-1-thiogalactopyranoside. *E. colis* strains and conditions for overproduction were depending on the construct and are listed in Table 4.

Table 4: Conditions for overproduction and way of purification of recombinant proteins

Construct	*E. coli* strain	Temperature	Time	Purification
dual targeting peptides	BL21 Lys	37 °C	4 h	inclusion bodies
STY8	BL21 Lys	16 °C	over night	soluble
OM64 TRP domain	RIPL	12 °C	over night	inclusion bodies
OM64 w/o TM	RIPL	18 °C	over night	soluble

2.3.4 Purification of soluble proteins

Pelleted bacteria from 1 l overproduction of constructs with His tag were resuspended in 25 ml lysis buffer (20 mM Tris pH 7.5, 200 mM NaCl, 20 mM imidazole, in case of OM64 w/o TM: PBS pH 7.3 (140 mM NaCl, 2.7 mM KCl, 10 mM Na_2HPO_4, 1.8 mM KH_2PO_4), 10 % glycerol, 20 mM imidazole). After cell disruption by a microfluidizer (Microfluidics, Westwood, USA) the solution was centrifuged at 20000 g, 4 °C for 30 min and the supernatant was rotated with 250 µl Ni Sepharose at 4 °C for 1 h. The beads were washed three times with 5 ml wash buffer (20 mM Tris pH 7.5, 200 mM NaCl, 40 mM imidazole, in case of OM64 w/o TM: PBS pH 7.3, 10 % glycerol, 40 mM imidazole). Recombinant proteins were eluted in 200 - 400 µl fractions with elution buffer (20 mM Tris pH 7.5, 200 mM NaCl, 200 mM imidazole, in case of OM64 w/o TM: PBS pH 7.3, 10 % glycerol, 200 mM imidazole).

2.3.5 Purification of proteins out of inclusion bodies

Unsoluble targeting peptides and TPR domains were purified out of inclusion bodies. Pelleted bacteria from 0.5 - 1 l overproduction were resuspended in 25 ml resuspend buffer (50 mM Tris pH 8.0, 200 mM NaCl, 5 mM β-mercaptoethanol). Cells were disrupted and centrifuged as described in 2.3.4. The pellet was washed one time with 20 ml detergent buffer (20 mM Tris pH 7.5, 200 mM NaCl, 1 % deoxycholic acid, 1 % nonidet P-40, 10 mM β-mercaptoethanol), two times with Triton buffer (20 mM Tris pH 7.5, 0.5 % Triton X-100, 5 mM β-mercaptoethanol) and two times with Tris buffer (20 mM Tris pH 8.0, 10 mM DTT). Centrifugation was done at 12000 g, 4 °C for 10 min. Finally the pellet was resuspended in 5 ml urea buffer (50 mM Tris pH 8.0, 100 mM NaCl, 7 M urea) and rotated for 1 h at room temperature. After centrifugation at 20000 g, room temperature for 15 min denaturated proteins were present in the supernatant.

2.3.6 Isolation of proteins from *A. thaliana*

A. thaliana leaves were homogenized in 300 µl homogenization medium (50 mM Tris pH 8.0, 10 mM EDTA, 2 mM EGTA, 10 mM DTT) using an electronic micropestle. The suspension was incubated for 10 min in the dark on ice then filtered and centrifuged at 9300 g, 4 °C for 10 min. Supernatant contained soluble proteins, pellet resuspended in homogenization medium contained membrane proteins.

2.3.7 Determination of protein concentration

Concentration of proteins was determined using Bradford reagent (0.1 % coomassie brilliant blue G-250, 5 % ethanol, 10 % phosphoric acid). 1 µl protein was mixed with 1:5 diluted Bradford reagent and absorption was measured against buffer at 595 nm.

2.3.8 Isothermal titration calorimetry (ITC)

Binding affinities of OM64 proteins to Hsp70 (CSGGAGPKIEEVD) and Hsp90 (CADAEGSKMEEVD) peptides (PSL, Heidelberg, Germany) were measured in cooperation with Ralf Heermann (Bioanalytic Core Facility, Ludwig-Maximilians-Universität München) by ITC using a MicroCal ITC200 (Malvern, Herrenberg, Germany). For control a chloroplast Hsp70 peptide (CESGPSESSGKEGPEGDVIDADFTDSK) having no TPR binding EEVD motif was used (PanaTecs, Heilbronn, Germany). Peptides were resuspended in OM64 elution buffer (PBS pH 7.3, 10 % glycerol, 200 mM imidazole, 2 mM DTT) and dialyzed against OM64 elution buffer using the Mini Dialysis Kit, 1 kDa cut-off (GE Healthcare) according to the manufacturer's instructions to removed TFA salts. 14 aliquots of 1 mM peptide were titrated in 150 sec intervals into a 30 - 50 µM solution of freshly purified OM64

protein at a temperature of 20 °C. After initial injection of 0.4 µl, peptide was injected in 3 µl aliquots to the protein until saturation was reached. Injection speed was 2 sec/µl with a string speed of 750 rpm. Onetime initial delay was 60 sec, reference power was set to 5 µcal/sec, feedback mode/gain was set to low. Binding curves were calculated with Origin7 MicroCal software (Northhampton, USA) using a 1:1 binding algorithm.

2.3.9 SDS polyacrylamide gel electrophoresis (SDS-PAGE)

Proteins were separated by SDS-PAGE using discontinuous gels according to (Laemmli, 1970) consisting of a stacking gel (5 % polyacrylamide) and a running gel (10 - 15 % polyacrylamide). Samples were loaded with SDS loading buffer (62.5 mM Tris pH 6.8, 2 % SDS, 10 % glycerol, 5 % β-mercaptoethanol, 0.004 % bromphenol blue). Gels were run in SDS running buffer (25 mM Tris, 192 mM glycine, 0.1 % SDS) and afterwards either stained with coomassie (45 % methanol, 9 % acetic acid, 0.2 % coomassie brilliant blue R-250) or used for western blotting (see 2.3.10).

2.3.10 Semi-dry electro blot and immunodetection of proteins

Proteins were electrotransferred out of an SDS gel onto a PVDF membrane using a semi-dry blotting apparatus. Blot was assembled as follows on the anode: three blotting papers in anode I buffer (20 % methanol, 300 mM Tris), two blotting papers in anode II buffer (20 % methanol, 25 mM Tris), activated membrane, gel, three blotting papers in cathode buffer (20 % methanol, 40 mM aminocapronic acid). Transfer was carried out for 1 h at 0.8 mA/cm^2, proteins on membrane were stained with ponceau solution (5 % acetic acid, 0.3 % ponceau S). For immunodetection of proteins membrane was blocked for 30 min with 5 % skimmed milk in TBST (20 mM Tris pH 7.6, 137 mM NaCl, 0.075 % Tween). Incubation with primary antibody was performed over night at 4 °C. After two times 15 min washing in TBST membrane was incubated for 1 h at room temperature with horse radish peroxidase conjugated secondary antibody. After three times 10 min washing in TBST membrane was incubated in equal volumes of development solution I (100 mM Tris pH 8.5, 1 % luminol, 0.44 % coomaric acid) and II (100 mM Tris pH 8.5, 0.018 % H_2O_2) and signal was detected with enhanced chemiluminescence using Image Quant LAS 400 (GE Healthcare).

2.3.11 Phosphorylation Assay

1,5 µg recombinant substrate protein was incubated with either 0.7 µl wheat germ lysate, 0.7 µl reticulocyte lysate or 1 µg recombinant kinase in the present of 13.5 µCi gamma ^{32}P-ATP (Hartmann Analytic, Braunschweig, Germany) in a total volume of 25 µl kinase buffer (20 mM Tris/HCl pH 7.5, 5 mM $MgCl_2$, 0.5 mM $MnCl_2$). The reaction was performed 15 min at room

temperature and stopped by the addition of 7.5 µl 4x SDS sample buffer. Proteins were separated by SDS-PAGE and phosphorylation signals were detected by phosphor plate imaging.

2.3.12 Detection of radiolabeled proteins

To visualize radiolabeled proteins dried SDS gels are exposed overnight to BAS-MS phosphor imaging plates (FUJIFILM) which are analyzed using a Typhoon scanner (GE healthcare).

2.3.13 Blue Native PAGE (BN-PAGE)

Solubilized samples (thylakoid membranes or mitochondria) were separated on native acrylamide gradient Bis-Tris gel (5 - 12 % polyacrylamide). Samples were loaded with BN loading buffer (750 mM aminocapronic acid, 5 % Serva-G 250), gel was run with cathode buffer (50 mM tricine, 15 mM Bis-Tris pH 7.0, 0.2 % Serva-G 250) and anode buffer (50 mM Bis-Tris pH 7.0). For second dimension one lane of the BN gel was placed on top of an SDS gel containing 4 M urea which was either silver stained to visualize proteins or used for western blot and immunodetection.

2.3.14 Silver staining of SDS gels

Gel was incubated for 1 h in fixation solution (50 % ethanol, 12 % acetic acid, 0.05 % formaldehyde) then washed three times for 30 min in 50 % ethanol. After 90 sec pre-impregnation in 0.02 % sodium thiosulfate and three times 30 sec washing in water impregnation of the gel was performed for 30 min in darkness using 0.2 % silver nitrate and 0.075 % formaldehyde. Gel was washed again in water then stained with development solution (6 % Na_2CO_3, 0.05 % formaldehyde, 0.0004 % sodium thiosulfate). After protein signals became visible reaction was stopped with stopping solution (50 % ethanol, 12 % acetic acid).

2.3.15 Co-Immunoprecipitation

To investigate binding of HCF136 mutants to 14-3-3 and binding of pFAD to chaperones 10 µl antiserum (14-3-3, Hsp70 or Hsp90) was coupled to the same amount of protein A sepharose. Coupling was performed in 400 µl PBS for 1 h rotating. After washing two times with PBS binding of wheat germ translated, ^{35}S labeled preprotein was performed for 30 min rotating at 4 °C. Beads were washed six times with PBS before transferring them on micro

spin column (BioRad, München, Germany). Proteins were eluted in SDS loading buffer and separated by SDS-PAGE and detected by phosphor plate imaging.

For mass spectrometric in vivo analyses of OM64 as well as for interaction studies between OM64 and the TOM complex the protein was enriched from isolated and solubilized mitochondria by immunoprecipitation using Pierce Co-IP Kit (Thermo Fisher Scientific).

2.3.16 Mass spectrometry

Mass spectrometric analyses were performed at the MSBioLMU core facility (Department Biology I, Ludwig-Maximilians-Universität München). Measurement of OM64 for identification of the phosphorylation site was done in cooperation with Heidi Pertl-Obermeyer (Department Biology I, Botany, Ludwig-Maximilians-Universität München).

2.3.17 Transformation of *A. tumefacium*

1 - 2 µg plasmid was added to GV3101 cells for stable transformation of *A. thaliana*. Cells were incubated 5 min on ice then 5 min in liquid nitrogen. Heat shock was performed for 5 min at 37 °C then 800 µl LB was added and cells were incubated shaking for 4 h at 28 °C before plated on LB plates with appropriate antibiotics. Cells were grown for 3 days at 28 °C.

2.4 Cell biological methods

2.4.1 Isolation of intact chloroplasts from *P. Sativum*

Approximately 200 g leaf material of 9 - 14 days old peas was mixed in isolation buffer (330 mM sorbitol, 20 mM MOPS, 13 mM Tris pH 7.6, 3 mM $MgCl_2$, 0.1 % BSA) filtered and centrifuged for 1 min at 1900 g, 4 °C. Intact chloroplasts were isolated out of the pellet via a discontinuous percoll gradient of 12 ml 40 % percoll solution (330 mM sorbitol, 50 mM HEPES pH 7.6, 40 % percoll) and 8 ml 80 % percoll solution (330 mM sorbitol, 50 mM HEPES pH 7.6, 80 % percoll) for 5 min at 8000 g, 4 °C and washed twice with washing buffer (330 mM sorbitol, 25 mM HEPES pH 7.6, 3 mM $MgCl_2$). The chlorophyll concentration was determined by measuring the optical density of 1 µl chloroplast solution in 1 ml 80 % acetone and calculated with the following formula:

mg chlorophyll / ml = 8.02 x (E663 - E750) + 20.2 x (E645 - E750)

2.4.2 Isolation of intact chloroplasts from *A. thaliana*

Approximately 50 g of 20 days old *A. thaliana* plants grown on plates with 1/2 MS medium (1 % sucrose, 0.05 % MES, 0.237 % MS salts, pH 5.7 with 1.2 % plant agar) were mixed

three times 2 sec in 25 ml isolation buffer (300 mM sorbitol, 5 mM $MgCl_2$, 5 mM EDTA, 20 mM HEPES pH 8.0, 10 mM $NaHCO_3$, 50 mM ascorbic acid) using a polytron mixer, filtering the solution between each mixing step. Lysate was centrifuged at 1500 g for 4 min, 4 °C using a swing-out rotor. Intact chloroplasts were isolated out of the pellet via a discontinuous percoll gradient of 7 ml 30 % percoll solution (162 mM sorbitol, 14.5 mM HEPES pH 8.0, 5.8 mM EDTA, 30 % percoll, 0.9 % PEG 6000, 0.3 % Ficoll, 0.3 % BSA) and 3 ml 82 % percoll solution (41 mM sorbitol, 4 mM HEPES pH 8.0, 1.5 mM EDTA, 40 % percoll, 2.6 % PEG 6000, 0.9 % Ficoll, 0.9 % BSA) for 5 min at 2000 g, 4 °C and washed with washing buffer (300 mM sorbitol, 0.5 mM $MgCl_2$, 50 mM HEPES pH 8.0). The chlorophyll concentration was determined as described above (2.4.2).

2.4.3 Isolation of intact mitochondria from *A. thaliana*

Approximately 100 g of 10 days old *A. thaliana* plants grown in liquid culture in 1/2 MS medium were pounded in a mortar in grinding buffer (0.3 M sucrose, 25 mM $Na_4P_2O_7$, 2 mM EDTA, 10 mM KH_2PO_4, 1 % PVP-40, 1 % BSA, 20 mM ascorbic acid, pH 7.5). Filtrated lysate was centrifuged for 5 min at 2500 g, 4 °C. Supernatant was centrifuged for 20 min at 17500 g, 4 °C. Pellet was washed in wash buffer (0.3 M sucrose, 10 mM TES, 0.07 % BSA, pH 7.5) and centrifuged for 5 min at 2500 g, 4 °C. Supernatant was again centrifuged for 20 min at 17500 g. Pellet was loaded on discontinuous percoll gradient consisting of 1.75 ml 60 % percoll solution, 2.5 ml 28 % percoll solution, and 2 ml 21 % percoll solution (all percoll solutions prepared with wash buffer) and centrifuged for 50 min at 26200 g, 4 °C. Mitochondria could be collected as a white band between 28 and 60 % percoll solution, were washed in wash buffer and centrifuged for 20 min at 20000 g, 4 °C. Pellet was resuspended in small volume of wash buffer and protein concentration was measured by Bradford assay.

2.4.4 Isolation of thylakoid membranes

Approximately 1 g leaf material of 21 days old *A. thaliana* plants grown on soil was mixed in 25 ml isolation medium (330 mM sorbitol, 50 mM HEPES pH 7.5, 2 mM EDTA, 1 mM $MgCl_2$, 5 mM ascorbic acid) using a polytron homogenizer. After filtration the homogenate was centrifuged at 760 g at 4 min, 4 °C. Pellet was resuspended in washing buffer (5 mM sorbitol, 50 mM HEPES pH 7.5) and centrifuged again. Pellet resuspended in TMK buffer (100 mM sorbitol, 50 mM HEPES pH 7.5, 5 mM $MgCl_2$) was incubated 10 min on ice, centrifuged and resuspended in a small volume of TMK buffer. Chlorophyll content was measured.

2.4.5 In vitro import into chloroplasts from *P. Sativum*

10 µg chlorophyll was used in a final reaction volume of 100 µl import buffer (330 mM sorbitol, 50 mM HEPES pH 7.6, 3 mM $MgCl_2$, 10 mM methionine, 10 mM cysteine, 0.2 % BSA, 3 mM ATP) together with 4 µl ^{35}S labeled, reticulocyte lysate translated preprotein. Import was performed for indicated times at 25 °C. Sample was loaded on 300 µl of 40 % percoll solution to reisolated intact chloroplasts by centrifugation at 4500 g, 5 min, 4 °C. Pellets were washed twice in 100 µl washing buffer (1100 g, 1 min, 4 °C) then resuspended in SDS loading buffer, heated for 3 min at 95 °C and loaded on SDS gel. Radioactive signals were detected by phosphor plate imaging.

2.4.6 In vitro import into chloroplasts from *A. thaliana*

10 µg chlorophyll was used in a final reaction volume of 100 µl import buffer (300 mM sorbitol, 50 mM HEPES pH 8.0, 3 mM $MgSO_2$, 50 mM ascorbic acid, 20 mM gluconate, 10 mM $NaHCO_3$, 0.2 % BSA, 4 mM $MgCl_2$, 10 mM methionine, 10 mM cysteine, 3 mM ATP) together with 4 µl ^{35}S labeled, reticulocyte lysate translated preprotein. Import was performed for indicated times at 25 °C. 100 µl wash buffer was added and samples were centrifuged at 1500 g for 1 min, 4 °C. Pellets were resuspended in SDS loading buffer, heated for 3 min at 95 °C and loaded on SDS gel. Radioactive signals were detected by phosphor plate imaging.

2.4.7 In vitro import into mitochondria from *A. thaliana*

50 µg mitochondria were used in a final reaction volume of 100 µl import buffer (0.3 M sucrose, 50 mM KCl, 10 mM MOPS, 5 mM KH_2PO_4, 0.1 % BSA, 1 mM $MgCl_2$, 1 mM methionine, 5 mM succinate, 5 mM DTT, 0.75 mM ATP, 0.2 mM ADP, pH 7.5) together with 4 µl ^{35}S labeled, reticulocyte lysate translated preprotein. Import was performed for indicated times at 350 rpm, 25 °C. For proteinase K digestion enzyme was added to a final concentration of 32 µg/ml and incubated 25 min on ice. 1 mM PMSF was used to quench the reaction. 100 µl wash buffer was added and samples were centrifuged at 16100 g for 5 min, 4 °C. Pellets were resuspended in SDS loading buffer, heated for 3 min at 95 °C and loaded on SDS gel. Radioactive signals were detected by phosphor plate imaging.

2.4.8 Solubilisation of mitochondria

For immunoprecipitation prior to mass spectrometry 200 µg, for BN-PAGE and Co-IP to detect interaction of OM64 with TOM complex 100 µg mitochondria were resuspended in 80 µl ACA buffer (750 mM aminocapronic acid, 50 mM Bis-Tris pH 7.0, 0.5 mM EDTA) and solubilized with digitonin (final concentration: 1 % for mass spectrometry, 0.5 % for BN-

PAGE and Co-IP) for 10 min on ice. After 10 min centrifugation at 13000 g, 4 °C supernatant was used for immunoprecipitation or loaded on a BN gel.

2.4.9 Solubilisation of thylakoid membranes

For analysis of photosynthetic protein complexes via BN-PAGE thylakoid membranes according to 30 µg chlorophyll were pelleted at 3300 g, 3 min, 4 °C, then solubilized in 70 µl ACA buffer with n-dodecyl β-D-maltoside (β-DM) (1.1 % final concentration) for 10 min on ice. After 10 min centrifugation at 18000g, 4 °C supernatant was loaded on BN-PAGE.

2.5 Plant biological methods

2.5.1 Plant growth conditions

Pea (*Pisum sativum*) was grown under long day conditions (14 h light / 10 h dark). *Arabidopsis thaliana* (ecotype Columbia and Wassilewskya) were either grown under long day conditions (16 h light / 8 h dark) or under greenhouse conditions.

2.5.2 Stable transformation of *A. thaliana* with *A. tumefacium*

400 ml LB medium was inoculated with preculture of transformed *A. tumefacium* strain GV3101 and grown over night. Cells were harvested by 20 min centrifugation at 1900 g, resuspended in Silwet medium (5 % sucrose, 0.05 % silwet L-77) and adjusted to OD_{600} of 0.8. Flowering *A. thaliana* plants were dipped for 5 sec in cell suspension. Seeds from transformed plants were selected on soil via resistance against BASTA.

2.5.3 Measurement of chlorophyll fluorescence

Chlorophyll a fluorescence of intact leaves was measured from plants after 10 min incubation in the dark using a pulse-modulated fluorimeter (Imaging PAM Mini or Microscopy, Walz, Effeltrich, Germany). The Fv/Fm ratio was determined which reflects the potential yield of the photochemical reaction.

3 Results

3.1 Phosphorylation of transit peptides of chloroplast targeted preproteins

Previously, it has been shown that transit peptides of chloroplast targeted preproteins can be phosphorylated within 14-3-3 binding motifs (Waegemann and Soll, 1996; May and Soll, 2000). The subsequent association of 14-3-3 proteins was shown to enhance import rates. Besides, dephosphorylation of the transit peptides prior to protein import was suggested to be required for efficient translocation (Waegemann and Soll, 1996; Lamberti et al., 2011a). To further investigate the role of the phosphorylation and dephosphorylation, especially regarding its relevance in vivo, the model preprotein pHCF136 was used for functional plant complementation studies.

3.1.1 In vitro characterization of pHCF136 phosphorylation

In a previous work it was shown that pHCF136 is phosphorylated in vitro within its transit peptide (Martin et al., 2006). The predicted transit peptide of HCF136 (amino acids 1 - 60) was fused to the mature sequence of SSU (mSSU) (Figure 3A) which is neither phosphorylated nor binds 14-3-3 (Fellerer et al., 2011; Lamberti et al., 2011b). The fusion construct was cloned into the pF3A vector to allow in vitro translation.

3.1.1.1 HCF136 transit peptide binds to 14-3-3

One typical 14-3-3 binding motif following the pattern [RHK][STALV].[ST].[PESRDIFTQ] was predicted in the transit peptide of HCF136 in position 33-38 (KASSSP) (Figure 3A). Phosphorylation is expected to occur within this binding motif. To investigate the role of the phosphorylation a phospho-mimicking construct (pHCF136 S35-37D) was created by side directed mutagenesis PCR. Besides, a construct that cannot be phosphorylated was produced (pHCF136 33-38A). To investigate 14-3-3 binding the different pHCF136-mSSU fusion constructs were in vitro translated in wheat germ lysate. This model cytosol contains endogenous 14-3-3 proteins. The translation product was co-immunoprecipitated with 14-3-3 antisera crosslinked to protein A sepharose. Uncoupled sepharose was used as a negative control. Indeed, pHCF136 WT was found to co-precipitate specifically with 14-3-3 (Figure 3B). Phospho-mimicry pHCF136 S35-37D does not interfere with 14-3-3 binding. Surprisingly, 14-3-3 binding was also not abolished by the phospho-deficient construct pHCF136 33-38A suggesting that an alternative binding site within the transit peptide can be used.

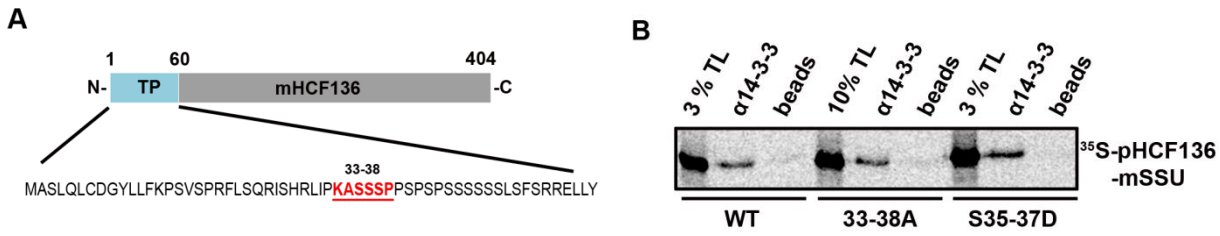

Figure 3: 14-3-3 binding of pHCF136. A) Position and sequence of the HCF136 transit peptide. The predicted 14-3-3 binding site (aa 33-38) is indicated. B) Co-immunoprecipitation of radiolabeled pHCF136 with 14-3-3 antisera. 3 % of the input (= translation product, TL) were loaded. Beads without coupled antisera were used as a negative control. Binding to 14-3-3 was observed for all three constructs pHCF136-mSSU WT, 33-38A and S35-37D. Figure taken from (Nickel et al., 2015).

3.1.1.2 Phospho-mimicry in the HCF136 transit peptide reduces import rate into isolated chloroplasts

To analyze the influence of the phosphorylation on the import behavior pHCF136 WT and the two mutated constructs pHCF136 S35-37D and pHCF136 33-38A were translated in reticulocyte lysate and imported in isolated pea chloroplasts for 5, 10 and 15 min. Successful import is made visible by a shift of the radiolabeled band to a lower molecular mass representing the mature protein after cleavage of transit peptide. pHCF136 33-38A imports to the same level as the WT construct, both showing efficient import already after 5 min (Figure 4). In contrast to that, phospho-mimicking construct pHCF136 S35-37D was not imported even after 15 min.

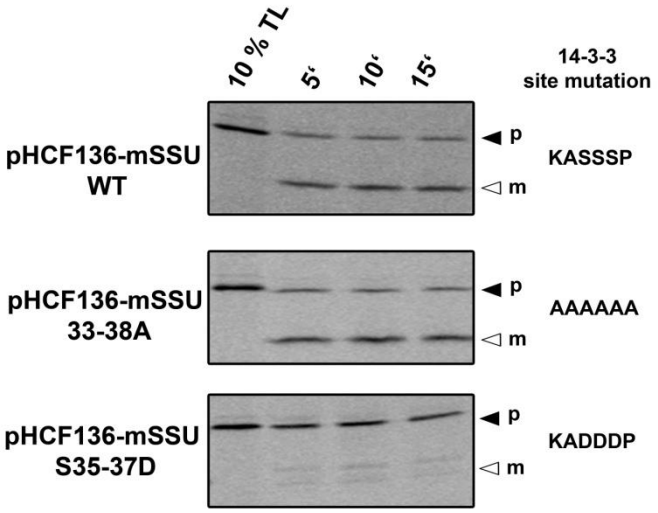

Figure 4: In vitro import of pHCF136 into isolated chloroplasts. Radiolabeled pHCF136-mSSU WT, 33-38A and S35-37D was imported into pea chloroplasts for the indicated time periods. 10 % of the translation product (TL) was loaded. The unprocessed preproteins (p) and the mature proteins (m) were detected. Comparable import efficiency was observed for pHCF136-mSSU WT and 33-38A, whereas almost no import could be detected for pHCF136-mSSU S35-37D. Figure taken from (Nickel et al., 2015).

3.1.2 In vivo characterization of pHCF136 phosphorylation

To investigate the consequences of impaired import in vivo the seedling lethal *hcf136* mutant was complemented with the three respective constructs. Complemented plants were used for functional analysis.

3.1.2.1 Complementation of *hcf136* with pHCF136 S35-37D results in growth defect and pale cotyledons

Since homozygous *hcf136* mutants are not fertile, heterozygous *hcf136* plants were transformed with *A. tumefaciens* carrying pHCF136 WT, pHCF136 33-38A and pHCF136 S35-37D, all under control of the 35S promoter. The progeny was screened for lines with a homozygous T-DNA insertion in the HCF136 gene and several independent lines were isolated for each construct. pHCF136 WT was fully able to complement the seedling lethal *hcf136* phenotype. The complementation with pHCF136 33-38A was likewise successful and the plants did not display any visible phenotype. Interestingly, plants complemented with pHCF136 S35-37D were heterogeneous in growth but all strikingly smaller compared to WT (Figure 5A). Besides, the plants have chlorotic cotyledons and in mature leaves a variegated phenotype was frequently observed. Homozygosity was confirmed by PCR (Figure 5B). To exclude that the phenotype was caused by insertion of the T-DNA at a random position in the genome two additional independent lines of pHCF136 S35-37D complementation (#8 and #22) were analyzed. Indeed, both displayed the same phenotype (Figure 6).

To monitor levels of HCF136 protein immunoblots with HCF136 specific antisera were performed with all complemented plant lines. To that end, cotyledons and leaves were distinguished, in case of *hcf136* S35-37D complementation also smaller and larger species. As expected, comparable amounts of HCF136 were found in cotyledons and leaves of WT and *hcf136* WT (Figure 5C). Regarding *hcf136* S35-37D, a reduction of HCF136 to less than 50 % of WT level was observed in leaves. The effect was slightly stronger in smaller plants compared to bigger species. The most pronounced reduction was observed in cotyledons where HCF136 was hardly detectable. Interestingly, in case of *hcf136* 33-38A complementation a slight increase in HCF136 levels compared to WT was observed in both, leaves and cotyledons. Levels of Cytf subunit of cytochrome b6f complex were unchanged in all samples and served as loading control.

To verify that the reduction in HCF136 levels was due to reduced import of the preprotein and not the result of a lower expression quantitative real time PCR was performed with the three complementation lines compared to WT (Figure 5D). Indeed, none of the transformants showed a reduction of the RNA level. Much more, due to 35S promoter expression levels of HCF136 were even increased 20-30 fold in *hcf136* WT, *hcf136* 33-38A as well as *hcf136* S35-37D all compared to WT.

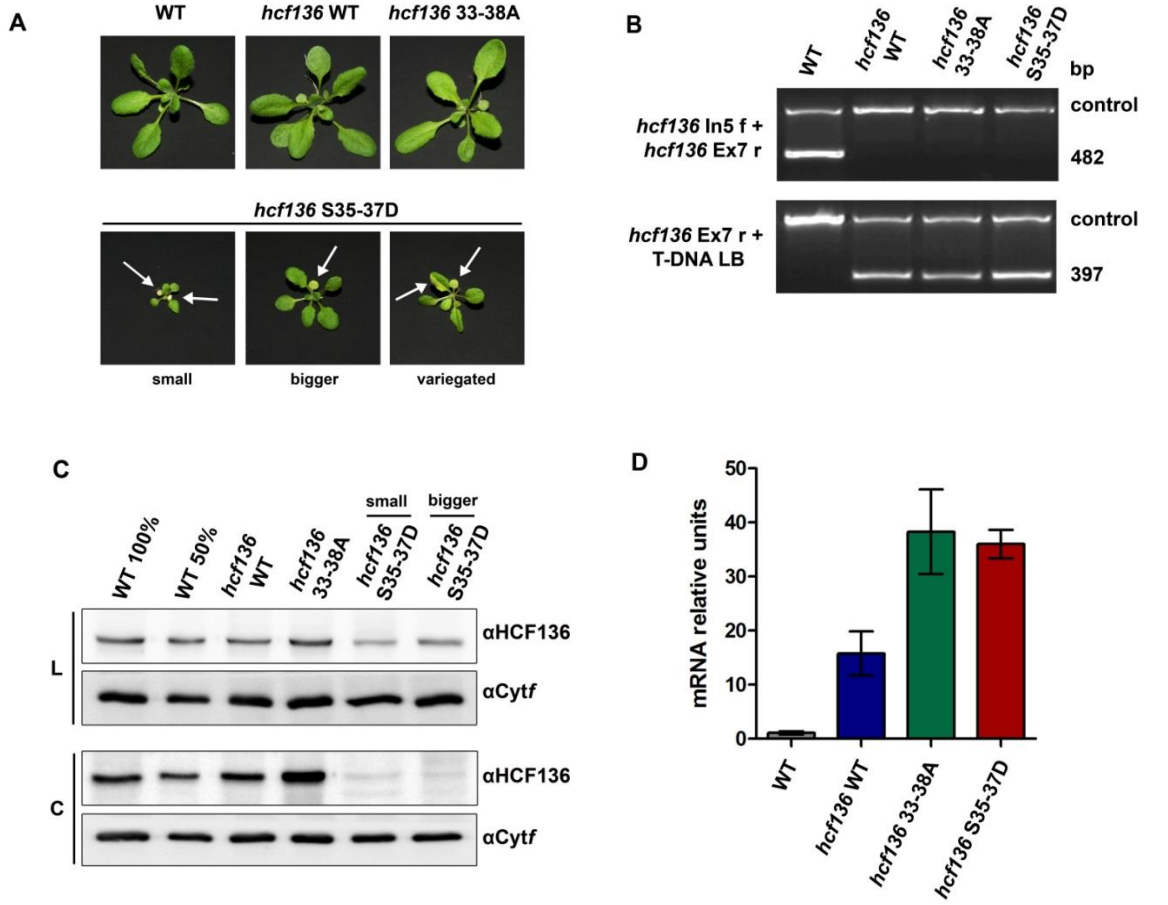

Figure 5: Complementation of the *hcf136* mutant. A) Phenotypes of 21 days old WT and mutant plants. Three examples of *hcf136* S35-37D are shown (small, bigger and variegated). Pale cotyledons and variegated leaves are indicated with arrows. B) Complemented *hcf136* mutant plants homozygous for the T-DNA insertion in the *hcf136* gene (*hcf136* WT, *hcf136* 33-38A and *hcf136* S35-37D) were identified by PCR. The three shown lines were used for further analyses. Oligonucleotides amplifying a fragment of OM64 were used as a control. C) Immunoblot analyses of complemented *hcf136* mutant plants. Leaves (L) and cotyledons (C) of WT, *hcf136* WT, *hcf136* 33-38A and *hcf136* S35-37D (smaller and bigger plants as shown in B)) were probed with antisera against HCF136 and Cyt*f* as loading control. Loading of 100 % corresponds to 10 µg protein. The same amount was loaded for the mutants. D) Quantification of expression levels of *HCF136* by quantitative real time RT-PCR HCF136 expression levels were normalized to OEP24 (n = 3 $\pm$ SD). Figure taken from (Nickel et al., 2015), modified.

3.1.2.2 Complementation of *hcf136* with pHCF136 S35-37D affects PSII function and assembly

Since HCF136 is a PSII assembly factor the functional analysis of the complemented lines focused on the in vivo impact on PSII. First, chlorophyll a fluorescence measurements were done to observe the photosynthetic performance of PSII. Here again leaves and cotyledons and in case of *hcf136* S35-37D smaller and bigger species were distinguished. The maximum quantum yield in *hcf136* WT and *hcf136* 33-38A was found to be comparable to WT at 0.78 - 0.8 in both, leaves and cotyledons (Figure 7A and B). Consistent with the

phenotype, a significant reduction of PSII yield was observed in *hcf136* S35-37D. In leaves and cotyledons of bigger plants PSII yield was reduced to 0.7 and 0.48, respectively, in smaller plants even to 0.63 in leaves and 0.42 in cotyledons. The two additional lines of pHCF136 S35-37D complementation (#8 and #22) showed the same reduction (Figure 7C).

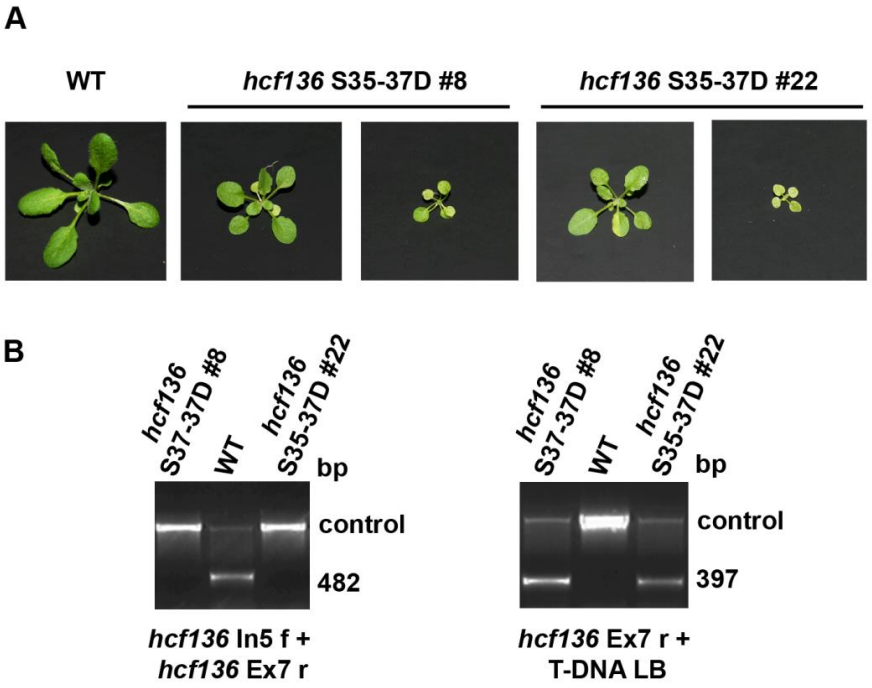

Figure 6: Analysis of *hcf136* S35-37D lines #8 and #22. A) The phenotype of two additional, independent *hcf136* S35-37D lines is shown. The same variation in size as well as pale cotyledons and variegated leaves were observed. B) Homozygocity for the T-DNA insertion in the *hcf136* gene was confirmed by PCR. Figure taken from (Nickel et al., 2015), modified.

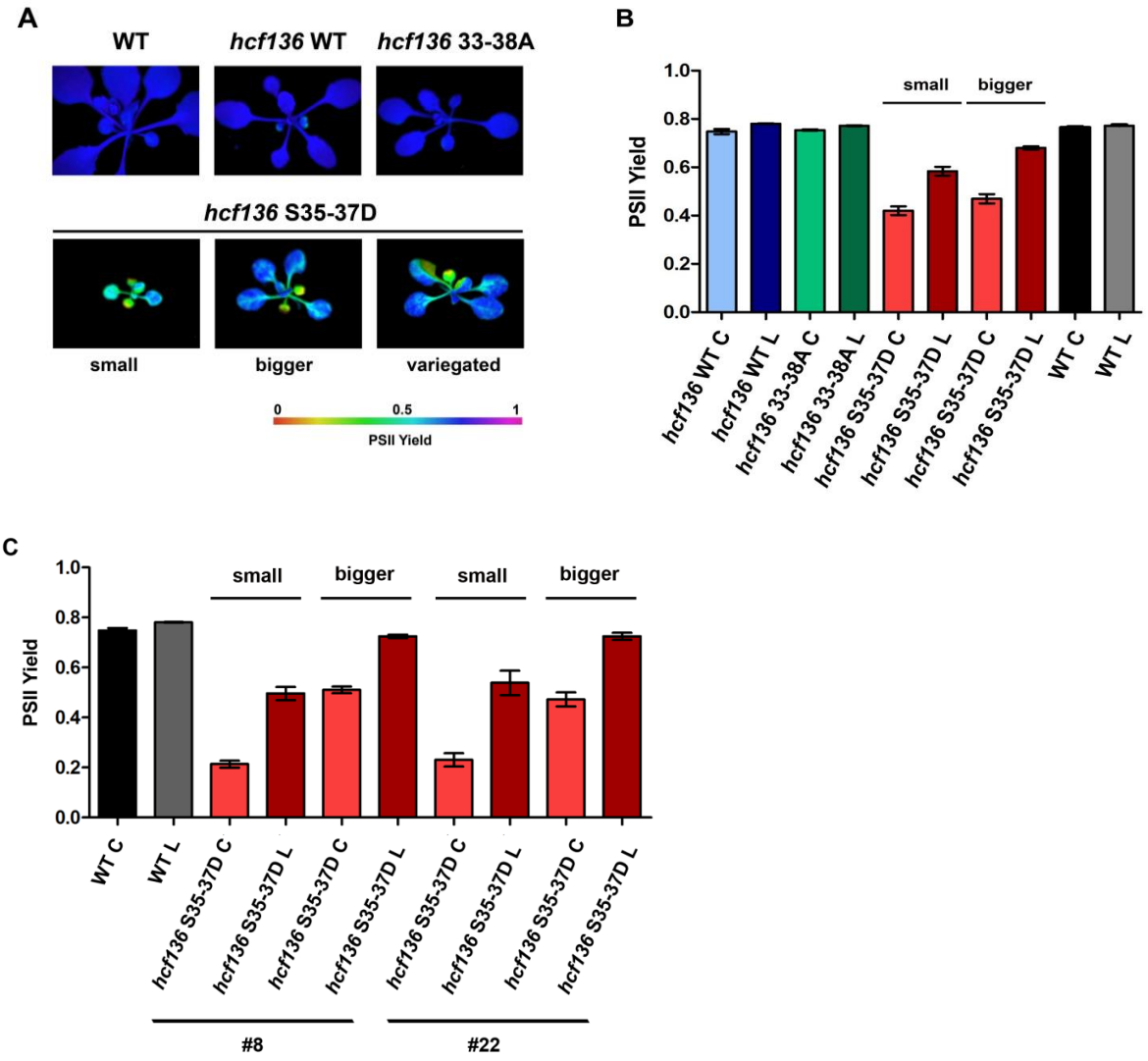

Figure 7: Photosynthetic performance is affected in complemented *hcf136* mutants. A) The PSII yield was monitored using an Imaging PAM system. A reduction in the PSII yield is visible in all three *hcf136* S35-37D species, especially in the cotyledons and in the variegated leaves. B) Quantification of PSII yield measurements as shown in A). L, leaves; C, cotyledons (n = 10 ± SD). C) PSII yield was measured for two additional *hcf136* S35-37D lines #8 and #22 in leaves (L) and cotyledons (C) (n = 10 ± SD). Figure taken from (Nickel et al., 2015), modified.

To further investigate whether the reduction in PSII yield is due to an impaired assembly of PSII, as it is reasonable regarding the function of HCF136, BN-PAGE analysis was performed. To that end, thylakoids were isolated from leaves as well as from cotyledons of WT and of complemented mutant lines. Solubilised thylakoids were separated in a first native dimension as well as in a second denaturing dimension. In *hcf136* WT and *hcf136* 33-38A PSII complexes were assembled comparatively to WT (Figure 8). Also in *hcf136* S35-37D leaves the PSII assembly was observed. In pale *hcf136* S35-37D cotyledons however, in both dimensions a clear reduction of PSII-LHCII supercomplexes, PSII dimer as well as PSII monomer and RC47 was observed. Besides, PSI was slightly reduced in this sample.

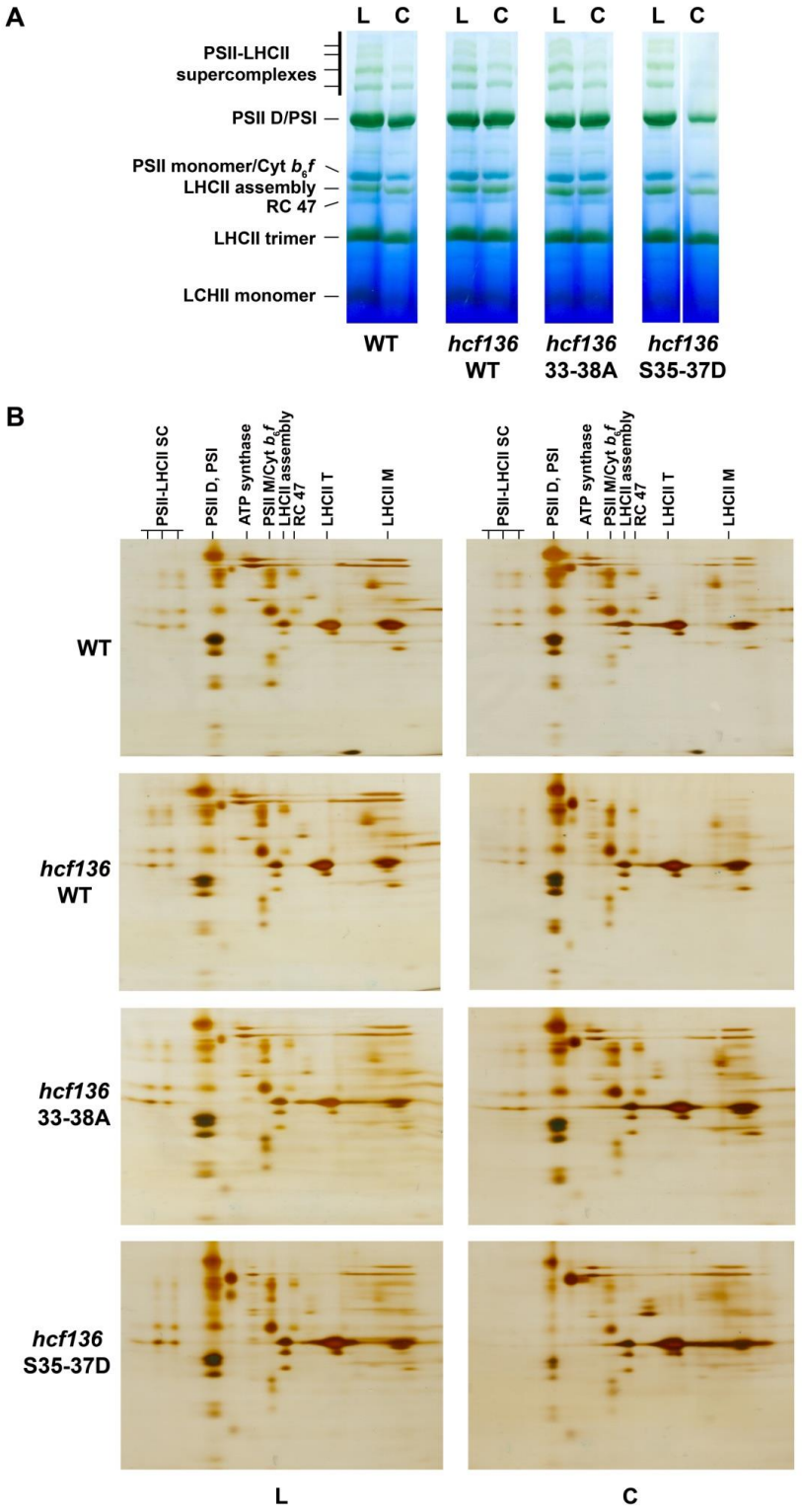

Figure 8: Assembly of photosynthetic complexes in complemented *hcf136* mutants. A) Thylakoids of WT, *hcf136* WT, *hcf136* 33-38A and *hcf136* S35-37D were isolated from leaves (L) and cotyledons (C) of 21 day old plants and solubilized photosynthetic complexes were separated by BN-PAGE in the first dimension. A reduction of PSII containing complexes is visible in *hcf136* S35-37D cotyledons. B) Thylakoid membrane complexes (from A)) were separated in a second dimension SDS-PAGE. *hcf136* S35-37D cotyledons are deficient of supercomplexes and PSII dimer, monomer as well as the RC47 are reduced. A slight reduction is also observed in the photosystem (PS)I. Figure taken from (Nickel et al., 2015).

To investigate protein levels of PSII components, immunoblot analyses were performed using antisera against D1 and CP47 (Figure 9). These two proteins were found to be reduced in *hcf136* S35-37D, especially in cotyledons. In leaves a more pronounced effect in smaller plants was observed. The PSI subunit PsaF accumulated to normal levels in *hcf136* S35-37D leaves but was slightly diminished in *hcf136* S35-37D cotyledons. In *hcf136* WT and *hcf136* 33-38A all three protein levels were found to be comparable to WT in both, leaves and cotyledons. Cytf of Cty b6f complex was unchanged in all samples and served as loading control.

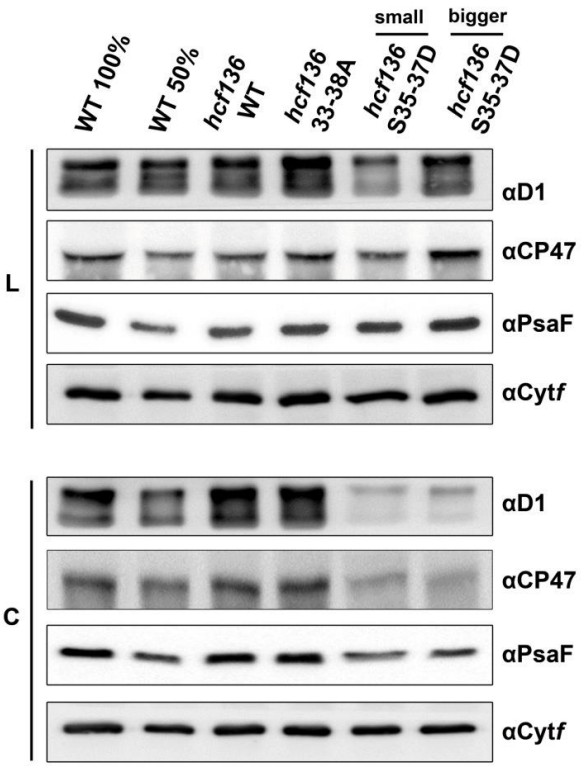

Figure 9: Accumulation of thylakoid membrane proteins in complemented *hcf136* mutants. Membrane proteins of WT, *hcf136* WT, *hcf136* 33-38A and *hcf136* S35-37D were isolated from leaves (L) and cotyledons (C) and probed with antisera against D1, CP47, Cyt*f* and PsaF. PSII subunits D1 and CP47 were clearly reduced in *hcf136* S35-37D cotyledons. Loading of 100 % corresponds to 10 µg protein. The same amount was loaded for the mutants. Figure taken from (Nickel et al., 2015).

3.2 Potential preprotein phosphatase

Recently, *Arabidopsis* purple acid phosphatase 2 (PAP2) was shown to interact with the presequence of a phosphorylated mitochondrial targeted preprotein (Law et al., 2015). PAP2 (At1g13900) is a tail-anchored protein located in the outer membrane of mitochondria and chloroplasts, exposing its enzymatic domain into the cytosol (Sun et al., 2012b). Besides, there exists the closely related protein PAP9 (At2g02450) which shows 72 % sequence

identity to PAP2. To investigate whether this phosphatase is involved in protein import, isolated chloroplast of *pap2* knockout plants were analyzed concerning their ability to import wheat germ lysate translated precursor proteins. Seeds were provided by Boon Leong Lim, University of Hong Kong, China. Two distinct preproteins which previously have been shown to be phosphorylated were tested, pSSU and pHCF136. Both showed no difference comparing mutant to WT in the linear range of the first 5 min of import (Figure 10A). To ensure that the preprotein is indeed present in a phosphorylated state, next, the translation product was incubated with STY8 kinase which is responsible for preprotein phosphorylation immediately before import reaction was performed. Again, chloroplasts of *pap2* do not shown a delayed import compared to WT chloroplasts (Figure 10B). Finally, a double-knockout of *PAP2* and *PAP9* was analyzed to consider the possibility that PAP9 functionally replaces PAP2. However, no difference in import behavior between WT and *pap2xpap9* could be observed, also not between pSSU which can be phosphorylated and phospho-deficient pSSU S31/34A (Figure 10C).

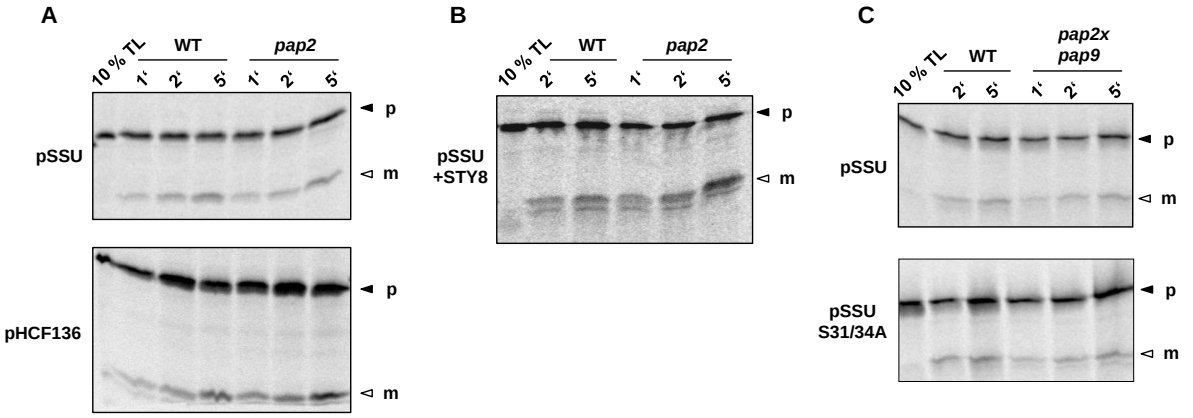

Figure 10: In vitro import of phosphorylated preproteins into isolated chloroplast from *A. thaliana* WT, *pap2* mutant (A, B) and *pap2xpap9* double mutant plants (C). Radiolabeled pSSU, pSSU S31/34A and pHCF136 was imported for the indicated time points, in case of (B) pSSU translation product was treated with STY8 kinase prior to import. 10 % of the input (translation product = TL) was loaded. Unprocessed preproteins (p) and imported mature proteins (m) were detected. Equal import efficiency between WT and mutant plants was observed under all conditions.

Previously, it was shown that mutant plants of STY kinases responsible for preprotein phosphorylation display an impaired greening process (Lamberti et al., 2011b). For mutants of the phosphatase a changed behavior in greening might be likely as well. Following, the greening process of single and double knock-out plants was investigated in comparison to WT plants. Etiolated plants were placed in the light and opening of the cotyledons was observed (Figure 11A). Weak differences can be seen six and eight hours after illumination.

However, *pap2* and *pap2xpap9* plants are not impaired but start opening the cotyledons slightly before WT plants. 25 hours after illumination the cotyledons of *pap2* and *pap2xpap9* plants are still slightly more open than the ones of WT plants. Furthermore, analysis of the photosynthetic performance indicates only weak differences between WT and mutant as well. The maximum quantum PSII yield of *pap2* and *pap2xpap9* plants four hours after illumination was found to be slightly higher than the one of WT plants (~ 0.35 compared to 0.25 after four hours) but still in the range of standard deviation (Figure 11B). At later time points PSII yield is comparable between WT and mutant plants. This indicates that PAP2 phosphatase activity is not required for chloroplast biogenesis during the greening process. Taken together, these results suggest that PAP2 is not involved in the import of phosphorylated chloroplast preproteins.

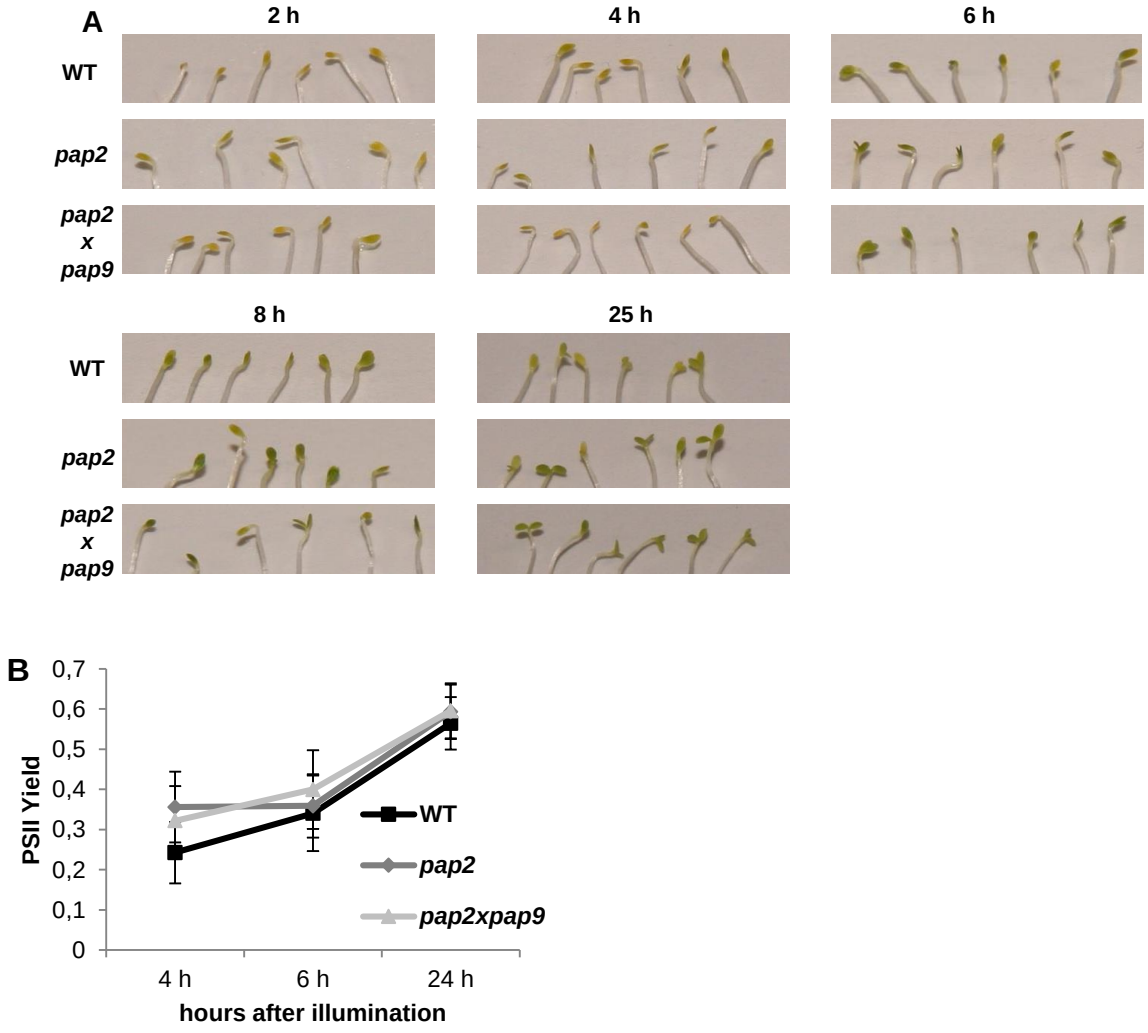

Figure 11: Greening assay of etiolated *pap2* and *pap2xpap9* plants in comparison to WT plants. A) Six representative seedlings are shown 2, 4, 6, 8 and 25 h after illumination. B) PSII yield was measured at indicated time points (n = 10 ± SD).

3.3 Phosphorylation of targeting peptide of dual targeted preproteins

During dual import a single preprotein with an ambiguous targeting signal is a substrate for import machineries of both organelles, mitochondria and chloroplasts. Since preproteins targeted to chloroplasts can be phosphorylated within their transit peptide, phosphorylation might also be involved in dual import.

The predicted targeting peptides of 17 dual targeted proteins (Carrie and Small, 2013) were cloned into pGEX6p1 vector to allow overproduction of peptides fused to an N-terminal GST tag. GST tag was chosen to enlarge the small sized (3 - 13 kDa) targeting peptides by approximately 25 kDa and in an attempt to make the highly hydrophobic peptides soluble. Nonetheless, the overproduction in a soluble form was not possible. Thus, proteins were purified out of inclusion bodies and solubilized in urea buffer. They were used in an in vitro kinase assay together with either wheat germ lysate, reticulocyte lysate or purified STY8 kinase. 7 out of 17 peptides showed phosphorylation in wheat germ lysate (Figure 12A). 4 out of these 7 peptides showed phosphorylation in reticulocyte lysate as well. Figure 12B shows peptides which are not phosphorylated in wheat germ lysate. One single peptide (At5g16200) displayed phosphorylation in reticulocyte lysate only and not in wheat germ lysate. Interestingly, this is one of the two peptides which were phosphorylated by STY8 kinase (Figure 12C). The other one (At4g33760) showed phosphorylation under all three conditions. pSSU which is known to be phosphorylated within the transit peptide was used as a positive control for STY8. Besides, STY8 displayed autophosphorylation, as described previously (Lamberti et al., 2011b). Finally, one targeting peptide (At2g04842) was used in a higher purified form, which was a kind gift from Erika Spånning, Stockholm University, Sweden (Berglund et al., 2009). After isolation out of inclusion bodies this peptide was cleaved from GST tag by CNBr. The peptide (aa 2 - 60) was precipitated and purified by ion affinity chromatography. Interestingly, this peptide showed a much stronger phosphorylation in both wheat germ and reticuloyte lysate compared to the same peptide in urea buffer (Figure 12D). An overview of the phosphorylation status of all tested targeting peptides under the three conditions can be seen in Table 5. Concluding from this screen ambiguous targeting peptides of dual targeted proteins can be phosphorylated but phosphorylation is no general phenomenon found in every dual targeted protein.

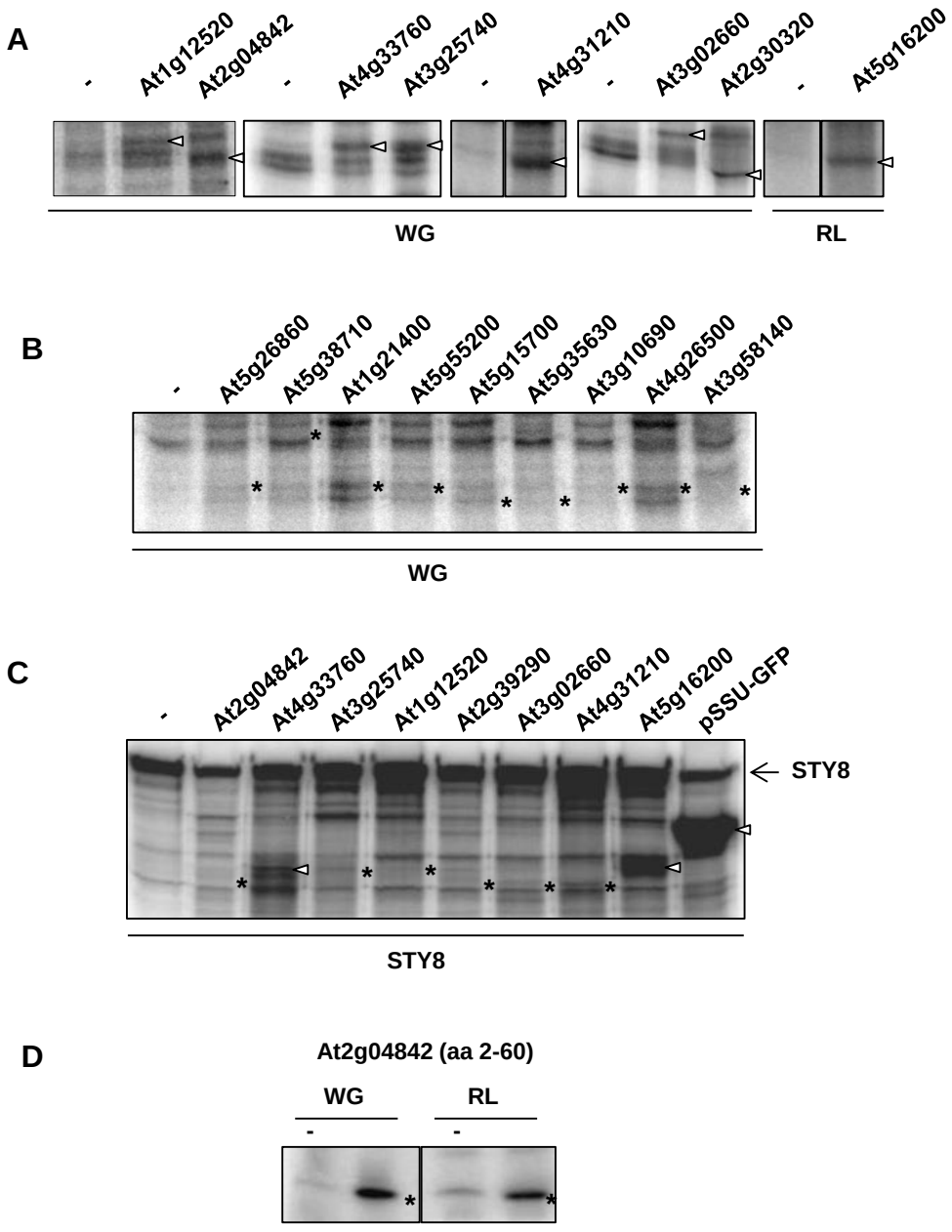

Figure 12: In vitro phosphorylation assay of dual targeting peptides. Peptides were radiolabeld by incubation with ^{32}P-ATP in the presence of either wheat germ lysate (WG), reticulocyte lysate (RL) or purified STY8 kinase. Autoradiographs are shown, positions of phosphorylated peptides are marked with an arrow head, positions of unphosphorylated peptides with an asterisk, - labels negative controls without peptide. A) Peptides showing phosphorylation using WG or RL. B) Peptides showing no phosphorylation using WG. C) Two out of eight peptides show phosphorylation using STY8 kinase. D) Further purification of peptide increases phosphorylation signal.

Table 5: Summary of phosphorylation status of all analyzed dual targeting peptides.

Accession number	Phosphorylation in wheat germ lysate	Phosphorylation in reticulocyte lysate	Phosphorylation by STY8 kinase
At1g12520	yes	no	no
At1g21400	no	no	N/A
At2g04842	yes	yes	no
At2g30320	yes	yes	N/A
At2g39290	no	N/A	no
At3g02660	yes	no	no
At3g10690	no	no	N/A
At3g25740	yes	yes	no
At3g58140	no	no	N/A
At4g26500	no	no	N/A
At4g31210	yes	no	no
At4g33760	yes	yes	yes
At5g15700	no	no	N/A
At5g16200	no	yes	yes
At5g26860	no	no	N/A
At5g38710	no	no	N/A
At5g55200	no	no	N/A

3.4 Phosphorylation of mitochondrial translocon docking protein

The overall subunit composition of the translocase of the outer mitochondrial membrane (TOM complex) from fungi, animals and plants is remarkably similar. Yet, in contrast to yeast and mammals plants lack a homolog of the mitochondrial receptor protein Tom70. However, plants possess the 64 kDa protein OM64 which is anchored in the outer mitochondrial membrane and phylogenetically related to chloroplast Toc64. Previously, OM64 was shown to be involved in mitochondrial protein import (Lister et al., 2007). A direct interaction between OM64 and the TOM complex however could not be shown yet (Lister et al., 2007).

3.4.1 OM64 is part of the TOM complex

OM64 is a low abundant protein predominantly expressed in roots (see expression profile in the appendix, Figure 21) (Aronsson et al., 2007). This aggravates in vivo detection of interactions. Following, in this study plants expressing OM64 under the control of a 35S promoter were generated (see below). From these plants mitochondria were isolated, solubilized with digitonin (0.5 % final concentration) and used for co-migration studies. On a

second dimension SDS gel following BN-PAGE OM64 can be detected in a complex with TOM subunits. A distinct spot of OM64 overlays with Tom40 and Tom20 (Figure 13A, marked by an arrow). Other parts of OM64 run in the previously reported lower molecular weight range (Lister et al., 2007). Additionally, OM64 can be detected in the higher molecular weight range around 669 kDa, which might be due to overexpression but interestingly overlay with Tom40 as well. To confirm the result of the co-migration study and see if indeed an interaction between OM64 and the TOM complex takes place co-immunoprecipitation with mitochondria solubilized as described above was performed. Co-IP using amino-reactive beads coupled to OM64 antiserum showed a specific interaction between OM64 and Tom40 as well as Tom20 (Figure 13B). For negative control beads were coupled to preimmune serum.

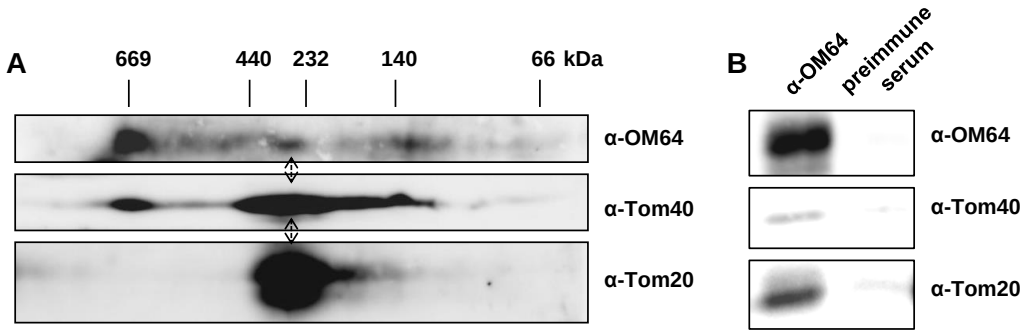

Figure 13: OM64 can be found in a complex with Tom40 and Tom20. A) BN-PAGE with second denaturating dimension of digitonin solubilized mitochondria. Immunoblot was performed using antisera against OM64, Tom40 and Tom20. Position of TOM complex is marked with an arrow. B) Co-IP of digitonin solubilized mitochondria. OM64 antiserum was coupled to the beads, preimmune serum was used as a negative control. Eluates were probed in an immunoblot with antisera against OM64, Tom40 and Tom20.

3.4.2 OM64 is phosphorylated within the TPR domain at position S568

Intriguingly, OM64 was found to be phosphorylated within its TPR domain. To ascertain the exact phosphorylation site, the TPR domain was cloned into pGEX6p1 vector to allow overproduction fused to an N-terminal GST tag. Subsequently all possible phosphorylation sites were exchanged into alanine residues. Since only small amounts of the hydrophobic TPR domain was found in the soluble fraction after overproduction, inclusion bodies were isolated and used for in vitro phosphorylation assays. Indeed, by subsequent analysis of the individual mutated proteins a single residue within the TPR domain was found to be phosphorylated: serine 568. The phosphorylation site was confirmed by using OM64 lacking the N-terminal transmembrane domain (OM64 w/o TM) which was cloned into pET21a vector

and could be purified in a soluble form by Ni^{2+} affinity purification (Figure 14B). Furthermore, S568 seems to be the only or at least the prevalent phosphorylation site in the cytosolic exposed domain of OM64. A schematic overview of the different OM64 constructs used in this work can be seen in Figure 14A. Interestingly, the serine residue representing the phosphorylation sites is conserved among dicotyledonous plant species (Figure 14C, for alignment of full-length protein see appendix, Figure 23). Compared to Toc64 however, which displays 67 % sequence identity within the TPR domain, the serine residue is not conserved (for alignment see appendix, Figure 24). Consistently, Toc64 TPR domain was found not to be phosphorylated (unpublished data, workgroup Soll). To confirm the phosphorylation site of OM64 in vivo mass spectrometry analysis is currently performed in cooperation with Heidi Pertl-Obermeyer (Department Biology I, Botany, Ludwig-Maximilians-Universität München). To this end, mitochondria from OM64 overexpression plants are isolated, solubilized with digitonin (1 % final concentration) and immunoprecipitated using amino-reactive beads coupled to OM64 antiserum. The eulate is digested with Lys-C protease and a phospho-peptide enrichment is performed prior to mass spectrometry.

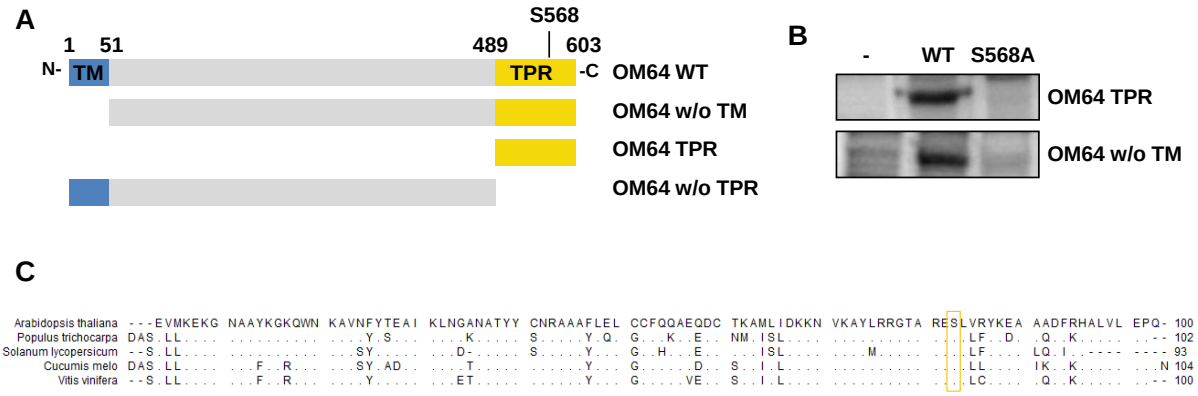

Figure 14: OM64 is phosphorylated at conserved residue S568 within the TPR domain. A) Scheme of different OM64 proteins used in this work. Phosphorylation site is marked. TM, transmembrane domain. B) Phosphorylation assay using either only the TPR domain of OM64 or OM64 w/o TM. Proteins present in WT form and in phospho-deficient S568A mutation were incubated with ^{32}P-ATP and reticulocyte lysate. Autoradiographs are shown. For negative control elution buffer instead of protein was used. C) Alignment of OM64 TPR domain shows the conservation of the phosphorylated serine residue in several dicotyledonous plant species.

3.4.3 Functional complementation of *Arabidopsis om64xtom20* mutants with different OM64 constructs

To investigate the role of the phosphorylation site in vivo, a complementation of *Arabidopsis* lacking OM64 was performed using different forms of OM64: OM64 WT (S568), phospho-

deficient OM64 S568A, phospho-mimicking OM64 S568D or S568E and OM64 without the TPR domain (OM64 w/o TPR). The chaperone binding TPR domain is most likely the functional part of OM64 for protein import. Previously, it was shown that the knockout of *om64* in combination with the knockout of all three relevant *tom20* isoforms is embryolethal (Duncan et al., 2013). Since an *om64* mutation alone does not have a growth phenotype (Aronsson et al., 2007), *om64xtom20* quadruple mutant was used as a background for the complementation to see which constructs of OM64 are able to abolish embryolethality. To this end, all constructs of OM64 were cloned into the binary vector pB7FWG2 and *om64xtom20* mutants were transformed using Agrobacteria. All constructs carried a stop codon at the end to prohibit expression of vector encoded GFP. Successful complementation was confirmed by monitoring the expression of OM64 protein. For that membrane proteins were isolated from leaf material and used for immunoblot analysis. 15 µg protein from the complemented plant lines were used and compared to 30 µg proteins from Col-0 (due to low expression). A clear overexpression due to the constitutive active 35S promoter can be detected (Figure 15A). The constantly appearing faint band (marked with an asterisk) is most likely an OM64 degradation product. It also appears when analyzing overproduced and purified OM64 protein on a coomassie stained SDS gel and was identified by mass spectrometry as OM64. *35S::OM64 WT* plants were used for interaction studies with the TOM complex seen in Figure 13 (3.4.1).

Since combined *om64* and *tom20* knockout is lethal, these plants are heterozygous for the main isoform of *Tom20*, *Tom20-2*. If the complementation with OM64 is successful, plants being homozygous for *tom20-2* should be present in the progeny, as it is the case for plants having a *tom20* triple knockout. gDNA was isolated and PCR was performed using one primer pair specific for *Tom20-2* WT and one primer pair including the left boarder of the T-DNA insertion. However, screening in total over 1000 plants up to the second generation after transformation no plant homozygous for *tom20-2* knockout was found, not even for complementation with *35S::OM64 WT* (Figure 15C). Probably, the 35S promoter which is present in the used pB7FWG2 vector is not properly active during embryogenesis which is why embryolethality cannot be prevented.

Therefore, in a second approach the complementation was done under control of the endogeneous OM64 promoter (*OM64::OM64*). To this end, genomic *OM64* including the promoter and terminator was cloned into pBGW and as before *om64xtom20* mutants were transformed with the four constructs using Agrobacteria. Indeed, already in F0 generation (out of seeds from transformed *Arabidopsis*) plants being homozygous for *tom 20-2* could be detected for *OM64::OM64 WT*, *OM64::OM64 S568A* and *OM64::OM64 S568E* (Figure 15D). For these plants as well, immunoblot analysis confirms the expression of OM64 (Figure 15B). Transformants carrying *OM64::OM64 w/o TPR* are still in the process of selection. Up to now

only four plants are available. With these the expression of the protein could already be confirmed (Figure 15B). For convincing genotyping however, a far larger number is required.

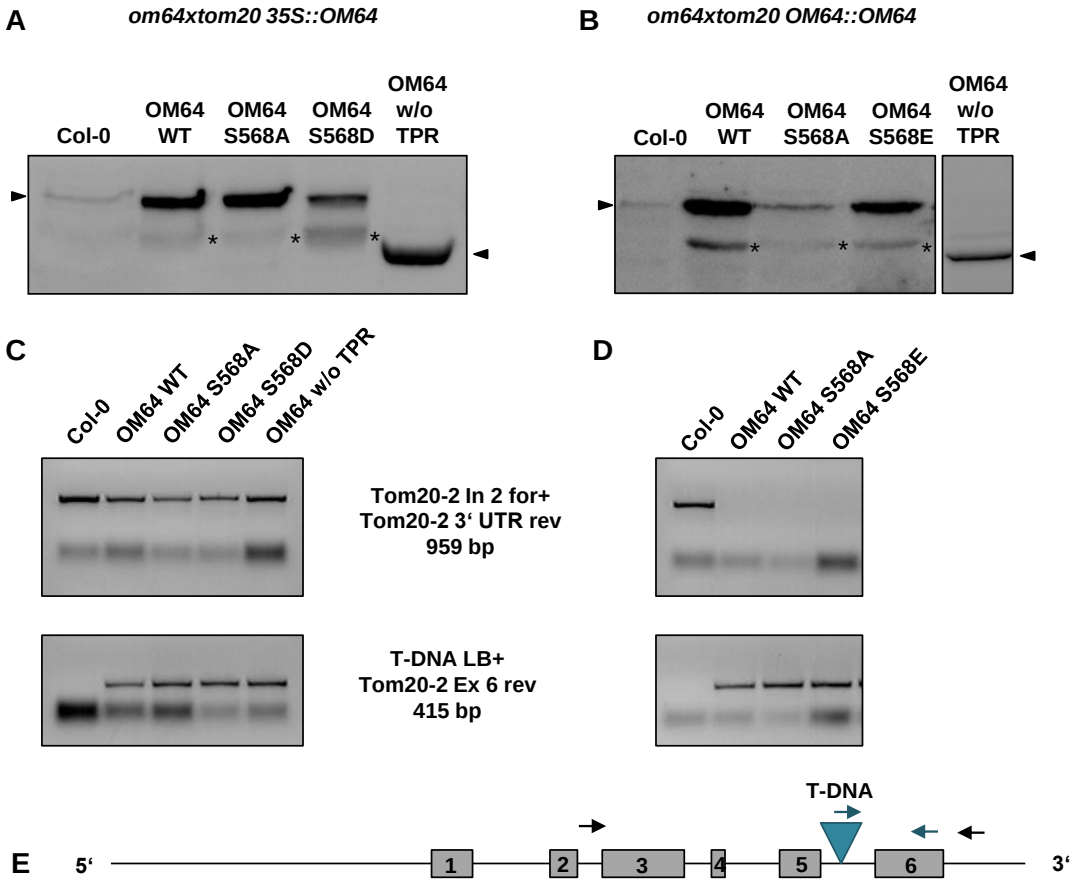

Figure 15: Complementation of *om64xtom20* mutants. Immunoblot analyses of complemented *om64xtom20* mutants with different *OM64* constructs under control of either 35S promoter (A) or endogenous promoter (B) confirm the expression of OM64. Membrane proteins were isolated from leaf material. 15 µg proteins from complemented plant lines *om64xtom20 35S::OM64* and 30 µg proteins from *om64xtom20 OM64::OM64* as well as from Col-0 were probed with antisera against OM64. Arrow head marks the correct sized protein, asterisk a degradation product. PCR with gDNA shows that complemented *om64xtom20* plants expressing OM64 under control of 35S promoter (C) stay heterozygous for *tom20-2* (as the original *om64xtom20* plants) while plants expressing OM64 under the control of its endogenous promoter (D) can be homozygous for T-DNA insertion in the *Tom20-2* gene. E) Schematic position of primers (black arrows for *Tom20-2* WT gene, blue arrows for T-DNA construct) on *Tom20-2* gDNA, exons marked with boxes, position of T-DNA with blue triangle.

3.4.4 Phosphorylation of OM64 is involved in mitochondrial protein import

Even though *om64* plants do not show a growth phenotype they have an impaired mitochondrial protein import. The import rate of the preprotein pFAD is 30 to 40 % lower in plants lacking OM64 meaning that FAD import at least partly depends on OM64 (Lister et al., 2007). To investigate the effect of the phosphorylation site of OM64 in this study pFAD was imported into mitochondria isolated from complemented plants. For this experiment plants resulting from the transformation of *om64xtom20* mutants with *35S::OM64* represent the

ideal tool since they still express Tom 20-2. *tom20-3 tom20-4* double knockout plants expressing Tom20-2 barely show any defects in growth and protein import (Lister et al., 2007). Consequently, in this study any detectable effects are due to the changed OM64. Radiolabeled pFAD was imported into mitochondria isolated from the four complemented plant lines for 5, 10 and 20 min (Figure 16A). Digestion with proteinase K at the latest time point (20' + PK) clearly shows the band of the protected mature protein. Indeed, in phospho-mimicking OM64 S568D plants pFAD is only imported to 30 to 40 % of OM64 WT levels. Interestingly, phospho-deficient OM64 S568A plants import pFAD almost like OM64 WT. OM64 w/o TPR plants show the same reduced import rate as OM64 S568D plants. For quantification mature FAD at each time point was normalized either to OM64 WT at 20 min (Figure 16B) to visualize the increase of the import over time or to OM64 WT at the same time point (Figure 16C) to better compare the amount of imported protein at each time point. The drastic reduction in import that could be observed shows that phosphorylation of OM64 is involved in import and suggests a negative regulatory effect on protein import. Furthermore, the crucial role of the TPR domain for the function of OM64 in FAD protein import can be seen.

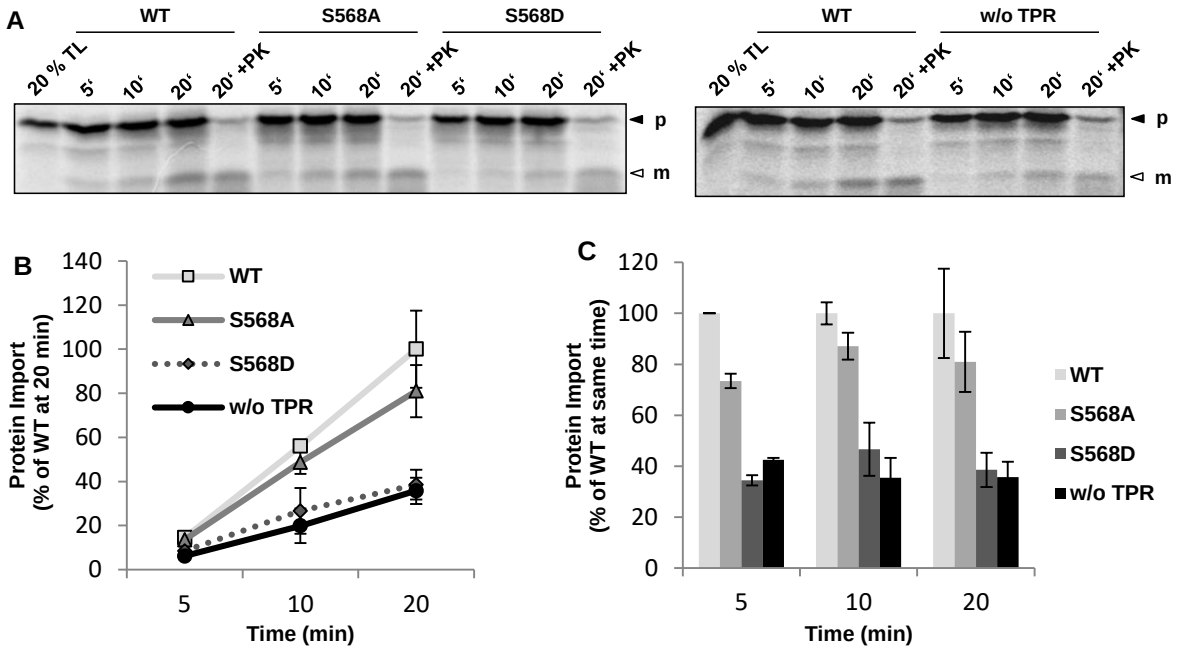

Figure 16: In vitro import into isolated mitochondria from complemented *om64xtom20* mutants. A) Radiolabeled FAD was imported for indicated time points into mitochondria of OM64 WT, OM64 S568A, OM64 S568D and OM64 w/o TPR domain, all heterozygous for Tom20-2. 20 % of the input (translation product = TL) was loaded. Autoradiographs are shown. Unprocessed preproteins (p) and imported mature proteins (m) were detected, proteinase K digestion of attached preproteins is marked with +PK. B, C) Quantification of import efficiency. Mature proteins were quantitated at each time point and normalized to OM64 WT either at 20 min (B) or at the same time point (C). Corresponding OM64 WT was set to 100 % (n ≥ 3 ± SD). OM64 S568A shows comparable import efficiency to OM64 WT while the efficiency of OM64 S568D and OM64 w/o TPR is reduced to less than 40 %.

Since preproteins can bind via an associated chaperone to the TPR domain of a docking protein a Co-IP was performed to investigate which chaperones bind to FAD. To this end, FAD was radiolabeled by in vitro translation in wheat germ lysate and incubated with sepharose A beads linked to antisera against either Hsp70 or Hsp90 (Figure 17). An interaction with both chaperones can be detected, though the one with Hsp70 is stronger.

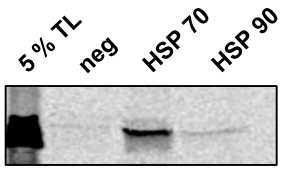

Figure 17: Chaperone binding of pFAD. Co-immunoprecipitation of radiolabeled pFAD with antisera against Hsp70 and Hsp90. 5 % of the input (TL) was loaded. Autoradiograph is shown. Beads without coupled antisera were used as a negative control. Strong binding of pFAD was observed in case of Hsp70, weak binding in case of Hsp90.

3.4.5 Phosphorylation of OM64 regulates the binding of Hsp90

In the next step the effect of the phosphorylation of OM64 on chaperone binding was investigated. To this end, OM64 w/o TM WT, S568A and S568E cloned in pET21a were overproduced in *E. coli* and purified as soluble proteins. For phospho-mimicry OM64 S568E was chosen since OM64 S568D could not be overproduced efficiently. Using isothermal titration calorimetry (ITC) at the Bioanalytic Core Facility, Ludwig-Maximilians-Universität München binding affinities of OM64 proteins to C-terminal Hsp70 (C-SGGAGPKIEEVD) and Hsp90 (C-ADAEGSKMEEVD) peptides were quantified. N-terminal cystein was added to the dodecapeptide for an initial attempt to use surface plasmon resonance for quantification. However, coupling of the peptides to the chip surface was not successful. To prevent building of disulfide bridges between the peptides due to the cystein residue, 2 mM DTT was added to OM64 elution buffer which was also used for resuspension of the peptides. For ITC the ligand (chaperone) is titrated to the protein (OM64) until saturation is reached. The small changes in energy occurring due to the binding event are measured and used to calculated K_d values for the interaction. Raw data (above) and fitted binding curve (below) of one representative experiment for interaction between OM64 and Hsp90 can be seen in Figure 18, thermodynamical parameters obtained for this measurement in Table 6. Binding affinities were calculated as a mean of two to three experiments (Table 7).

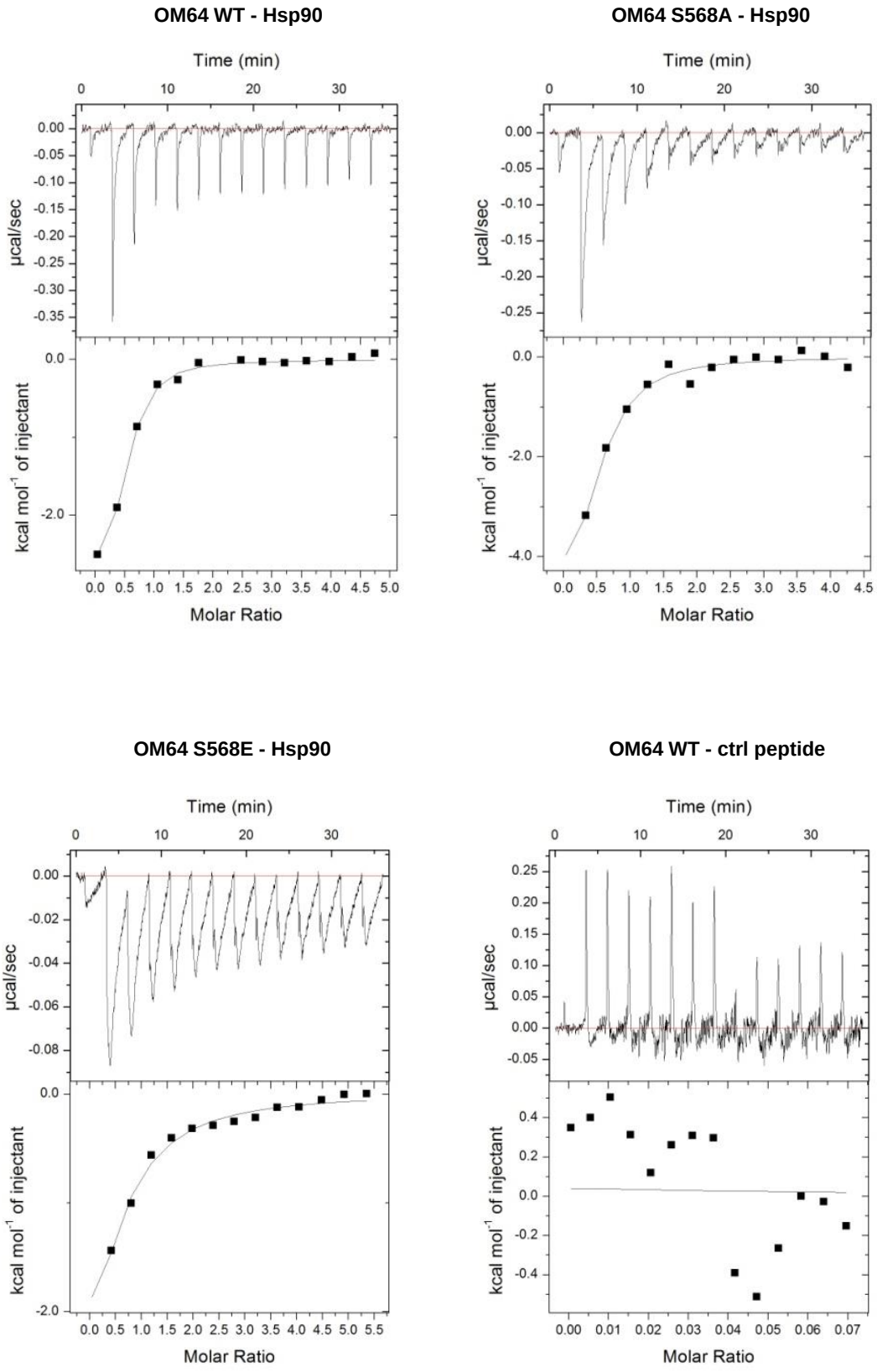

Figure 18: Binding of different OM64 variants to Hsp90 peptide analyzed with ITC. Hsp90 peptide was titrated to OM64 proteins. Obtained raw data (above) and fitted binding curve using a 1:1 binding ratio together with measured thermodynamical parameters (below) can be seen. As a control a chloroplast Hsp70 peptide was used showing no binding to OM64 WT (on the right).

Table 6: Obtained thermodynamical parameters for ITC measurements seen in Figure 18. N is the stoichiometry; Chi^2 divided by the degrees of freedom is the quality of fit of the binding curve; ΔH is the change in enthalpy; ΔS is the change in entropy.

Thermodynamical parameter	OM64 WT - Hsp90	OM64 S568A - Hsp90	OM64 S568E - Hsp90
N	0.408 ± 0.0236	0.446 ± 0.117	0.331 ± 0.299
Chi2/DoF	2351	22380	3007
ΔH [cal/mol]	-3379 ± 235.6	-6107 ± 1945	-7308 ± 7080
ΔS [cal/mol/deg]	12.5	1.84	-4.61

Table 7: Affinities of different OM64 variants to Hsp90 peptide. Mean of 2-3 measurements ± SD.

OM64 variant	K_d [µM]
WT	10±3
S568A	15±6
S568E	39±3

Each spike of the raw data represents one injection of the peptide to the protein and the resulting temperature change which is measured. All three reactions of the different OM64 variants and Hsp90 are exothermic that is favorable as can be seen by the downwards pointing peaks as well as by the negative changes in enthalpy (ΔH, Table 6). However, the change in entropy (ΔS) only shows positive (meaning favorable) values for OM64 WT and S568A, while the binding of OM64 S568E to Hsp90 is described by a thermodynamically unfavorable loss of entropy. The binding curve is calculated by the integration of the peak area and fitting to a 1:1 binding model which is expected for the interaction of a TPR domain with a chaperone. Already regarding the run of the curve a reduced affinity of OM64 S568E to Hsp90 can be seen. The slope is clearly reduced compared to OM64 WT and saturation is reached later. This trend as well as the different changes in entropy are reflected in the K_d values. The affinity of OM64 WT to Hsp90 is described by a K_d value of 10 µM. The K_d value of phospho-deficient OM64 S568A lies in the range of OM64 WT (15 µM) while the affinity of phospho-mimicking OM64 S568E to Hsp90 is fourfold reduced (39 µM). Chi^2 represents the quality of fit of the binding curve. The increased value in case of OM64 S568A compared to WT and S568E reflects the outlier of the measured values seen in the binding curve. The stoichiometry described by N with values around 0.4 indicates that approximately only 40 % of OM64 protein is in a conformational state able to bind the ligand. For a 1:1 binding which can be expected for the interaction between OM64 and heat shock proteins an ideal N value of 1 would show that 100 % of the protein is able to bind the ligand. The reduced values

measured in this case can be explained by the fact that OM64 protein is prone to aggregation. This reduces the amount of protein available for an interaction. As a control a chloroplast Hsp70 peptide was titrated to OM64 WT, showing no binding as expected (Figure 18 right). Unfortunately, no binding could be detected for OM64 with Hsp70 peptide. To exclude any binding problems due to the chosen peptide the experiment was repeated with overproduced full length Hsp70 protein, however binding could not be detected as well. Summarizing, phospho-mimicry of OM64 reduces the affinity to the chaperone Hsp90 as can be seen by fourfold increased K_d value (OM64 WT 10 µM compared to OM64 S568E 39 µM).

4 Discussion

4.1 Phosphorylation of transit peptides of chloroplast targeted preproteins

Many chloroplast proteins are nucleus encoded, synthesized in the cytosol and are posttranslationally imported into the chloroplasts. For correct targeting the proteins are synthesized as preproteins, equipped with a mostly N-terminal transit peptide. Protein import into chloroplasts can involve phosphorylation of the preprotein (Waegemann and Soll, 1996). Preproteins can be phosphorylated within the 14-3-3 binding site and the subsequent association of 14-3-3 enhances import rates presumably by enhancing the affinity to the TOC complex (May and Soll, 2000). Besides, it was shown that dephosphorylation of the transit peptide at the organellar surface prior to the actual import is crucial for efficient translocation (Waegemann and Soll, 1996; Lamberti et al., 2011a). Previous studies have been mainly performed in vitro; therefore in this work relevance of the phosphorylation in vivo should be investigated. To this end the phosphorylated preprotein pHCF136 (Martin et al., 2006) was used for functional plant complementation studies.

4.1.1 14-3-3 binds to an alternative binding site within HCF136 transit peptide

The transit peptide of HCF136 (amino acids 1 - 60) was fused to the mature sequence of SSU. The predicted 14-3-3 binding site in position 33-38 (KASSSP, pHCF136 WT) was mutated on the one hand to a phospho-mimicking construct (KADDDP, pHCF136 S35-37D), on the other hand to a phospho-deficient mutant (AAAAAA, pHCF136 33-38A). The three constructs were tested in a co-immunoprecipitation regarding their ability to bind 14-3-3. Surprisingly, not only pHCF136 WT and pHCF136 S35-37D were found to co-precipitate specifically with 14-3-3 but also phospho-deficient pHCF136 33-38A still bound 14-3-3. Since the transit peptides were fused to the mature sequence of SSU which was shown not to bind 14-3-3 (Fellerer et al., 2011) this result suggests that 14-3-3 binds to an alternative phosphorylated binding site within the HCF136 transit peptide. Indeed, two amino acid regions (KPSVSP 14-19 and PSPSP 39-43) can be found which are similar to the predicted binding motif [RHK][STALV].[ST].[PESRDIFTQ], merely displaying an alternative amino acid in the first position. Likewise, in the transit peptide of the model protein SSU 14-3-3 was previously observed to bind to a slightly unusual motif (May and Soll, 2000). Due to the presence of multiple serine residues in the transit peptide of pHCF136 the determination of the exact phosphorylation site or sites was not feasible. Regarding the result of the co-immunoprecipitation, pHCF136 33-38A cannot be taken as an entirely non-phosphorylated construct but rather as an internal control for random amino acid substitution.

4.1.2 Dephosphorylation of HCF136 transit peptide is required for import into chloroplasts in vitro

In an in vitro import assay the three constructs of HCF136 transit peptides were compared concerning their capability to target and successfully import the fused SSU protein into chloroplasts. Both pHCF136 WT and pHCF136 33-38A showed efficient import already after 5 min meaning that a random mutation within the amino acids 33-38 does not affect the import competence per se. Interestingly, phospho-mimicking construct pHCF136 S35-37D was not imported even after 15 min. A similar effect was observed previously for in vitro import as well as for fluorescence localization studies in *A. thaliana* protoplasts using a phospho-mimicry mutant of pSSU (Lamberti et al., 2011a). Moreover it has been shown that addition of unspecific phosphatase inhibitor NaF prohibits import of phosphorylated preproteins (Waegemann and Soll, 1996). Besides, the introduction of a thiophosphate group at the transit peptide which is dephosphorylated significantly slower than a phosphate group hinders import as well (Waegemann and Soll, 1996). Therefore, dephosphorylation of preproteins by an yet unidentified phosphatase is an obligatory prerequisite prior to translocation through the membrane and seems to be a common feature in chloroplast preprotein import.

4.1.3 Dephosphorylation of HCF136 transit peptide plays a role in import into chloroplasts in vivo

Seedling lethal *hcf136* mutants were complemented with the three previously used constructs of the gene: pHCF136 WT, pHCF136 33-38A and phospho-mimicking pHCF136 S35-37D. All three complementations gave rise to fertile plants but only pHCF136 WT and pHCF136 33-38A could fully restore the wild type phenotype. In case of *hcf136* S35-37D plants were heterogeneous in growth but all smaller compared to WT. Besides, the plants had strikingly chlorotic cotyledons and often variegated parts in mature leaves. Immunoblot analyses confirmed an expected reduction of HCF136 proteins level in *hcf136* S35-37D which is even more pronounced in the cotyledons. Since qRT-PCR revealed the presence of pHCF136 S35-37D RNA the reduced protein level can only be due to an impaired protein import.

HCF136 is a chaperone-like PSII assembly factor which associates with an early PSII precomplex. It is conserved from cyanobacteria to higher plants. HCF136 catalyzes the interaction of D2 and cytochrom b559 which together form the reaction center precomplex (Plücken et al., 2002). The following assembly of D1 gives rise to the reaction center to which further subunits like coupling protein 47 and 43 are subsequently added. In the absence of HCF136, D1 is synthesized but no functional reaction center complex can be assembled, therefore D1 is degraded (Plücken et al., 2002). Due to the physiological role of HCF136, the

complemented *hcf136* mutant lines in this work have been investigated regarding PSII function and assembly. As expected, measurement of the PSII yield of intact plants shows a functional impairment of PSII in *hcf136* S35-37D again especially in the cotyledons. Besides, BN-PAGE using thylakoid membranes clearly showed an impairment of PSII assembly in *hcf136* S35-37D cotyledons. All PSII assembly forms from early RC47 up to late PSII-LHCII supercomplexes were reduced. Even more, immunoblot analyses showed a reduction of PSII subunits D1 and CP47 which was also observed in *hcf136* mutant plants where no PSII assembly can take place (Plücken et al., 2002). The fact that BN-PAGE and immunoblot analyses show a reduction of PSI as well as PSI subunit PsaF in *hcf136* S35-37D cotyledons correlates with the observation that PSI is affected in *hcf136* mutant under normal light conditions (Plücken et al., 2002). However, under low light the specific effect of HCF136 on PSII becomes evident (Plücken et al., 2002).

Summarizing the results of this study, it can be suggested that (de-)phosphorylation of pHCF136 prior to import into chloroplasts might also play a role in vivo. Phospho-mimicking pHCF136 S35-37D can obviously not be dephosphorylated and therefore its translocation into chloroplasts is highly impaired. The fact that no or at least less functional HCF136 is reaching the thylakoids is visualized in vivo by impairment of PSII in assembly and function. Interestingly, these experiments always show clear differences comparing cotyledons and mature leaves in *hcf136* S35-37D plants. It seems that in vivo import of pHCF136 S35-37D in cotyledons is almost completely abolished whereas in the mature leaves pHCF136 S35-37D can be imported to some extent. This suggests that preprotein phosphorylation and especially dephosphorylation plays a role in the early developmental stages where many proteins are needed for chloroplast biogenesis. Similarly, plants lacking the three STY kinases which are responsible for transit peptide phosphorylation show an impaired chloroplast differentiation (Lamberti et al., 2011b). The occurrence of differently sized *hcf136* S35-37D plants and variegated leaves might indicate that a certain threshold level of mature HCF136 is needed for normal chloroplast biogenesis. Due to external or internal slightly varying conditions in the cell, import might be further reduced in some areas of the leaf and thus lead to the variegated phenotype containing chloroplasts lacking functional PSII. For *hcf136* 33-38A mutant plants a slight increase in HCF136 levels compared to WT was observed in immunoblot analyses. Since in case of pHCF136 33-38A no additional dephosphorylation at the predicted 14-3-3 binding site is necessary while the import enhancing 14-3-3 is nonetheless bound, this preprotein is imported with a higher efficiency and therefore accumulate to higher levels within the complemented plants.

Taken together, this study presents a first in vivo investigation of the potential impact of chloroplast preprotein dephosphorylation. The data support previous results and confirm the known model, suggesting that preprotein phosphorylation is used especially during early

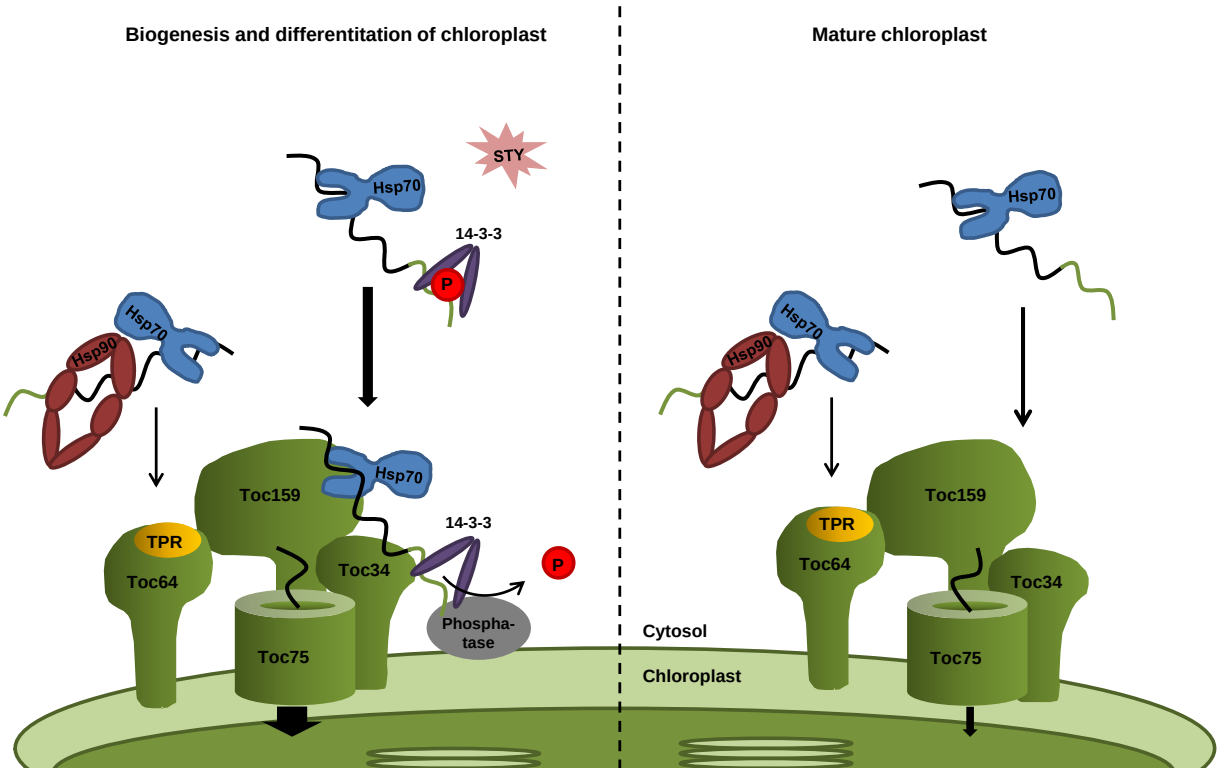

Figure 19: Regulatory effect of preprotein phosphorylation and dephosphorylation on preprotein import rates into chloroplasts. Chloroplast preproteins can be bound by Hsp70 alone, by Hsp70 and Hsp90 which enables interaction with Toc64 or by Hsp70 and 14-3-3 (guidance complex) which targets the preprotein to the receptor proteins Toc34 and Toc159. During early development of chloroplasts many nucleus encoded proteins are required for example for the formation of the photosystems. Import rates are increased by preprotein phosphorylation leading to the formation of the guidance complex together with a high expression of preprotein phosphatase enabling the translocation. In mature chloroplasts a lower number of proteins is needed. Therefore, phosphorylation might be reduced and expression of phosphatase downregulated.

developmental stages and besides as a tissue specific tool to regulate preprotein import efficiency. During posttranslational import into chloroplasts preproteins are thought to be first bound by Hsp70 directly after translation in the cytosol. They can be escorted to the TOC complex like this or they can be bound by further chaperones. Either preproteins are targeted together with Hsp90 to the TPR domain containing docking protein Toc64. Or transit peptides can be phosphorylated and subsequently bound by 14-3-3. This Hsp70 and 14-3-3 containing guidance complex enhances binding to the receptor proteins Toc34 and Toc159 and increases translocation rate three- to fourfold. During etiolation and differentiation of the plastids an increased number of nucleus encoded proteins is required to be imported into the chloroplasts. Following, the import rate is increased by phosphorylation of the preproteins and formation of the guidance complex (Figure 19). Prior to translocation the preprotein has to be dephosphorylated. In mature chloroplasts an elevated preprotein import is not necessary, following phosphorylation might not play a prominent role in adult parts of the

plant. Probably, also the phosphatase is less abundant in mature chloroplasts. The still pending identification of the phosphatase will give new insides into this topic. The question remains why plants first equip their urgent preproteins with a phosphate group to enhance their import rate but then hinders the translocation by adding the mandatory step of dephosphorylation. Most likely, it represents a second layer of regulation and enables the plant to fine-tune the import rates. They can either be increased by phosphorylation together with a high expression of the phosphatase or decreased by a downregulation of STY kinases and the phoshatase. Like this, plants can best adapt to different developmental and environmental conditions.

4.2 Potential preprotein phosphatase

The kinases responsible for phosphorylation of chloroplast preproteins (STY kinases) are already characterized (Lamberti et al., 2011b). The phosphatase however, remains yet to be identified. Recently, *Arabidopsis* PAP2 dually targeted to mitochondria and chloroplasts was shown to interact with the presequence of a phosphorylated mitochondrial targeted preprotein and might potentially be involved in mitochondrial import (Law et al., 2015). Since PAP2 is also present in chloroplasts it was analyzed for its involvement in chloroplast protein import.

Purple acid phosphatases (PAPs) represent a large group of unspecific phosphatases found in plants, mammals and fungi that catalyze the hydrolysis of activated phosphoric acid esters and anhydrides at a pH range from 4 to 7 (Schenk et al., 2000). Plant PAPs are structurally divers proteins playing a role in growth and development under both normal and stress conditions (Zhu et al., 2005). Since the expression of several PAPs is induced by phosphate starvation stress they are thought to function in phosphate metabolism (Haran et al., 2000; Li et al., 2002; Bozzo et al., 2004; Zimmermann et al., 2004). Besides, they might play a role in flower development (Kim and Gynheung, 1996; Zhu et al., 2005), in metabolism of reactive oxygen species during senescence (Del Pozo et al., 1999) and in carbon metabolism (Sun et al., 2012b). Biochemical in vitro assays show a broad range of substrates, high activity can be found among other on ATP, ADP, GTP, dATP, polyphosphate and phosphoenolpyruvate (Cashikar et al., 1997; Bozzo et al., 2004; Zhu et al., 2005). The ability to dephosphorylate phosphoproteins however, does not seems to be a general characteristic of plant PAPs. A tomato PAP has been found active on phosphotyrosine but hardly on phosphoserine and -threonine (Bozzo et al., 2004). One *Arabidopsis* PAP (PAP23) showed high activity on phosphoserine, low activity on phosphothreonine and no activity on phosphotyrosine (Zhu et al., 2005). A PAP from red kidney bean was found not to be active on phosphotyrosine and -threonine at all (Cashikar et al., 1997).

In *Arabidopsis* 29 PAPs exist which can be grouped into eight subgroups (Li et al., 2002). One subgroup, consisting of PAP2 (At1g13900) and PAP9 (At2g02450), is characterized by a plant-specific C-terminal transmembrane domain (Sun et al., 2012b). The two proteins share 72 % sequence similarity. PAP2 was shown to be dually targeted to mitochondria and chloroplasts via the transmembrane domain and C-terminally anchored in the outer membrane, exposing its enzymatic domain into the cytosol (Sun et al., 2012a). To investigate if PAP2 acts as a preprotein phosphatase during protein import chloroplasts of *pap2* knockout mutant were isolated and an in vitro import with phosphorylated preproteins was performed. However, no difference between WT and *pap2* could be observed. Even the *pap2xpap9* double-knockout mutant can still efficiently import preproteins into isolated chloroplast. Concluding from these results, PAP2 is not involved in preprotein dephosphorylation. Furthermore, PAP2 was never shown to be able to dephosphorylate phosphoproteins but is thought to function in the modulation of carbon metabolism (Sun et al., 2012b). Overexpression of PAP2 leads to higher levels of sucrose, hexose sugars and several TCA metabolites and to an increased activity of the metabolic enzyme sucrose phosphate synthase (Sun et al., 2012b). Besides, *pap2* and *pap2xpap9* plants do not show a phenotype apart from a slightly shorter hypocotyl (Sun et al., 2012b). Even during etiolation which was investigated within this work *pap2* and *pap2xpap9* plants are not impaired. On the contrary, they rather seem to open their cotyledons slightly before WT plants. Though, this might be due to variations within the WT seeds since measured PSII yield values of *pap2* and *pap2xpap9* plants strikingly resemble values for WT plants under the same condition reported before (e.g. ~0.35 at 4 hours after illumination (Lamberti et al., 2011b)). During early plant development and differentiation of the plastids many proteins are required within the chloroplast. Therefore, etiolation visualizes the regulatory effect of phosphorylation of preproteins on import kinetics. In the case of *sty8 sty17 sty46* mutants no preprotein phosphorylation can occur (Lamberti et al., 2011b). Hence, an impaired greening process compared to WT plants can be observed because the import enhancing effect of the phosphorylation is missing. If the phosphatase is lacking a similar effect might be likely. Though preproteins are phosphorylated and following bind faster to the TOC complex, in the end they are not imported as fast as proteins in WT plants because the phosphate group cannot be removed. It could be speculated that due to permanent phosphorylation even a more drastic effect might be possible, similar as can be seen for *hcf136* S35-37D plants. However, it is likely that not all of the preproteins destined for import are phosphorylated. Following, there is a sufficient number of unphosphorylated preproteins entering the chloroplast and enable plastid development. *pap2* and *pap2xpap9* plants however, do not show any impairment at all. Summarizing, it seems unlikely that PAP2 is a preprotein phosphatase of chloroplast transit peptides or if so not the only one. Possibly, PAP2 and/or

PAP9 might have overlapping functions with other unknown phosphatases and therefore in *pap2xpap9* plants dephosphorylation might not be entirely abolished.

4.3 Phosphorylation of targeting peptides of dual targeted preproteins

Like chloroplast transit peptides also dual targeting peptides are enriched in serine residues which are able to be phosphorylated (Berglund et al., 2009). Therefore, it seems likely that dual targeting peptides can be phosphorylated as it is the case for chloroplast transit peptides. In this work 17 dual targeting peptides were overproduced and tested in an in vitro kinase assay. Indeed, 8 peptides showed phosphorylation. Thus, phosphorylation might also be involved in dual import.

Phosphorylation of chloroplast transit peptides was shown to enhance import rates into chloroplasts (May and Soll, 2000). For plant mitochondrial preproteins there was for long time no evidence that phosphorylation plays a role during import. Thus, it is tempting to speculate that phosphorylation in dual import might be a way to direct targeting of ambiguous signals towards chloroplasts, rather than towards mitochondria. Recently however, it was shown that also mitochondrial targeting peptides can be phosphorylated (Fellerer, 2012; Law et al., 2015). Unlike in yeast and mammals, plant targeting signals of mitochondrial preproteins are enriched in serine residues, as it can be observed for chloroplast transit peptides and dual targeting peptides. Even though up to now only two mitochondrial preproteins were shown to be phosphorylated, it is probable that in plants phosphorylation can also be involved in mitochondrial import. Furthermore, for two dual targeted proteins (histidyl- and cysteinyl-tRNA synthetase) it was previously shown by fluorescence tagging that in vivo localization was not changed towards either mitochondria or chloroplasts upon mutation of predicted phosphorylation sites to alanine (Nakrieko et al., 2004). Following, phosphorylation seems to be involved in chloroplast, mitochondrial as well as dual import but most likely does not influence the distinction of the organelles.

Interestingly, the result of the phosphorylation assay of one peptide was not always consistent comparing wheat germ lysate and reticulocyte lysate. However, this could also be seen for the two phosphorylated mitochondrial proteins. The presequence of MORF3 is phosphorylated by wheat germ lysate and purified STY kinases, but hardly in reticulocyte lysate (Law et al., 2015). Yet, mitochondrial NFU4 is phosphorylated by wheat germ lysate as well as reticulocyte lysate (Fellerer, 2012). Thus, it is unlikely that the kinase of mitochondrial proteins is plant specific as it is the case for chloroplast proteins. Since STY kinases are plants specific chloroplast preproteins are thought to be only phosphorylated in wheat germ lysate and not in mammalian reticulocyte lysate (Martin et al., 2006; Lamberti et al., 2011b). In this screen only two out of eight peptides were phosphorylated by STY8.

Therefore, it might by possible that different kinases are responsible for the phosphorylation of chloroplast, mitochondrial and dual targeted preproteins.

Finally, the intensity of phosphorylation obviously depends on purification method of the peptide. At2g04842 (threonyl-tRNA synthetase) shows much stronger phosphorylation after cleavage from GST tag and further purification steps compared to the usage of inclusion bodies directly. It cannot be excluded that other peptides would also show (stronger) phosphorylation after further purification. The removal of denaturalizing urea from the buffer enable folding of the peptide which might support phosphorylation. It was reported that protein folding can create phosphorylation motifs (Duarte et al., 2014). However, targeting peptides are mostly unfolded anyway. Comprising, it can be concluded that some dual targeting peptides are phosphorylated in vitro but phosphorylation of these peptides is most likely no general phenomenon and not responsible for organelle specificity during dual import.

4.4 Mitochondrial TPR domain containing docking protein OM64

The TOM complex is responsible for the recognition of proteins at the mitochondrial surface and their translocation across the outer mitochondrial membrane. It was first discovered in *Neurospora crassa* (Kiebler et al., 1990) and yeast (Moczko et al., 1992) and later described in plants (Jänsch et al., 1998), mammals (Suzuki et al., 2000) and recently in the parasitic protozoa *Trypanosoma brucei* (Mani et al., 2015). Yeast TOM complex consists of a stable 400 kDa core complex, also called general import pore, that is formed by Tom40, Tom22 and the three small Tom proteins Tom7, Tom6 and Tom5 (Dekker et al., 1998). Only after very mild solubilization of the mitochondrial membrane Tom20 is found in association with the TOM complex (Meisinger et al., 2001). Same holds true for mammalian TOM complex (Suzuki et al., 2000). The binding of Tom70 to the TOM complex is still weaker, even after mild solubilization it cannot be found in association with the TOM complex in yeast (Meisinger et al., 2001). Only in *N. crassa*, a TOM complex containing both Tom20 and Tom70 could be isolated (Künkele et al., 1998). Thus, Tom70 is thought to interact only transitory with the TOM complex. In plants no homolog of Tom70 exists. However, OM64 was found in the outer membrane of mitochondria, an N-terminal anchored protein exposing a TPR domain into the cytosol, as Tom70 does. Om64 is a paralog of the chloroplast TPR domain containing docking protein Toc64. The involvement of OM64 in protein import was shown before (Lister et al., 2007). Within this work for the first time an interaction of OM64 with the TOM complex could be detected.

4.4.1 OM64 is part of the TOM complex

OM64 is a low abundant protein as can be seen by analyzing Genevestigator data (see appendix, Figure 22) as well as the fact that currently only two ESTs are available. Therefore, the in vivo detection of interactions is aggravated. Following, in this work an overexpressing line of OM64 was generated and used for interaction studies. Indeed, with BN-PAGE as well as with Co-IP an association with the TOM complex could be detected.

In *Arabidopsis* a stable TOM complex consisting of Tom40, Tom20, Tom9 and the three small Toms can be isolated (Werhahn et al., 2003). The molecular mass of the TOM complex was estimated between 230 (Lister et al., 2007) and 390 kDa (Werhahn et al., 2003). In this work Tom40 and Tom20 could be found to co-migrate with OM64 in a complex of similar size when analyzing solubilized mitochondria by BN-PAGE. Tom40 shows a signal in the lower molecular weight as well, which might be a reported subcomplex of Tom40 and the small Toms at 100 kDa (Werhahn et al., 2003). OM64 can also be detected in a range below 140 kDa which was also previously reported (Lister et al., 2007). It might be as well part of a subcomplex or, as it could be seen for Tom70 (Schmidt et al., 2011) migrate as a dimer. Large parts of OM64 can also be found in the high molecular weight range around 669 kDa which surprisingly overlay with Tom40 as well. This large complex might be due to the overexpression of OM64. In addition to the co-migration data from BN-PAGE, an interaction between OM64 and Tom40 as well as Tom20 could be shown by co-immunoprecipitation of solubilized mitochondria with OM64 antiserum. Thus, OM64 can be considered as part of the TOM complex.

4.4.2 Phosphorylation of OM64 influences protein import

Phosphorylation as a regulative mechanism was shown to influence protein import not only regarding preproteins (Waegemann and Soll, 1996) but also on the level of the translocon proteins. Different receptor proteins and other translocon subunits in chloroplast and yeast mitochondria have been shown to be regulated by phosphorylation (Sveshnikova et al., 2000; Schmidt et al., 2011). OM64 as well was found to be phosphorylated within its TPR domain. Via a site directed mutagenesis approach one residue, namely S568, was determined to be the phosphorylation site. It is possible that full length OM64 has one or several further phosphorylation sites outside the TPR domain since OM64 w/o TM S568A shows a weak signal in a phosphorylation assay. However, it is obvious that S568 is the main phosphorylation site, at least in vitro. Mass spectrometric analysis of isolated mitochondria is currently performed to confirm the phosphorylation site in vivo. Interestingly, this serine residue is conserved within OM64 between different dicotyledonous species. This fact makes it likely that the phosphorylation of OM64 is a general regulatory mechanism in dicots, not only present in *Arabidopsis*. The phosphorylation site however, is not conserved

in monocotyledonous species. The phylogenetic distribution of OM64 in general is restricted to vascular plants while it is absent in green and red algae, as well as in other lower plant lineages like *Physcomitrella patens* (Carrie et al., 2010). Thus, it might be likely that other yet undiscovered docking proteins are present in these clades.

The question arose which function the phosphorylation site fulfills in vivo. To investigate this issue plants were generated expressing either OM64 WT, phospho-deficient OM64 S568A or phospho-mimicking OM64 S568D or S568E. Furthermore, a construct expressing OM64 without the TPR domain was used. Since *om64* knockout does not show a phenotype, *tom20xom64* quadruple mutant including a knockout of all three Tom20 isoforms was chosen as a background for complementation. *tom20xom64* knockout is lethal, therefore plants are heterozygous for *Tom20-2*. This makes it an ideal tool for the investigation of different OM64 constructs since the appearance of plants being homozygous for *tom20-2* in the progeny of transformed plants indicating a functional OM64. However, in a first attempt expressing OM64 under control of a 35S promoter no homozygous *tom20-2* plants were found, not even using *35S::OM64 WT*. Since the expression of OM64 was confirmed by immunoblot analysis the transformation itself as well as the expression in adult plants was successful. *tom20xom64* knockout is embryolethal therefore the only explanation for the missing homozygous *tom20-2* plants is that the used 35S promoter is not properly active during embryogenesis. The *35S* promoter has been previously used to complement embryolethal mutants in *Arabidopsis* (Albert et al., 1999; Chen et al., 2001; Kim and Huang, 2004). However, it was also reported that the *35S* promoter is not active during early stages of embryogenesis (Odell et al., 1994; Custers et al., 1999; Sunilkumar et al., 2002). Indeed, the expression of OM64 is increased in dry and 24 h imbibed seeds and furthermore in the shoot apex and in the root of an early developed plant (Winter et al., 2007) (see appendix, Figure 21). This shows that OM64 is active during embryogenesis and early development. If no homozygous *tom20-2* plants are present no OM64 was expressed during embryogenesis to prevent the embryolethal phenotype. Therefore, in a second approach the complementation was done expressing OM64 under its endogenous promoter which should be active during all physiological needed time points. Indeed, in this case homozygous *tom20-2* plants were found, confirming the explanation that 35S promoter was not active during embryogenesis. Homozygous *tom20-2* plants were detected for all different phosphorylation site constructs, *OM64::OM64 WT*, *OM64::OM64 S568A* and *OM64::OM64 S568E*. This means that the phosphorylation site of OM64 is not essential for germination or viability. However, a detailed phenotyping needs to be done to compare the plants during later development. *tom20* triple knockout displays a slower growth rate compared to Col-0 (Lister et al., 2007). It will be interesting to see, if OM64 mutations can add an additional effect to that. The complementation with *OM64::OM64 w/o TPR* is still in the process of selection. Expression

of the protein could already be confirmed but the result of genotyping is still pending. Yeast Tom70 bearing a mutation in the TPR domain which disables chaperone binding cannot complement the lethal *tom70 tom20* knockout (Young et al., 2003b). From this result it is expected that the TPR domain is also essential for the function of OM64 and no homozygous *tom20-2* plants will be present.

Though the plants derived from the complementation using the 35S promoter cannot be used for the analysis of OM64 by phenotyping in a *tom20* triple knockout background, they represent a suitable tool to investigate the role of the phosphorylation site in protein import. Even more, in this case it is ideal to have Tom20-2 present since like this any effects in protein import are due to the mutated OM64 and not due to the missing Tom20. To investigate the role of phosphorylation during import the preprotein FAD was used, whose import was shown before to depend on OM64 (Lister et al., 2007). Mitochondria with phospho-deficient OM64 S568A can import FAD with the same efficiency as OM64 WT. In OM64 w/o TPR as well as in phospho-mimicking OM64 S568D the import rate of FAD is reduced to 30 - 40%. This shows on the one hand how important the TPR domain for the function of OM64 is which reflects the results in yeast (Young et al., 2003b). On the other hand, this clearly demonstrates the relevance of the phosphorylation site in vivo, showing that phosphorylation inhibits the preprotein import. Apparently, FAD import depends only partly on OM64 since even without OM64 it is still imported to some extent. Same was observed in yeast for the import of ADP/ATP carrier which is imported to 75 % via Tom70 and to 25 % via Tom20 (Steger et al., 1990). Furthermore, it can be seen that the effect of phospho-mimicry is more drastic in the in vitro import (showing an import rate comparable to *om64*) than in the plant complementation where OM64 S568E is able to complement *om64*. Evidently, more complex mechanisms are at work in vivo. OM64 can directly interact with mitochondrial preproteins (Lister et al., 2007). It is not known yet if this occurs via the TPR domain or at a distinct position. Possibly, this causes the reduced in vivo effect observed for plant complementation.

4.4.3 Phosphorylation of OM64 influences chaperone binding

Proteins with a clamp type TPR domain can interact with Hsp70 and Hsp90 (Scheufler et al., 2000). In the cytosol these chaperones can escort the newly synthesized preproteins and help targeting them to their destination organelle (Young et al., 2003b; Qbadou et al., 2006). Thus, TPR domain containing docking proteins can be found in each organelle throughout different kingdoms of life (Schlegel et al., 2007; Mani et al., 2015). The TPR domain of OM64 was shown to bind Hsp70 and Hsp90 (Schweiger et al., 2013; Panigrahi et al., 2014). Taking into account that phospho-mimicry of OM64 inhibits protein import in vitro it might be likely

that phosphorylation changes the binding affinities to chaperones and like this regulates import rates. To test this hypothesis binding affinities of OM64 WT, S568A and S568E to C-terminal Hsp70 and Hsp90 peptides were quantified with isothermal titration calorimetry (ITC). Concerning Hsp90, indeed a clear inhibitory effect of the phospho-mimicry could be detected, binding affinity of OM64 S568E (K_d = 39 µM) was four times lower than that of OM64 WT (K_d = 10 µM). The affinity of OM64 S568A was in the range of OM64 WT. All measured interactions are characterized by a negative change in enthalpy (ΔH) which describes an exothermal and favorable reaction but consistently to the K_d values, the change in entropy (ΔS) only shows positive that is favorable values for OM64 WT and S/A, while the binding of OM64 S568E to Hsp90 is described by a thermodynamically unfavorable loss of entropy.

Surprisingly, with this method no binding between OM64 and Hsp70 could be detected. To exclude that this result was due to the used Hsp70 peptide the experiment was repeated with full length Hsp70, however also detecting no binding. Since binding between OM64 and Hsp70 has been reported before, a methodological problem is probable. Nonetheless, describing binding affinities with different methods can lead to different results. Surface plasmon resonance spectroscopy with OM64 and full length chaperones indicated that OM64 prefers Hsp70 over Hsp90 (Schweiger et al., 2013) while regarding a molecular dynamics approach OM64 is not supposed to discriminate between Hsp70 and Hsp90 at all (Panigrahi et al., 2014). Furthermore, plant mitochondrial preproteins where shown to preferentially bind Hsp70 (Fellerer, 2012), in contrast to mammals where preproteins are bound by both Hsp70 and Hsp90 (Fan et al., 2006). In this work however, FAD whose import depends on OM64 was shown to interact with both Hsp70 and Hsp90, although the binding of Hsp70 is stronger. Yet, it has to be taken into account that Hsp70 binding in general is more unspecific, thus possibly more easily formed under in vitro conditions. Further, Hsp90 often takes over clients from Hsp70 (Dittmar and Pratt, 1997). Possibly, co-chaperones of Hsp90 are not active in vitro and therefore Hsp90 binding is aggravated to detect. To further investigate the changed binding affinity of OM64 due to phosphorylation in a next step a crystallization of OM64 WT and S568E together with chaperone peptide will be performed.

Summarizing, still no clear conclusion can be drawn which (if only one) chaperone is preferentially bound by OM64. Preproteins that are targeted to the receptor protein Tom20 are associated with Hsp70 (Figure 20). In case of OM64 most likely both Hsp70 and Hsp90 are involved in targeting. Apart from this issue, the measured K_d values could confirm the result of the in vitro import. Phosphorylation of the TPR domain of OM64 changes the affinity toward chaperones and thereby downregulates protein import. This was previously observed for Tom70 as well. Tom70 is phosphorylated not within its TPR domain but close to the chaperone binding site. Phospho-mimicry decreases protein import rates by reducing the

binding of Hsp70 (Schmidt et al., 2011). Therefore, negative regulation by phosphorylation is a new similarity between OM64 and its functional counterpart in yeast. Phosphorylation within a TPR domain was reported for human HOP and yeast homolog Sti1. In both cases phospho-mimicry reduces binding affinity to Hsp70 (Röhl et al., 2015). In addition, a phospho-mimicking mutant of HOP at a phosphorylation site outside the TPR domain negatively affects the interaction with Hsp90 (Daniel et al., 2008). On the other side, also chaperones can be phosphorylated. Phosphorylation of yeast Hsp90 leads to a decrease in its activity (Soroka et al., 2012) and phospho-mimicry at the C-terminus of both Hsp70 and Hsp90 changes affinities to TPR domain containing co-chaperones (Assimon et al., 2015). Thus, OM64 is one of the latest examples showing that phosphorylation on the one hand regulates the interaction between TPR domain and chaperone and on the other hand is involved during protein import.

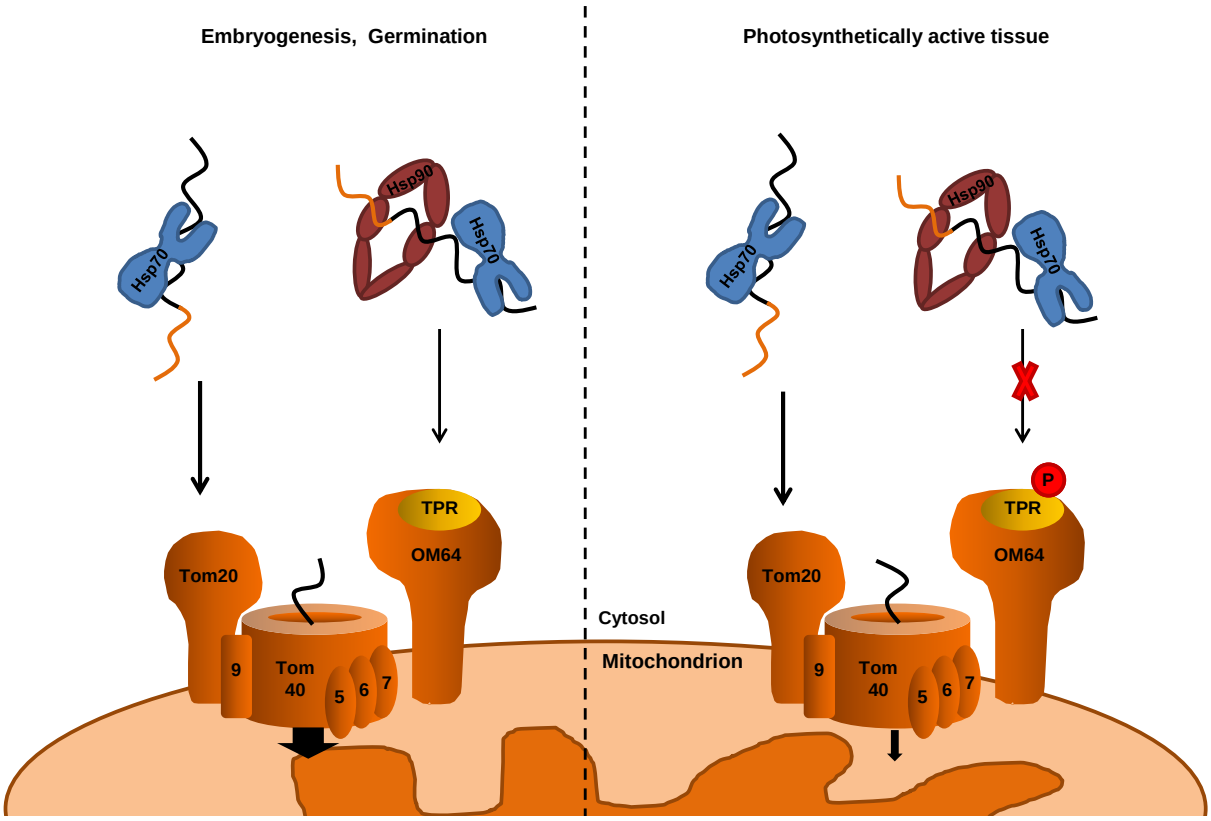

Figure 20: Model of function of OM64 phosphorylation. Mitochondrial preproteins can interact either with Hsp70 alone or with both Hsp70 and Hsp90. Tom20 can directly interact with mitochondrial presequences while the TPR domain of OM64 binds to the chaperones. During embryogenesis and germination an increased mitochondrial import is required and OM64 is present in an active unphosphorylated state. In adult plants and photosynthetically active tissue a reduced number of proteins is needed in mitochondria. OM64 is phosphorylated to decrease protein import by inhibiting chaperone binding.

The question remains under which physiological conditions phosphorylation of OM64 occurs. To answer this in a next step the kinase of OM64 has to be identified and analyzed in its expression profile. In yeast Tom70 is phosphorylated by protein kinase A (PKA) (Gerbeth et al., 2013). The activation of PKA is glucose induced, following representing a metabolic switch from respiration to fermentation. This involves lower mitochondrial activity and therefore a decreased need in imported proteins. Phosphorylation of Tom70 inhibits binding of Hsp70 and thereby reduces protein import rates (Gerbeth et al., 2013). What could this mean for plants? Possibly, OM64 phosphorylation is induced in the light since energy production by photosynthesis reduces the need for mitochondrial activity and phosphorylation of OM64 inhibits chaperone binding and like this protein import (Figure 20). An active OM64 is probably especially required during early germination which is supported by the fact that OM64 is expressed during early plant development. An increased mitochondrial protein import facilitates a switch from a dormant to an active metabolic state which is needed to drive germination (Murcha et al., 2014).

5 Literature

Abe, Y., Shodai, T., Muto, T., Mihara, K., Torii, H., Nishikawa, S.-i., Endo, T., and Kohda, D. (2000). Structural basis of presequence recognition by the mitochondrial protein import receptor Tom20. Cell **100,** 551-560.

Ahting, U., Waizenegger, T., Neupert, W., and Rapaport, D. (2005). Signal-anchored proteins follow a unique insertion pathway into the outer membrane of mitochondria. Journal of Biological Chemistry **280,** 48-53.

Albert, S., Després, B., Guilleminot, J., Bechtold, N., Pelletier, G., Delseny, M., and Devic, M. (1999). The EMB 506 gene encodes a novel ankyrin repeat containing protein that is essential for the normal development of Arabidopsis embryos. Plant J **17,** 169-179.

Aronsson, H., Boij, P., Patel, R., Wardle, A., Topel, M., and Jarvis, P. (2007). Toc64/OEP64 is not essential for the efficient import of proteins into chloroplasts in Arabidopsis thaliana. Plant J **52,** 53-68.

Assimon, V.A., Southworth, D.R., and Gestwicki, J.E. (2015). Specific Binding of Tetratricopeptide Repeat Proteins to Heat Shock Protein 70 (Hsp70) and Heat Shock Protein 90 (Hsp90) Is Regulated by Affinity and Phosphorylation. Biochemistry **54,** 7120-7131.

Attardi, G., and Schatz, G. (1988). Biogenesis of mitochondria. Annual review of cell biology **4,** 289-331.

Bauer, J., Chen, K., Hiltbunner, A., Wehrli, E., Eugster, M., Schnell, D., and Kessler, F. (2000). The major protein import receptor of plastids is essential for chloroplast biogenesis. Nature **403,** 203-207.

Becker, T., Hritz, J., Vogel, M., Caliebe, A., Bukau, B., Soll, J., and Schleiff, E. (2004). Toc12, a novel subunit of the intermembrane space preprotein translocon of chloroplasts. Molecular biology of the cell **15,** 5130-5144.

Berglund, A.K., Spanning, E., Biverstahl, H., Maddalo, G., Tellgren-Roth, C., Maler, L., and Glaser, E. (2009). Dual targeting to mitochondria and chloroplasts: characterization of Thr-tRNA synthetase targeting peptide. Molecular plant **2,** 1298-1309.

Bhushan, S., Kuhn, C., Berglund, A.-K., Roth, C., and Glaser, E. (2006). The role of the N-terminal domain of chloroplast targeting peptides in organellar protein import and miss-sorting. FEBS letters **580,** 3966-3972.

Bozzo, G.G., Raghothama, K.G., and Plaxton, W.C. (2004). Structural and kinetic properties of a novel purple acid phosphatase from phosphate-starved tomato (Lycopersicon esculentum) cell cultures. Biochemical Journal **377,** 419-428.

Bracher, A., and Hartl, F.U. (2006). Hsp90 structure: when two ends meet. Nature structural & molecular biology **13,** 478-480.

Brocard, C., and Hartig, A. (2006). Peroxisome targeting signal 1: is it really a simple tripeptide? Biochimica et Biophysica Acta (BBA)-Molecular Cell Research **1763,** 1565-1573.

Carrie, C., and Small, I. (2013). A reevaluation of dual-targeting of proteins to mitochondria and chloroplasts. Biochimica et biophysica acta **1833,** 253-259.

Carrie, C., Murcha, M.W., and Whelan, J. (2010). An in silico analysis of the mitochondrial protein import apparatus of plants. BMC Plant Biol **10,** 249.

Cashikar, A.G., Kumaresan, R., and Rao, N.M. (1997). Biochemical characterization and subcellular localization of the red kidney bean purple acid phosphatase. Plant physiology **114,** 907-915.

Chen, J.-G., Ullah, H., Young, J.C., Sussman, M.R., and Jones, A.M. (2001). ABP1 is required for organized cell elongation and division in Arabidopsis embryogenesis. Genes & Development **15,** 902-911.

Chew, O., Lister, R., Qbadou, S., Heazlewood, J.L., Soll, J., Schleiff, E., Millar, A.H., and Whelan, J. (2004). A plant outer mitochondrial membrane protein with high amino

acid sequence identity to a chloroplast protein import receptor. FEBS letters **557,** 109-114.

Cohen, P. (2002). The origins of protein phosphorylation. Nature cell biology **4,** E127-E130.

Custers, J., Snepvangers, S., Jansen, H., Zhang, L., and van Lookeren Campagne, M. (1999). The 35S-CaMV promoter is silent during early embryogenesis but activated during nonembryogenic sporophytic development in microspore culture. Protoplasma **208,** 257-264.

Daniel, S., Bradley, G., Longshaw, V.M., Söti, C., Csermely, P., and Blatch, G.L. (2008). Nuclear translocation of the phosphoprotein Hop (Hsp70/Hsp90 organizing protein) occurs under heat shock, and its proposed nuclear localization signal is involved in Hsp90 binding. Biochimica et Biophysica Acta (BBA)-Molecular Cell Research **1783,** 1003-1014.

de Boer, A.H., van Kleeff, P.J., and Gao, J. (2013). Plant 14-3-3 proteins as spiders in a web of phosphorylation. Protoplasma **250,** 425-440.

Dekker, P.J., Ryan, M.T., Brix, J., Müller, H., Hönlinger, A., and Pfanner, N. (1998). Preprotein translocase of the outer mitochondrial membrane: molecular dissection and assembly of the general import pore complex. Molecular and cellular biology **18,** 6515-6524.

Del Pozo, J.C., Allona, I., Rubio, V., Leyva, A., De La Peña, A., Aragoncillo, C., and Paz-Ares, J. (1999). A type 5 acid phosphatase gene from Arabidopsis thaliana is induced by phosphate starvation and by some other types of phosphate mobilising/oxidative stress conditions. The Plant Journal **19,** 579-589.

Dittmar, K.D., and Pratt, W.B. (1997). Folding of the Glucocorticoid Receptor by the Reconstituted hsp90-based Chaperone Machinery THE INITIAL hsp90· p60· hsp70-DEPENDENT STEP IS SUFFICIENT FOR CREATING THE STEROID BINDING CONFORMATION. Journal of Biological Chemistry **272,** 13047-13054.

Duarte, M.L., Pena, D.A., Ferraz, F.A.N., Berti, D.A., Sobreira, T.J.P., Costa-Junior, H.M., Baqui, M.M.A., Disatnik, M.-H., Xavier-Neto, J., and de Oliveira, P.S.L. (2014). Protein folding creates structure-based, noncontiguous consensus phosphorylation motifs recognized by kinases. Science signaling **7,** ra105-ra105.

Duncan, O., Murcha, M.W., and Whelan, J. (2013). Unique components of the plant mitochondrial protein import apparatus. Biochimica et biophysica acta **1833,** 304-313.

Fan, A.C., Bhangoo, M.K., and Young, J.C. (2006). Hsp90 functions in the targeting and outer membrane translocation steps of Tom70-mediated mitochondrial import. Journal of Biological Chemistry **281,** 33313-33324.

Faou, P., and Hoogenraad, N.J. (2012). Tom34: a cytosolic cochaperone of the Hsp90/Hsp70 protein complex involved in mitochondrial protein import. Biochimica et Biophysica Acta (BBA)-Molecular Cell Research **1823,** 348-357.

Fellerer, C. (2012). Molecular chaperones involved in preprotein targeting to plant organelles. Dissertation.

Fellerer, C., Schweiger, R., Schöngruber, K., Soll, J., and Schwenkert, S. (2011). Cytosolic HSP90 cochaperones HOP and FKBP interact with freshly synthesized chloroplast preproteins of Arabidopsis. Molecular plant **4,** 1133-1145.

Fransen, M., Amery, L., Hartig, A., Brees, C., Rabijns, A., Mannaerts, G.P., and Van Veldhoven, P.P. (2008). Comparison of the PTS1-and Rab8b-binding properties of Pex5p and Pex5Rp/TRIP8b. Biochimica et Biophysica Acta (BBA)-Molecular Cell Research **1783,** 864-873.

Gerbeth, C., Mikropoulou, D., and Meisinger, C. (2013). From inventory to functional mechanisms: regulation of the mitochondrial protein import machinery by phosphorylation. The FEBS journal **280,** 4933-4942.

Hachiya, N., Mihara, K., Suda, K., Horst, M., Schatz, G., and Lithgow, T. (1995). Reconstitution of the initial steps of mitochondrial protein import.

Hanahan, D. (1985). Techniques for transformation of E. coli. DNA cloning **1,** 109-135.

Haran, S., Logendra, S., Seskar, M., Bratanova, M., and Raskin, I. (2000). Characterization of Arabidopsis acid phosphatase promoter and regulation of acid phosphatase expression. Plant physiology **124,** 615-626.

Hartl, F.U., Bracher, A., and Hayer-Hartl, M. (2011). Molecular chaperones in protein folding and proteostasis. Nature **475,** 324-332.

Hinnah, S.C., Wagner, R., Sveshnikova, N., Harrer, R., and Soll, J. (2002). The chloroplast protein import channel Toc75: pore properties and interaction with transit peptides. Biophysical journal **83,** 899-911.

Howell, K.A., Millar, A.H., and Whelan, J. (2006). Ordered assembly of mitochondria during rice germination begins with promitochondrial structures rich in components of the protein import apparatus. Plant molecular biology **60,** 201-223.

Jänsch, L., Kruft, V., Schmitz, U.K., and Braun, H.-P. (1998). Unique composition of the preprotein translocase of the outer mitochondrial membrane from plants. Journal of Biological Chemistry **273,** 17251-17257.

Jarvis, P., Chen, L.-J., Li, H.-m., Peto, C.A., Fankhauser, C., and Chory, J. (1998). An Arabidopsis mutant defective in the plastid general protein import apparatus. Science **282,** 100-103.

Karlin, S., and Brocchieri, L. (1998). Heat shock protein 70 family: multiple sequence comparisons, function, and evolution. Journal of molecular evolution **47,** 565-577.

Keegstra, K., Olsen, L.J., and Theg, S.M. (1989). Chloroplastic precursors and their transport across the envelope membranes. Annual review of plant biology **40,** 471-501.

Kessler, F., Blobel, G., Patel, H.A., and Schnell, D.J. (1994). Identification of two GTP-binding proteins in the chloroplast protein import machinery. Science **266,** 1035-1039.

Kiebler, M., Pfaller, R., Söllner, G., Horstmann, H., Pfanner, N., and Neupert, W. (1990). Identif ication of a mitochondrial receptor complex required for recognit ion and membrane insertion of precursor proteins. Nature **348,** 13.

Kim, H.U., and Huang, A.H. (2004). Plastid lysophosphatidyl acyltransferase is essential for embryo development in Arabidopsis. Plant physiology **134,** 1206-1216.

Kim, S.R., and Gynheung, A. (1996). RESEARCH ARTICLES: Isolation and Characterization of a Pollen-specific cDNA Clone from Easter Lily. Journal of Plant Biology **39,** 197-202.

Komiya, T., Rospert, S., Koehler, C., Looser, R., Schatz, G., and Mihara, K. (1998). Interaction of mitochondrial targeting signals with acidic receptor domains along the protein import pathway: evidence for the 'acid chain'hypothesis. The EMBO Journal **17,** 3886-3898.

Kouranov, A., and Schnell, D.J. (1997). Analysis of the interactions of preproteins with the import machinery over the course of protein import into chloroplasts. The Journal of cell biology **139,** 1677-1685.

Kriechbaumer, V., von Loffelholz, O., and Abell, B.M. (2012). Chaperone receptors: guiding proteins to intracellular compartments. Protoplasma **249,** 21-30.

Krimm, I., Gans, P., Hernandez, J.F., Arlaud, G.J., and Lancelin, J.M. (1999). A coil–helix instead of a helix–coil motif can be induced in a chloroplast transit peptide from Chlamydomonas reinhardtii. European journal of biochemistry **265,** 171-180.

Künkele, K.-P., Heins, S., Dembowski, M., Nargang, F.E., Benz, R., Thieffry, M., Walz, J., Lill, R., Nussberger, S., and Neupert, W. (1998). The preprotein translocation channel of the outer membrane of mitochondria. Cell **93,** 1009-1019.

Kyriakis, J.M. (2014). In the beginning, there was protein phosphorylation. Journal of Biological Chemistry **289,** 9460-9462.

Laemmli, U.K. (1970). Cleavage of structural proteins during the assembly of the head of bacteriophage T4. nature **227,** 680-685.

Lamberti, G., Drurey, C., Soll, J., and Schwenkert, S. (2011a). The phosphorylation state of chloroplast transit peptides regulates preprotein import. Plant signaling & behavior **6,** 1918-1920.

Lamberti, G., Gügel, I.L., Meurer, J., Soll, J., and Schwenkert, S. (2011b). The cytosolic kinases STY8, STY17, and STY46 are involved in chloroplast differentiation in Arabidopsis. Plant physiology **157,** 70-85.

Law, Y.-S., Zhang, R., Guan, X., Cheng, S., Sun, F., Duncan, O., Murcha, M.W., Whelan, J., and Lim, B.L. (2015). Phosphorylation and Dephosphorylation of the

Presequence of Precursor MULTIPLE ORGANELLAR RNA EDITING FACTOR3 during Import into Mitochondria from Arabidopsis. Plant physiology **169,** 1344-1355.

Lee, S., Lee, D.W., Lee, Y., Mayer, U., Stierhof, Y.-D., Lee, S., Jürgens, G., and Hwang, I. (2009). Heat shock protein cognate 70-4 and an E3 ubiquitin ligase, CHIP, mediate plastid-destined precursor degradation through the ubiquitin-26S proteasome system in Arabidopsis. The Plant cell **21,** 3984-4001.

Leibovitch, M., Bublak, D., Hanic-Joyce, P.J., Tillmann, B., Flinner, N., Amsel, D., Scharf, K.D., Mirus, O., Joyce, P.B., and Schleiff, E. (2013). The folding capacity of the mature domain of the dual-targeted plant tRNA nucleotidyltransferase influences organelle selection. The Biochemical journal **453,** 401-412.

Li, D., Zhu, H., Liu, K., Liu, X., Leggewie, G., Udvardi, M., and Wang, D. (2002). Purple acid phosphatases of Arabidopsis thaliana comparative analysis and differential regulation by phosphate deprivation. Journal of Biological Chemistry **277,** 27772-27781.

Lindquist, S., and Craig, E. (1988). The heat-shock proteins. Annual review of genetics **22,** 631-677.

Lister, R., Carrie, C., Duncan, O., Ho, L.H., Howell, K.A., Murcha, M.W., and Whelan, J. (2007). Functional definition of outer membrane proteins involved in preprotein import into mitochondria. The Plant cell **19,** 3739-3759.

Lister, R., Chew, O., Lee, M.-N., Heazlewood, J.L., Clifton, R., Parker, K.L., Millar, A.H., and Whelan, J. (2004). A transcriptomic and proteomic characterization of the Arabidopsis mitochondrial protein import apparatus and its response to mitochondrial dysfunction. Plant physiology **134,** 777-789.

Mani, J., Desy, S., Niemann, M., Chanfon, A., Oeljeklaus, S., Pusnik, M., Schmidt, O., Gerbeth, C., Meisinger, C., and Warscheid, B. (2015). Mitochondrial protein import receptors in Kinetoplastids reveal convergent evolution over large phylogenetic distances. Nature communications **6**.

Margulis, L. (1970). Origin of eukaryotic cells: evidence and research implications for a theory of the origin and evolution of microbial, plant, and animal cells on the Precambrian earth. (Yale University Press New Haven).

Martin, T., Sharma, R., Sippel, C., Waegemann, K., Soll, J., and Vothknecht, U.C. (2006). A protein kinase family in Arabidopsis phosphorylates chloroplast precursor proteins. The Journal of biological chemistry **281,** 40216-40223.

May, T., and Soll, J. (2000). 14-3-3 proteins form a guidance complex with chloroplast precursor proteins in plants. The Plant cell **12,** 53-63.

Meisinger, C., Ryan, M.T., Hill, K., Model, K., Lim, J.H., Sickmann, A., Müller, H., Meyer, H.E., Wagner, R., and Pfanner, N. (2001). Protein import channel of the outer mitochondrial membrane: a highly stable Tom40-Tom22 core structure differentially interacts with preproteins, small tom proteins, and import receptors. Molecular and cellular biology **21,** 2337-2348.

Mhawech, P. (2005). 14-3-3 proteins—an update. Cell research **15,** 228-236.

Michaud, M., Maréchal-Drouard, L., and Duchêne, A.-M. (2010). RNA trafficking in plant cells: targeting of cytosolic mRNAs to the mitochondrial surface. Plant molecular biology **73,** 697-704.

Miras, S., Salvi, D., Piette, L., Seigneurin-Berny, D., Grunwald, D., Reinbothe, C., Joyard, J., Reinbothe, S., and Rolland, N. (2007). Toc159-and Toc75-independent import of a transit sequence-less precursor into the inner envelope of chloroplasts. Journal of Biological Chemistry **282,** 29482-29492.

Moberg, P., Nilsson, S., Ståhl, A., Eriksson, A.-C., Glaser, E., and Mäler, L. (2004). NMR Solution Structure of the Mitochondrial F 1 β Presequence from Nicotiana plumbaginifolia. Journal of molecular biology **336,** 1129-1140.

Moczko, M., Bömer, U., Kübrich, M., Zufall, N., Hönlinger, A., and Pfanner, N. (1997). The intermembrane space domain of mitochondrial Tom22 functions as a trans binding site for preproteins with N-terminal targeting sequences. Molecular and cellular biology **17,** 6574-6584.

Moczko, M., Dietmeier, K., Söllner, T., Segui, B., Steger, H.F., Neupert, W., and Pfanner, N. (1992). Identification of the mitochondrial receptor complex in Saccharomyces cerevisiae. FEBS letters **310,** 265-268.

Morgante, C.V., Rodrigues, R.A., Marbach, P.A., Borgonovi, C.M., Moura, D.S., and Silva-Filho, M.C. (2009). Conservation of dual-targeted proteins in Arabidopsis and rice points to a similar pattern of gene-family evolution. Molecular Genetics and Genomics **281,** 525-538.

Murcha, M.W., Wang, Y., Narsai, R., and Whelan, J. (2014). The plant mitochondrial protein import apparatus - the differences make it interesting. Biochimica et biophysica acta **1840,** 1233-1245.

Nada, A., and Soll, J. (2004). Inner envelope protein 32 is imported into chloroplasts by a novel pathway. Journal of cell science **117,** 3975-3982.

Nakrieko, K.-A., Mould, R.M., and Smith, A.G. (2004). Fidelity of targeting to chloroplasts is not affected by removal of the phosphorylation site from the transit peptide. European Journal of Biochemistry **271,** 509-516.

Nickel, C., Soll, J., and Schwenkert, S. (2015). Phosphomimicking within the transit peptide of pHCF136 leads to reduced photosystem II accumulation in vivo. FEBS Lett **589,** 1301-1307.

Odell, J.T., Hoopes, J.L., and Vermerris, W. (1994). Seed-specific gene activation mediated by the Cre/lox site-specific recombination system. Plant physiology **106,** 447-458.

Panigrahi, R., Whelan, J., and Vrielink, A. (2014). Exploring ligand recognition, selectivity and dynamics of TPR domains of chloroplast Toc64 and mitochondria Om64 from Arabidopsis thaliana. Journal of molecular recognition : JMR **27,** 402-414.

Pearl, L.H., and Prodromou, C. (2006). Structure and mechanism of the Hsp90 molecular chaperone machinery. Annu. Rev. Biochem. **75,** 271-294.

Peeters, N., and Small, I. (2001). Dual targeting to mitochondria and chloroplasts. Biochimica et Biophysica Acta (BBA)-Molecular Cell Research **1541,** 54-63.

Perry, A.J., Hulett, J.M., Likić, V.A., Lithgow, T., and Gooley, P.R. (2006). Convergent evolution of receptors for protein import into mitochondria. Current biology **16,** 221-229.

Plücken, H., Müller, B., Grohmann, D., Westhoff, P., and Eichacker, L.A. (2002). The HCF136 protein is essential for assembly of the photosystem II reaction center in Arabidopsis thaliana. FEBS letters **532,** 85-90.

Pollmann, S., Neu, D., Lehmann, T., Berkowitz, O., Schäfer, T., and Weiler, E.W. (2006). Subcellular localization and tissue specific expression of amidase 1 from Arabidopsis thaliana. Planta **224,** 1241-1253.

Pujol, C., Maréchal-Drouard, L., and Duchêne, A.-M. (2007). How can organellar protein N-terminal sequences be dual targeting signals? In silico analysis and mutagenesis approach. Journal of molecular biology **369,** 356-367.

Qbadou, S., Becker, T., Mirus, O., Tews, I., Soll, J., and Schleiff, E. (2006). The molecular chaperone Hsp90 delivers precursor proteins to the chloroplast import receptor Toc64. The EMBO journal **25,** 1836-1847.

Ramage, L., Junne, T., Hahne, K., Lithgow, T., and Schatz, G. (1993). Functional cooperation of mitochondrial protein import receptors in yeast. The EMBO Journal **12,** 4115.

Rao, S., Schmidt, O., Harbauer, A.B., Schonfisch, B., Guiard, B., Pfanner, N., and Meisinger, C. (2012). Biogenesis of the preprotein translocase of the outer mitochondrial membrane: protein kinase A phosphorylates the precursor of Tom40 and impairs its import. Molecular biology of the cell **23,** 1618-1627.

Rehling, P., Brandner, K., and Pfanner, N. (2004). Mitochondrial import and the twin-pore translocase. Nature reviews Molecular cell biology **5,** 519-530.

Rimmer, K.A., Foo, J.H., Ng, A., Petrie, E.J., Shilling, P.J., Perry, A.J., Mertens, H.D., Lithgow, T., Mulhern, T.D., and Gooley, P.R. (2011). Recognition of mitochondrial targeting sequences by the import receptors Tom20 and Tom22. Journal of molecular biology **405,** 804-818.

Robin, M.-A., Prabu, S.K., Raza, H., Anandatheerthavarada, H.K., and Avadhani, N.G. (2003). Phosphorylation enhances mitochondrial targeting of GSTA4-4 through increased affinity for binding to cytoplasmic Hsp70. Journal of Biological Chemistry **278,** 18960-18970.

Robin, M.-A., Anandatheerthavarada, H.K., Biswas, G., Sepuri, N.B.V., Gordon, D.M., Pain, D., and Avadhani, N.G. (2002). Bimodal targeting of microsomal CYP2E1 to mitochondria through activation of an N-terminal chimeric signal by cAMP-mediated phosphorylation. Journal of Biological Chemistry **277,** 40583-40593.

Röhl, A., Rohrberg, J., and Buchner, J. (2013). The chaperone Hsp90: changing partners for demanding clients. Trends in biochemical sciences **38,** 253-262.

Röhl, A., Tippel, F., Bender, E., Schmid, A.B., Richter, K., Madl, T., and Buchner, J. (2015). Hop/Sti1 phosphorylation inhibits its co-chaperone function. EMBO reports **16,** 240-249.

Saitoh, T., Igura, M., Obita, T., Ose, T., Kojima, R., Maenaka, K., Endo, T., and Kohda, D. (2007). Tom20 recognizes mitochondrial presequences through dynamic equilibrium among multiple bound states. The EMBO Journal **26,** 4777-4787.

Sambrook, J., Fritsch, E.F., and Maniatis, T. (1989). Molecular cloning. (Cold spring harbor laboratory press New York).

Schenk, G., Guddat, L., Ge, Y., Carrington, L., Hume, D., Hamilton, S., and De Jersey, J. (2000). Identification of mammalian-like purple acid phosphatases in a wide range of plants. Gene **250,** 117-125.

Scheufler, C., Brinker, A., Bourenkov, G., Pegoraro, S., Moroder, L., Bartunik, H., Hartl, F.U., and Moarefi, I. (2000). Structure of TPR domain–peptide complexes: critical elements in the assembly of the Hsp70–Hsp90 multichaperone machine. Cell **101,** 199-210.

Schlegel, T., Mirus, O., von Haeseler, A., and Schleiff, E. (2007). The tetratricopeptide repeats of receptors involved in protein translocation across membranes. Molecular biology and evolution **24,** 2763-2774.

Schleiff, E., and Becker, T. (2011). Common ground for protein translocation: access control for mitochondria and chloroplasts. Nature Reviews Molecular Cell Biology **12,** 48-59.

Schmidt, O., Harbauer, A.B., Rao, S., Eyrich, B., Zahedi, R.P., Stojanovski, D., Schonfisch, B., Guiard, B., Sickmann, A., Pfanner, N., and Meisinger, C. (2011). Regulation of mitochondrial protein import by cytosolic kinases. Cell **144,** 227-239.

Schneider, G., Sjöling, S., Wallin, E., Wrede, P., Glaser, E., and von Heijne, G. (1998). Feature-extraction from endopeptidase cleavage sites in mitochondrial targeting peptides. Proteins: Structure, Function, and Bioinformatics **30,** 49-60.

Schweiger, R., Müller, N.C., Schmitt, M.J., Soll, J., and Schwenkert, S. (2012). AtTPR7 is a chaperone-docking protein of the Sec translocon in Arabidopsis. J Cell Sci **125,** 5196-5207.

Schweiger, R., Soll, J., Jung, K., Heermann, R., and Schwenkert, S. (2013). Quantification of interaction strengths between chaperones and tetratricopeptide repeat domain-containing membrane proteins. The Journal of biological chemistry **288,** 30614-30625.

Seedorf, M., Waegemann, K., and Soll, J. (1995). A constituent of the chloroplast import complex represents a new type of GTP-binding protein. The Plant Journal **7,** 401-411.

Shirasu, K. (2009). The HSP90-SGT1 chaperone complex for NLR immune sensors. Annual review of plant biology **60,** 139-164.

Sohrt, K., and Soll, J. (2000). Toc64, a new component of the protein translocon of chloroplasts. The Journal of cell biology **148,** 1213-1222.

Soll, J. (2002). Protein import into chloroplasts. Current opinion in plant biology **5,** 529-535.

Soroka, J., Wandinger, S.K., Mäusbacher, N., Schreiber, T., Richter, K., Daub, H., and Buchner, J. (2012). Conformational switching of the molecular chaperone Hsp90 via regulated phosphorylation. Molecular cell **45,** 517-528.

Steger, H.F., Söllner, T., Kiebler, M., Dietmeier, K.A., Pfaller, R., Trülzsch, K.S., Tropschug, M., Neupert, W., and Pfanner, N. (1990). Import of ADP/ATP carrier

into mitochondria: two receptors act in parallel. The Journal of cell biology **111,** 2353-2363.

Stengel, A., Benz, J.P., Soll, J., and Bölter, B. (2010). Redox-regulation of protein import into chloroplasts and mitochondria: similarities and differences. Plant signaling & behavior **5,** 105-109.

Sun, F., Carrie, C., Law, S., Murcha, M.W., Zhang, R., Law, Y.S., Suen, P.K., Whelan, J., and Lim, B.L. (2012a). AtPAP2 is a tail-anchored protein in the outer membrane of chloroplasts and mitochondria. Plant signaling & behavior **7,** 927-932.

Sun, F., Suen, P.K., Zhang, Y., Liang, C., Carrie, C., Whelan, J., Ward, J.L., Hawkins, N.D., Jiang, L., and Lim, B.L. (2012b). A dual-targeted purple acid phosphatase in Arabidopsis thaliana moderates carbon metabolism and its overexpression leads to faster plant growth and higher seed yield. New Phytologist **194,** 206-219.

Sunilkumar, G., Mohr, L., Lopata-Finch, E., Emani, C., and Rathore, K.S. (2002). Developmental and tissue-specific expression of CaMV 35S promoter in cotton as revealed by GFP. Plant molecular biology **50,** 463-479.

Suzuki, H., Okazawa, Y., Komiya, T., Saeki, K., Mekada, E., Kitada, S., Ito, A., and Mihara, K. (2000). Characterization of rat TOM40, a central component of the preprotein translocase of the mitochondrial outer membrane. Journal of Biological Chemistry **275,** 37930-37936.

Sveshnikova, N., Soll, J., and Schleiff, E. (2000). Toc34 is a preprotein receptor regulated by GTP and phosphorylation. Proceedings of the National Academy of Sciences of the United States of America **97,** 4973-4978.

Taipale, M., Jarosz, D.F., and Lindquist, S. (2010). HSP90 at the hub of protein homeostasis: emerging mechanistic insights. Nature reviews Molecular cell biology **11,** 515-528.

Tillmann, B., Röth, S., Bublak, D., Sommer, M., Stelzer, E.H., Scharf, K.-D., and Schleiff, E. (2015). Hsp90 is involved in the regulation of cytosolic precursor protein abundance in tomato. Molecular plant **8,** 228-241.

van Wilpe, S., Ryan, M.T., Hill, K., Maarse, A.C., Meisinger, C., Brix, J., Dekker, P.J., Moczko, M., Wagner, R., and Meijer, M. (1999). Tom22 is a multifunctional organizer of the mitochondrial preprotein translocase. Nature **401,** 485-489.

Vestweber, D., Brunner, J., Baker, A., and Schatz, G. (1989). A 42K outer-membrane protein is a component of the yeast mitochondrial protein import site.

von Braun, S.S., Sabetti, A., Hanic-Joyce, P.J., Gu, J., Schleiff, E., and Joyce, P.B. (2007). Dual targeting of the tRNA nucleotidyltransferase in plants: not just the signal. Journal of experimental botany **58,** 4083-4093.

von Heijne, G. (1986). Mitochondrial targeting sequences may form amphiphilic helices. The EMBO Journal **5,** 1335.

Waegemann, K., and Soll, J. (1996). Phosphorylation of the transit sequence of chloroplast precursor proteins. Journal of Biological Chemistry **271,** 6545-6554.

Waegemann, K., Paulsen, H., and Soll, J. (1990). Translocation of proteins into isolated chloroplasts requires cytosolic factors to obtain import competence. FEBS letters **261,** 89-92.

Werhahn, W., Jänsch, L., and Braun, H.-P. (2003). Identification of novel subunits of the TOM complex from Arabidopsis thaliana. Plant Physiology and Biochemistry **41,** 407-416.

Werhahn, W., Niemeyer, A., Jänsch, L., Kruft, V., Schmitz, U.K., and Braun, H.-P. (2001). Purification and characterization of the preprotein translocase of the outer mitochondrial membrane from Arabidopsis. Identification of multiple forms of TOM20. Plant physiology **125,** 943-954.

Winter, D., Vinegar, B., Nahal, H., Ammar, R., Wilson, G.V., and Provart, N.J. (2007). An "Electronic Fluorescent Pictograph" browser for exploring and analyzing large-scale biological data sets. PloS one **2,** e718.

Young, J.C. (2010). Mechanisms of the Hsp70 chaperone system This paper is one of a selection of papers published in this special issue entitled "Canadian Society of Biochemistry, Molecular & Cellular Biology 52nd Annual Meeting-Protein Folding:

Principles and Diseases" and has undergone the Journal's usual peer review process. Biochemistry and Cell Biology **88,** 291-300.

Young, J.C., Barral, J.M., and Hartl, F.U. (2003a). More than folding: localized functions of cytosolic chaperones. Trends in biochemical sciences **28,** 541-547.

Young, J.C., Hoogenraad, N.J., and Hartl, F.U. (2003b). Molecular chaperones Hsp90 and Hsp70 deliver preproteins to the mitochondrial import receptor Tom70. Cell **112,** 41-50.

Young, J.C.M., I.; Hartl, F. U. (2001). Hsp90: a specialized but essential protein-folding tool. The Journal of cell biology **154,** 267-274.

Zeytuni, N., and Zarivach, R. (2012). Structural and functional discussion of the tetra-trico-peptide repeat, a protein interaction module. Structure **20,** 397-405.

Zhang, M., Windheim, M., Roe, S.M., Peggie, M., Cohen, P., Prodromou, C., and Pearl, L.H. (2005). Chaperoned ubiquitylation--crystal structures of the CHIP U box E3 ubiquitin ligase and a CHIP-Ubc13-Uev1a complex. Molecular cell **20,** 525-538.

Zhang, X.-P.G., Elzbieta. (2002). Interaction of plant mitochondrial and chloroplast signal peptides with the Hsp70 molecular chaperone. TRENDS in Plant Science **7**.

Zhu, H., Qian, W., Lu, X., Li, D., Liu, X., Liu, K., and Wang, D. (2005). Expression patterns of purple acid phosphatase genes in Arabidopsis organs and functional analysis of AtPAP23 predominantly transcribed in flower. Plant molecular biology **59,** 581-594.

Zimmermann, P., Regierer, B., Kossmann, J., Frossard, E., Amrhein, N., and Bucher, M. (2004). Differential expression of three purple acid phosphatases from potato. Plant Biology **6,** 519-528.

6 Appendix

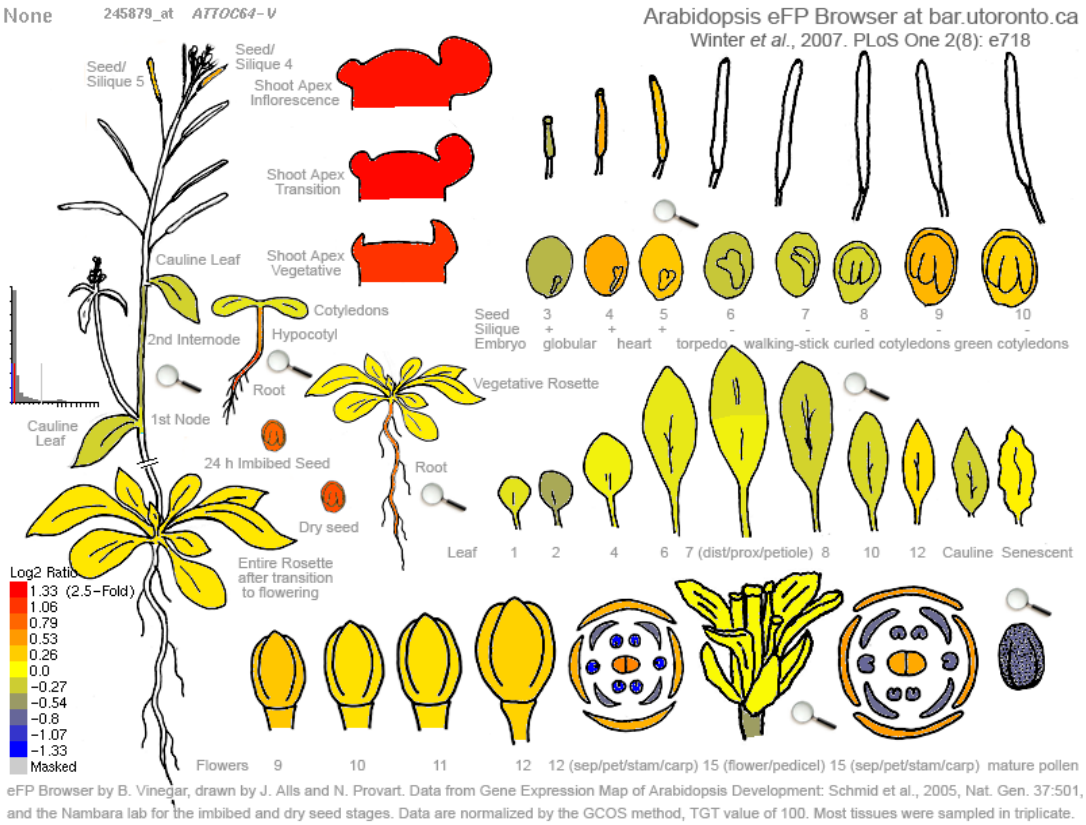

Figure 21: Relative expression levels of OM64 (=Toc64-V) in *Arabidopsis* plant. OM64 is mainly expressed in shoot apex, seeds, roots and during embryogenesis. Data from Arabidopsis eFP Browser (http://bbc.botany.utoronto.ca) (Winter et al., 2007).

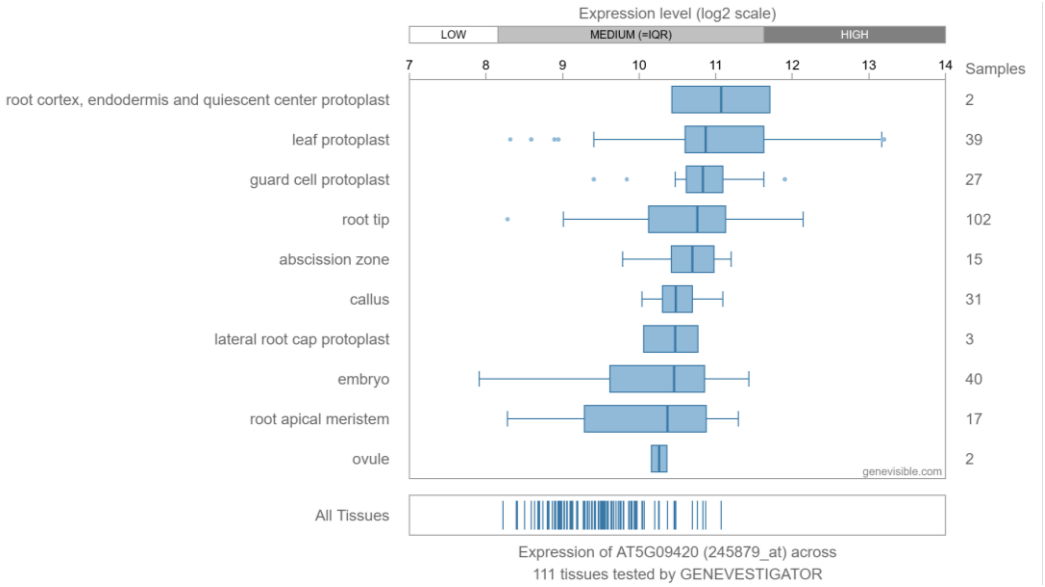

Figure 22: OM64 expression in different tissues. OM64 is a low to medium abundant protein with highest expression in root tissue and in the embryo. Data from Affymetrix Arabidopsis ATH1 Genome Array, Genevestigator (https://genevisible.com).

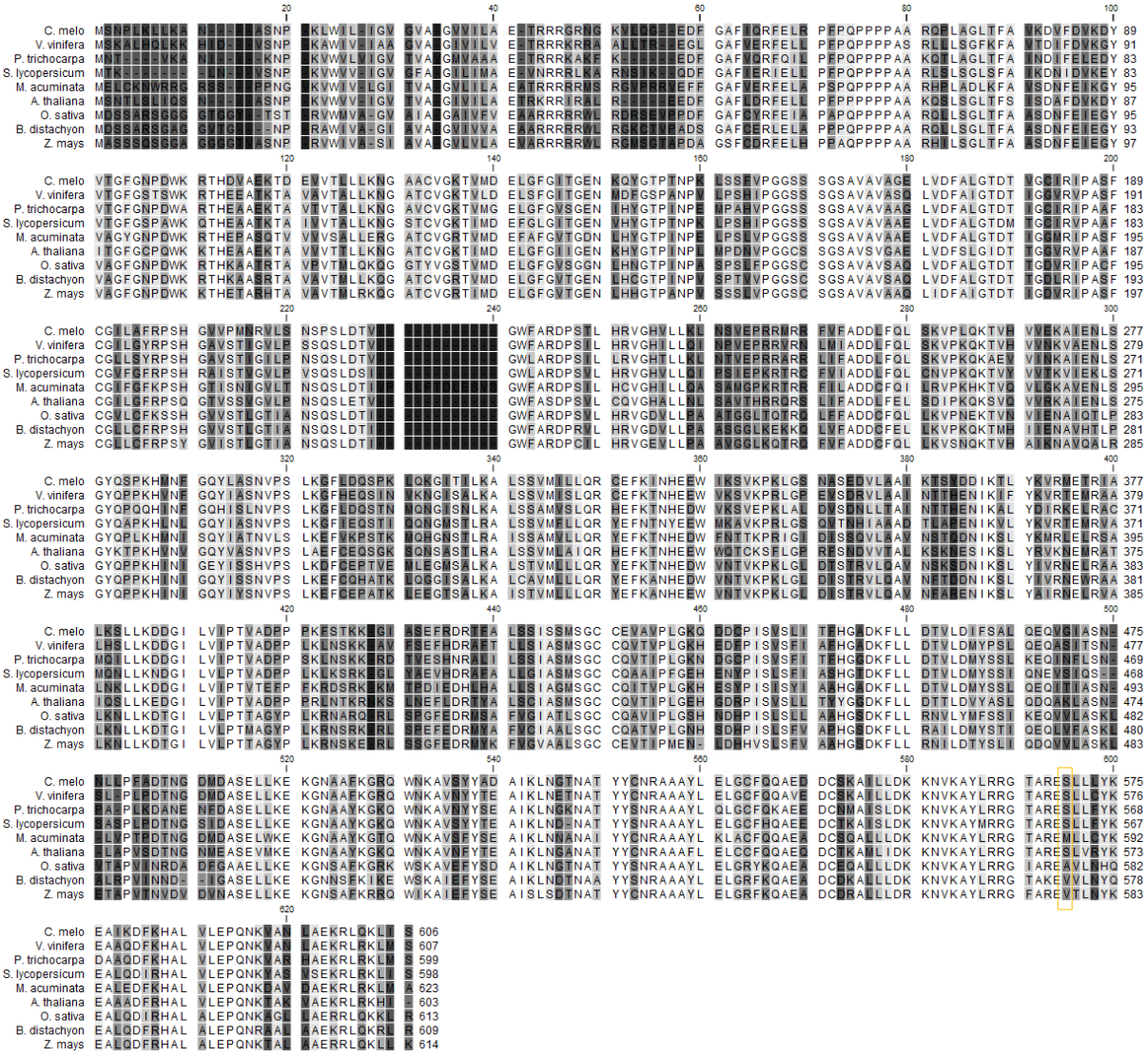

Figure 23: Alignment of OM64 protein of different mono- and dicotyledonous species. Black background color represents 0 % conservation, white background 100 % conservation. Phosphorylation site in *Arabidopsis* is marked.

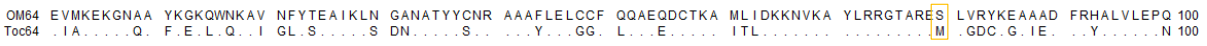

Figure 24: Alignment of TPR domain of OM64 and Toc64. Phosphorylation site of OM64 is marked.

Danksagung

An dieser Stelle möchte ich mich bei allen bedanken, die zu der Entstehung dieser Arbeit beigetragen haben.

Mein erster und größter Dank geht an PD Dr. Serena Schwenkert, der besten Betreuerin, die man sich wünschen kann. Immer ein offenes Ohr, immer motivierend, begeistert und optimistisch.

Dann möchte ich Prof. Soll für seine Unterstützung danken und dafür, dass ich meine Arbeit in seiner AG durchführen konnte.

Meinen Kooperationspartnern PD Dr. Ralf Heermann danke ich für die ITC Messungen und Dr. Heidi Obermeyer-Pertl für die OM64 MS Messungen. Prof. Dr. Boon Leong Lim danke ich für die Bereitstellung der *pap2* Samen.

Bei all meinen Kollegen möchte ich mich für die nette Zeit bedanken, für den Spaß im Laboralltag, für die Hilfsbereitschaft und die gute Stimmung. Insbesondere möchte ich Pit danken für die leckeren Kuchen und die vielen Gespräche. Und natürlich ausdrücklich meinem Banknachbarn Thomas für seine unerschütterlich gute Laune, für den geteilten (großen) Frust und die geteilten (kleinen) Erfolge.

Ganz besonders möchte ich meiner Familie danken, vor allem meinen Eltern, auf die ich mich immer verlassen kann, die stets hinter mir stehen und ohne die ich es nie bis nach hier geschafft hätte.

Und das Wichtigste zum Schluss: ein ganz großer Dank an Uwe. Für alles und von ganzem Herzen.

Curriculum Vitae

Personal data

Family name:	Nickel
First name:	Anna-Elisa Catharina
Date of birth:	25.09.1986
Place of birth:	Düren, Germany

Education and Research Experience

since 01/2013	Post-graduate studies Ludwig-Maximilians-Universität München, Germany PhD thesis: Role of protein phosphorylation in preprotein targeting to plant organelles
10/2010-09/2012	Master's degree: Molecular and Cellular Biology Philipps Universität Marburg, Germany Master thesis: The role of SK channels in neuronal damage caused by oxidative stress
10/2007-09/2010	Bachelor's degree: Biochemistry Universität Ulm, Germany Bachelor thesis: Regulation of KLF4 expression by DNA methylation in different B-cell subtypes and B-cell lymphomas
09/1997-06/2006	General matriculation standard Landrat-Lucas-Gynmasium Leverkusen, Germany

Publications

Nickel C, Brylok T, Schwenkert S (2016) In Vivo Radiolabeling of Arabidopsis Leaves and Separation of Thylakoid Membrane Complexes by Blue Native PAGE. Plant Proteostasis, Humana Press, Springer Science+Business Media New York, ISBN 978-1-4939-3757-8.

Nickel C, Soll J, Schwenkert S (2015) Phosphomimicking within the transit peptide of pHCF136 leads to reduced photosystem II accumulation in vivo. FEBS Letters, 589(12):1301-7.

Richter M, Nickel C, Apel L, Kaas A, Dodel R, Culmsee C, Dolga AM (2015) SK channel activation modulates mitochondrial respiration and attenuates neuronal HT-22 cell damage induces by H2O2. Neurochemistry international, 81:63-75.

Veröffentlichungen

Teile dieser Arbeit wurden veröffentlicht in:

Nickel C, Soll J, Schwenkert S (2015) Phosphomimicking within the transit peptide of pHCF136 leads to reduced photosystem II accumulation in vivo. FEBS Letters, 589(12):1301-7.

Andere Teile dieser Arbeit sind ebenfalls zur Veröffentlichung vorgesehen. Folgendes Manuskript wird zur Zeit erarbeitet:

Nickel C, Schweiger R, Heermann R, Jung K, Soll J, Schwenkert S (2016) Phosphorylation of the outer membrane mitochondrial protein OM64/Tom64 influences protein import into mitochondria.

Eidesstattliche Versicherung

Ich versichere hiermit an Eides statt, dass die vorgelegte Dissertation von mir selbstständig und ohne unerlaubte Hilfe angefertigt wurde. Ich habe weder anderweitig versucht, eine Dissertation einzureichen oder eine Doktorprüfung durchzuführen, noch habe ich diese Dissertation oder Teile derselben einer anderen Prüfungskommission vorgelegt.

München, den _____ _____

Catharina Nickel